Tectonics of Europa

Simon A. Kattenhorn
University of Idaho

Terry Hurford
NASA Goddard Space Flight Center

Europa has experienced significant tectonic disruption over its visible history. The description, interpretation, and modeling of tectonic features imaged by the Voyager and Galileo missions have resulted in significant developments in four key areas addressed in this chapter: (1) The characteristics and formation mechanisms of the various types of tectonic features; (2) the driving force behind the tectonics; (3) the geological evolution of its surface; and (4) the question of ongoing tectonics. We elaborate upon these themes, focusing on the following elements: (1) The prevalence of global tension, combined with the inherent weakness of ice, has resulted in a wealth of extensional tectonic features. Crustal convergence features are less obvious but are seemingly necessary for a balanced surface area budget in light of the large amount of extension. Strike-slip faults are relatively common but may not imply primary compressive shear failure, as the constantly changing nature of the tidal stress field likely promotes shearing reactivation of preexisting cracks. Frictional shearing and heating thus contributed to the morphologic and mechanical evolution of tectonic features. (2) Many fracture patterns can be correlated with theoretical stress fields induced by diurnal tidal forcing and long-term effects of nonsynchronous rotation of the icy shell; however, these driving mechanisms alone probably cannot explain all fracturing. Additional sources of stress may have been associated with orbital evolution, polar wander, finite obliquity, ice shell thickening, endogenic forcing by convection and diapirism, and secondary effects driven by strike-slip faulting and plate flexure. (3) Tectonic resurfacing has dominated the ~40–90 m.y. of visible geological history. A gradual decrease in tectonic activity through time coincided with an increase in cryomagmatism and thermal convection in the icy shell, implying shell thickening. Hence, tectonic resurfacing gave way to cryomagmatic resurfacing through the development of broad areas of crustal disruption called chaos. (4) There is no definitive evidence for active tectonics; however, some tectonic features have been noted to postdate chaos. A thickening icy shell equates to a decreased tidal response in the underlying ocean, but stresses associated with icy shell expansion may still sufficiently augment the contemporary tidal stress state to allow active tectonics.

1. INTRODUCTION AND HISTORICAL PERSPECTIVE

It took 369 years after the discovery of Europa, the smallest of the Galilean moons, before humans finally managed a close look at this icy world as the Voyager spacecraft sped by in 1979. The analysis of Voyager images of Europa (e.g., *Finnerty et al.,* 1981; *Pieri,* 1981; *Helfenstein and Parmentier,* 1980, 1983, 1985; *Lucchitta and Soderblom,* 1982; *McEwen,* 1986; *Schenk and McKinnon,* 1989), which had resolutions of 2 km to tens of kilometers per pixel, resulted in the identification of a multitude of superposed crosscutting lineaments. The overall appearance, much akin to a "ball of string" (*Smith et al.,* 1979), spoke of a history of intense tectonic activity (Fig. 1), but a paucity of large impact craters suggested a geologically young surface. The surface deformation suggested an efficient tectonic resurfacing process, perhaps accompanied by cryovolcanism, resulting in a broad classification of Europa's surface into tectonic terrain and chaotic or mottled (cryomagmatically disaggregated) terrain (*Smith et al.,* 1979; *Lucchitta and Soderblom,* 1982). Hence, competing tectonic and endogenic processes have both been important in shaping Europa's geology. The notion of a tectonically active world implied an effective tidal forcing of the icy shell, leading researchers to hypothesize about the presence of a liquid ocean beneath the icy exterior of the moon (see chapter by Alexander et al.).

Detailed analyses of higher-resolution (tens to hundreds of meters per pixel) Galileo spacecraft images 20 years after Voyager resulted in a more precise classification of the many types of lineaments (e.g., troughs, ridges, bands, cycloids, strike-slip faults) and a reexamination of lineament-formation mechanisms (e.g., summary in *Pappalardo et al.,* 1999). In many studies, crosscutting relationships among multiple episodes of lineaments allowed a complex tectonic history to be unraveled. Cryomagmatism and chaos formation (see chapter by Collins and Nimmo) generally postdated tectonic resurfacing, although there was broad overlap between tectonic and cryomagmatic processes and some tectonic features are clearly geologically young (see chapter by Doggett et al.). Most of the emphasis in tectonic analyses of Galileo data was given to determining what caused individual features to form in the first place, and what mech-

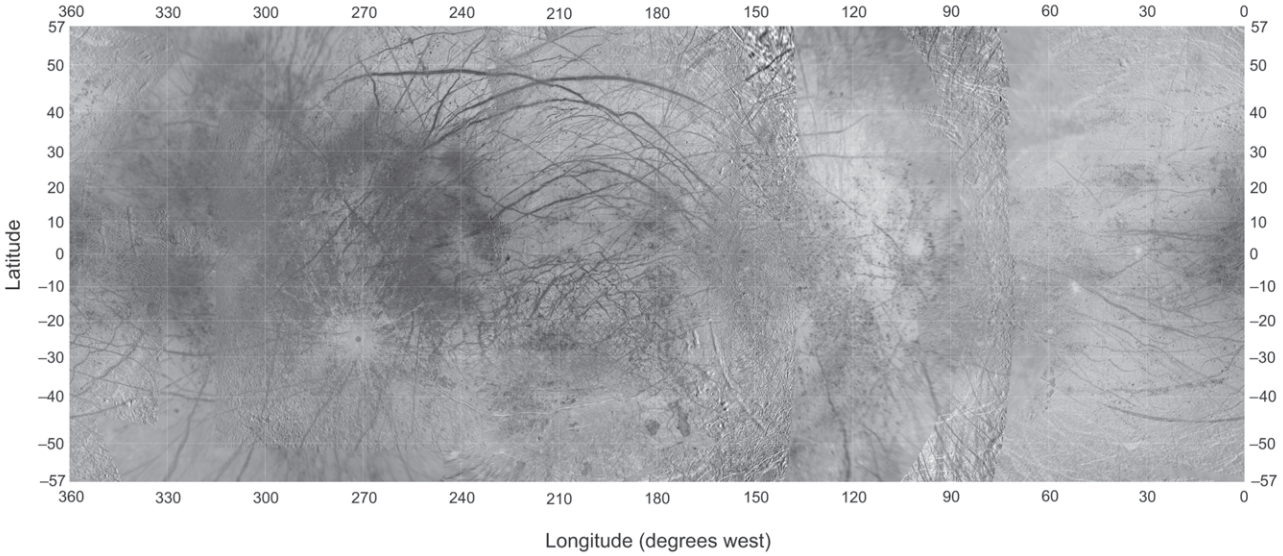

Fig. 1. Global mosaic of Europa, in Mercator projection, based on Voyager and Galileo imagery (courtesy of USGS, Flagstaff). The center is at longitude 180°W and the latitude range is +57° to –57°.

anisms resulted in their morphologic and geometric differences. Over the past dozen or so years, this work has produced a convincing framework for the role of tidal stresses in deforming the icy shell to produce fracturing, assisted by some amount of buildup of stress due to nonsynchronous rotation (see chapter by Sotin et al.). These stresses can be quantified and show a remarkable correlation to many lineament orientations after accounting for the effects of longitudinal migration of the icy shell by nonsynchronous rotation. The magnitude of the tidal distortion required for pervasive fracturing of the icy shell strongly suggests the presence of a tidally responding ocean beneath a relatively thin shell that was repeatedly stressed and strained. The presence of such an ocean is also strongly implied by Galileo magnetometer measurements (*Kivelson et al.,* 2000; see chapter by Khurana et al.).

The goal of this chapter is to provide a thorough examination of the wide range of tectonic features that pervasively damaged the icy shell of Europa during its visible geological history and their implications for characterizing the nature of the icy shell, the interior dynamics, the tidal deformation history, and the prospects for active tectonics. To accomplish this, the chapter is divided into three main components. First, we discuss the tectonic features themselves, summarizing their likely formation mechanisms in terms of being extensional, compressive, or lateral shearing structures. Second, we provide an overview of the causal factors that drive tectonic deformation at all scales, focusing on the production of stresses in the icy shell through tidal forcing and other means. Finally, we examine the tectonic history of Europa interpreted from the various types of tectonic features placed in the context of the tidal stress history. In so doing, we also address a number of topical issues such as the evidence for diminishing tectonic activity through time, reasons for the disparate geometries of lineaments, and the prospect of active tectonics. We do not speculate on the exact thickness of the icy shell in this chapter other than to infer that it is sufficiently thin (likely <30 km) to enable a strong tidal response in the underlying ocean, and consequently inducing tectonic deformation of the shell. One reason for this omission is that any constraints on icy shell thickness based on tectonic features are inconclusive. Second, fractures that have been used to deduce brittle or elastic thicknesses do not necessarily capture the entire thickness of the icy shell (e.g., *Billings and Kattenhorn,* 2005), much of which may be behaving inelastically depending on the timescale of deformation (see chapter by Nimmo and Manga). Various terms have been used to describe tectonic features on Europa. We aim to define and standardize the relevant terms adopted in this chapter and that of Prockter and Patterson with the glossary found in Table 1.

2. DEFORMATION STYLES

2.1. Extensional Tectonics

Analyses of low-resolution Voyager images followed by higher-resolution Galileo images resulted in the recognition and characterization of ubiquitous fractures in Europa's icy shell (Fig. 2). The prevalence of linear or curvilinear lineaments (e.g., *Lucchitta and Soderblom,* 1982) led to comparisons to terrestrial tension cracks, resulting in a body of published works that interpreted the majority of europan lineaments as tensile features (e.g., *McEwen,* 1986*; Leith and McKinnon,* 1996). Exceptions included the identification of lateral offset lineaments, interpreted to be strike-slip faults (see section 2.3). The assumption that tensile failure predominates in the icy shell is supported by numerous lines of evidence. First, ice has been shown to be particularly weak in tension under terrestrial conditions and in low-tem-

TABLE 1. Glossary of terms used to describe tectonic features on Europa.

band — A general term used to describe a tabular feature that formed by dilation (*dilational band*), contraction (*convergence band*), and/or strike-slip motions (*band-like strike-slip fault*). A *dilational band* is *lineated* (faulted or ridged varieties) or *smooth*. In low-resolution images, relative albedo may be used to distinguish between a *bright band*, *gray band*, or *dark band*.

band-like strike-slip fault — A type of *strike-slip fault* that morphologically resembles a *dilational band* and implies an oblique cumulative opening vector.

bright band — A term used to refer to high-relative-albedo, tabular features in low-resolution imagery. These bands may have experienced some combination of dilation, strike-slip, and/or convergence.

chaos — Regions of crustal disruption or disaggregation related to an underlying endogenic process such as cryomagmatism.

complex ridge — See *ridge complex*. Use of this term is discouraged.

convergence band — a tabular zone that appears to represent missing crust after tectonic reconstructions are undertaken, implying a localized zone of contraction.

crack — See *trough*.

cycloid — Curved, cuspate structures that form in chains of arcuate segments linked at sharp cusps. If a central *trough* is flanked by ridge edifices, the feature is called a *cycloidal ridge*. Also called a *flexus* (plural *flexūs*).

cycloidal fracture — A type of *trough* that forms arcuate segments linked at sharp cusps. They are the ridgeless progenitor of a *cycloidal ridge*.

cycloidal ridge — A *cycloid* that has developed ridges to either side of a central *trough*.

dark band — A term sometimes used to refer to a low-albedo *dilational band*.

dilational band — A tabular zone of dilation in the icy shell where intrusion of new crustal material occurred between the walls of a crack. Also called a *pull-apart band*. If fine, internal lineations are observed, the term *lineated band* may be used. The lineations may be defined by *normal faults* (hence, a *faulted band*) or by parallel *ridges* (a *ridged band*). If no lineations are observable (commonly a resolution effect), the term *smooth band* may be used.

diurnal tidal stress — The stress produced globally in the icy shell in response to the oscillating tidal response of the satellite during its eccentric orbit.

double ridge — See *ridge*.

endogenic fracture — A type of *trough* that forms above or adjacent to a zone of endogenic activity in the icy shell, thus commonly occurring adjacent to regions of *chaos*.

faulted band — A type of *lineated band* in which the lineations are caused by *normal faults* that have dissected the surface of the *dilational band*.

flexure fracture — A type of *trough* that forms alongside a *ridge* in response to flexing of the icy shell beside a *ridge*.

flexus — See *cycloid*.

fold — A rare form of contractional deformation in which the icy shell warps into anticlinal and synclinal undulations, such as within *dilational bands*.

fold hinge fracture — A type of *trough* that forms along the crest of an anticline.

gray band — A term sometimes used to refer to an intermediate relative albedo *dilational band*.

lineated band — A type of *dilational band* characterized by a fine lineated internal texture. This term may be used generically regardless of the inferred cause of the lineation. Two varieties are *faulted bands* and *ridged bands*.

nonsynchronous rotation — The proposed process by which the icy shell gradually migrates longitudinally eastward (i.e., about the rotational poles) in response to rotational torques. As a result, all locations on the surface migrate across the tidal bulges, resulting in a global component of stress that may contribute to the tectonics.

normal fault — An extensional shear fracture across which a vertical component of motion is inferred. Interpreted to define the lineations within a *faulted band*.

protoridge — The progenitor of a *ridge*, composed of a central trough flanked by poorly developed edifices. Also called a *raised-flank trough*.

pull-apart band — See *dilational band*.

raised-flank trough — See *protoridge*.

ridge — The most common tectonically related feature on Europa, comprising a central crack or trough flanked by two raised edifices, up to a few hundred meters high and less than 5 km wide. Also called a *double ridge*.

ridge complex — Several adjacent ridges that can be mutually parallel or commonly sinuous and anastomosing. Individual ridges in the complex are readily identifiable.

ridged band — A type of *lineated band* in which the lineations are created by numerous parallel ridges that define the *dilational band*.

ridged plains — The oldest and most expansive portions of the surface of Europa, composed of a multitude of low, generally high-albedo *ridges, bands,* and other structures that were repeatedly overprinted by younger features. Also called *subdued plains*.

ridge-like strike-slip fault — A type of *strike-slip fault* that morphologically resembles a *ridge*.

small-circle depressions — Up to 1.5-km-deep depressions in the icy shell that form broad, circular map patterns centered ~25° from the equator in an antipodal relationship on the leading and trailing hemispheres.

smooth band — A type of *dilational band* lacking an observable internal lineated texture, commonly in response to image resolution constraints, that may include small-scale hummocks.

strike-slip fault — A lineament along which older crosscut features were translated laterally during shearing.

subdued plains — See *ridged plains*.

tailcrack — A type of *trough* that forms where tension occurs at the tip of a *strike-slip fault* in response to fault motion.

tectonic fracture — A type of linear or broadly curving *trough* that forms locally or regionally, probably in response to tensile tidal stress.

triple band — A now-discouraged term originally used to describe lineaments in low-resolution imagery that appeared as a bright central stripe flanked by dark edges. Such features were ultimately identified in higher-resolution images to be predominantly *ridge complexes* flanked by dark materials, but may also be *double ridges* or *bright bands* flanked by dark materials.

trough — A ridgeless fracture with a visible width that results in a linear indentation at the surface of the icy shell. Also called a *crack*.

perature experiments, with tensile strengths of perhaps hundreds of kilopascals to as much as ~2 MPa (cf. *Schulson,* 1987, 2001; *Rist and Murrell,* 1994; *Lee et al.,* 2005). Second, unlike Earth, Europa's surface experiences absolute tension on a regular basis due to oscillating tidal bulges during the diurnal cycle (see section 4.1.5 and chapter by Sotin et al.). Third, some lineaments of particular ages typically form as multiple, parallel sets analogous to terrestrial tension joint sets. Fourth, the majority of lineaments on Europa do not appear to show lateral offsets, implying only crack-orthogonal motions (mode I cracks, in fracture mechanics terminology). Finally, there is clear evidence of complete dilational separation of parts of the icy shell, with infill of material from below to create new surface area within the dilated crack. A number of tensile tectonic features have been identified on the basis of these lines of evidence, including ridges, cycloids, dilational bands, and troughs. Additionally, normal faults on Europa indicate that extensional tectonics can occur through shear failure where there is deviatoric tension in a compressive stress field. Inferred extensional features, called small-circle depressions (*Schenk et al.,* 2008), form an antipodal pattern in the leading and trailing hemispheres, but an explicit formation mechanism has not been identified (see section 4.1.7).

2.1.1. Ridges. The most common lineaments on Europa are ridges, also referred to as *double ridges* due to the typical morphology in which a central crack or trough is flanked by two raised edifices (e.g., Androgeos Linea in Fig. 2b). As a result, ridges typically appear in medium- to high-resolution surface images as having a central dark stripe (the trough) flanked by two bright thicker stripes (the raised edifices; Fig. 3c), and may extend from a few kilometers to in excess of 1000 km across the surface. Ridges are analyzed in great detail elsewhere in this book (see chapter by Prockter and Patterson) but are also described here due to their prominence among Europa's tectonic features. Not only are ridges the most common type of structural lineament on Europa, they are also the most persistent, being the primary component of the very oldest *ridged plains* of the icy surface (*Figueredo and Greeley,* 2000*; Kattenhorn,* 2002; *Doggett et al.,* 2007) as well as constituting some of the youngest geological features. Hence, whatever process is responsible for their development must have been an ongoing process throughout Europa's visible geological history. Ridges of different ages commonly occur in disparate orientations, resulting in a complex network of multiply crosscutting generations of ridge sets and indicating significant changes in stress fields through time (see sections 5.1 and 5.2). Topographically, ridges range from barely perceptible in parts of the background plains to as high as several hundred meters (*Malin and Pieri,* 1986; *Greenberg et al.,* 1998; *Greeley et al.,* 2000). Individual ridge widths are typically around a few hundreds of meters (<400 m) but higher ridges tend to be wider, with maximum

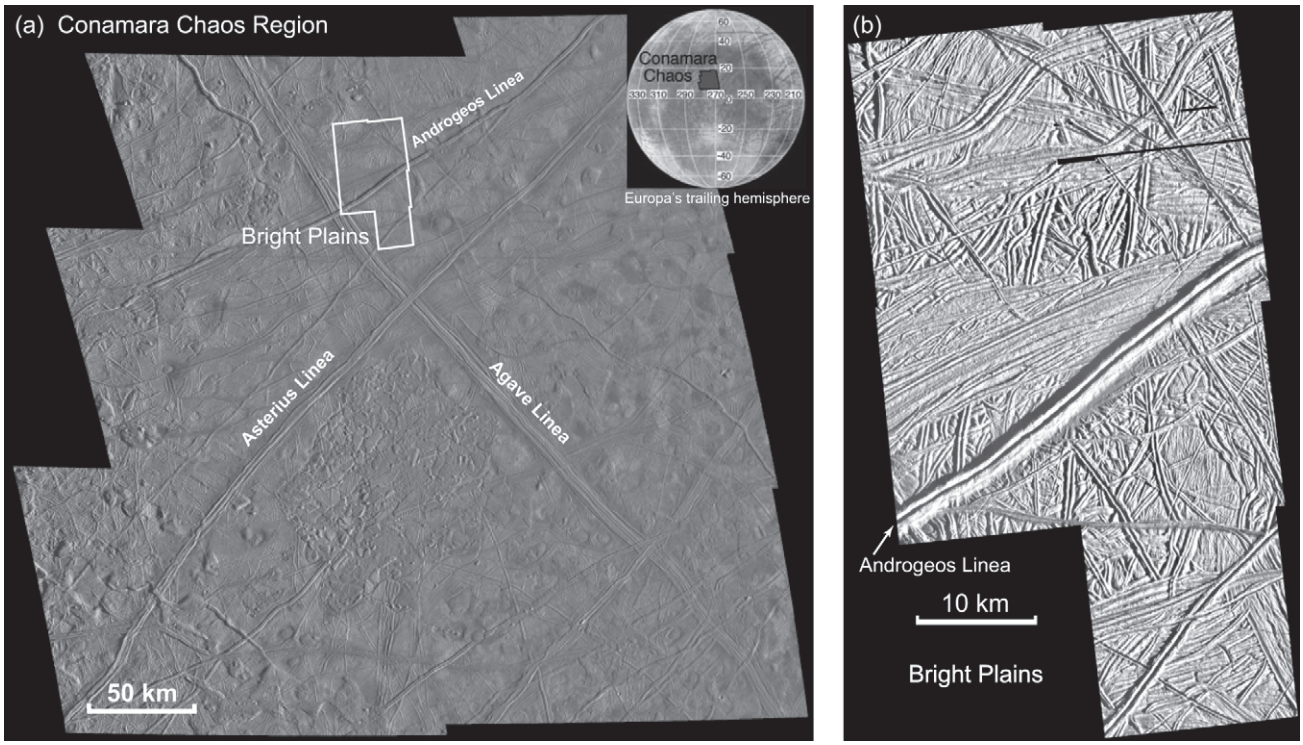

Fig. 2. **(a)** Conamara Chaos in the northern trailing hemisphere (orthographic mosaic E6ESDRKLIN01). The region is dominated by the prominent tectonic lineaments Asterius and Agave Lineae and the cryomagmatically disrupted region of chaos south of where the two lineaments cross. **(b)** The Bright Plains region (Galileo mosaic E6ESBRTPLN02) highlights the wide range of tectonic features in different orientations that characterizes much of the europan surface. This region shows ridges, dilational bands, and troughs, with the prominent Androgeos Linea cutting across the center of the image. Images courtesy of the NASA Space Photography Laboratory at Arizona State University.

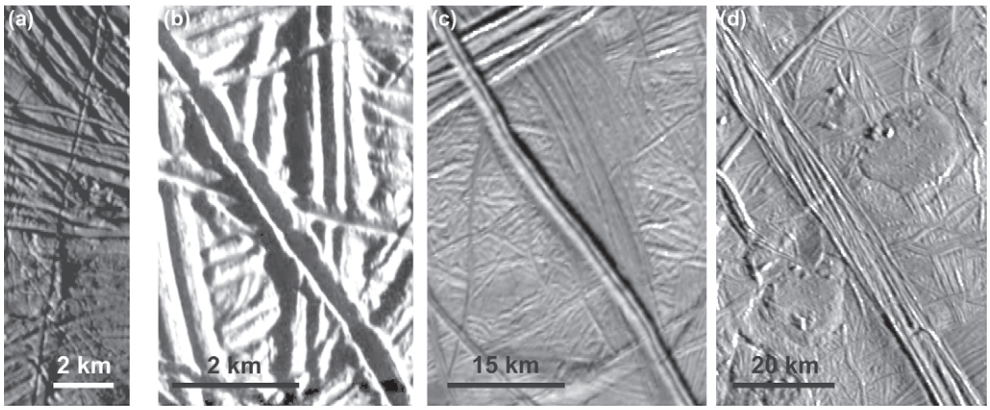

Fig. 3. Progressive evolution of fractures from **(a)** simple troughs to the development of **(b)** nascent ridges, then **(c)** fully developed ridges, and finally **(d)** a ridge complex. The image in **(a)** was taken during Galileo's E11orbit, image 420626739; those in **(b)**–**(d)** are all from the Conamara Chaos and Bright Plains region shown in Fig. 2, taken during Galileo's E6 orbit. The ridge in **(c)** is Androgeos Linea. The ridge complex in **(d)** is Agave Linea.

surface widths of <5 km (*Coulter et al.,* 2009). *Kattenhorn* (2002) examined the 20 m/pixel "Bright Plains" images (Fig. 2b) and concluded that ridges became higher, wider, and fewer in number during the geological sequence in that region.

Ridges do not necessarily occur in isolation but may develop prominent lineaments comprising several, commonly braided and inosculating, superposed ridges up to 15 km wide (Fig. 3d). Such features are called *ridge complexes* (e.g., *Greenberg et al.,* 1998) but are sometimes referred to as *complex ridges* (*Figueredo and Greeley,* 2000, 2004; *Greeley et al.,* 2000) and imply that an early formed ridge may create a zone of weakness that localizes and superposes later ridge development (Patterson and Head, in preparation), possibly accompanied by shearing (*Aydin,* 2006). Prominent examples include Agave and Asterius Lineae in the Conamara Chaos region (Fig. 2a). In low-resolution images, ridge complexes commonly appear bright with flanking dark stripes, and were originally referred to as triple bands (*Lucchitta and Soderblom,* 1982), now a defunct term as it does not imply any explicit geological feature type. Ridges and ridge complexes can produce a surface line-load that impinges on the elastic portion of the icy shell, resulting in downward flexing to either side of the ridge (*Tufts,* 1998; *Head et al.,* 1999; *Kattenhorn,* 2002; *Billings and Kattenhorn,* 2005; *Hurford et al.,* 2005). The associated bending stresses may induce flanking lines of tension fractures to either side of the ridge (see section 2.1.4).

A key observation about ridges is that they appear to represent an advanced stage in a genetic sequence of lineament development (*Geissler et al.,* 1998a; *Head et al.,* 1999) (Fig. 3). This idea stemmed from the fact that some ridges change in morphology along their trend, becoming less prominent along their lengths with a central crack flanked by underdeveloped edifices (Fig. 3b). This less-evolved stage has been called a *protoridge* (*Kattenhorn,* 2002) or a *raised-flank trough* (*Head et al.,* 1999). Ultimately, the protoridge may disappear along its trend to reveal its progenitor: a ridgeless crack called a *trough* (Fig. 3a). This sequence of development has been interpreted to imply that all ridges originate as troughs that form as tension cracks, evolving into protoridges and then finally ridges (Fig. 3c) or sometimes ridge complexes (Fig. 3d), although the nature of this evolution (i.e., the ridge growth process) is neither straightforward nor generally agreed upon.

The majority of published models of ridge development assume that they are fundamentally tensile features, but with differing mechanisms to explain the manner in which the ridge edifices are constructed. *Kadel et al.* (1998) attributed ridge growth to the effects of gas-driven cryovolcanic fissure eruptions. Weaknesses of this model include no explanation for a subsurface source of cryovolcanic material and the inherent difficulty in attempting to account for the remarkably consistent morphology of ridges, commonly for hundreds of kilometers along their lengths. A linear diapirism model (*Head et al.,* 1999) invokes buoyant upwelling of ice beneath a tension crack near the surface, resulting in an upward bending of the brittle carapace to either side of the central crack, thus forming ridges. Problems with this model include no explicit mechanism to explain why such upwelling would occur beneath a surface crack (although see the shear heating discussion below, for one possibility) and it necessitates that the preexisting terrain is preserved within the upwarped ridge slopes. This final point does not seem to be characteristic of europan ridges even though some examples have been described (*Giese et al.,* 1999; *Head et al.,* 1999; *Cordero and Mendoza,* 2004). The along-trend morphology of a well-developed ridge is invariably unaffected by the nature of the ridged plains it crosses, which may imply that upward warping of these plains is not the primary process by which ridges are created. Mass wasting could conceivably have removed the original surface roughness along ridges; however, ridge slopes are typically less than 30° and on average only about 10° (*Coulter*

et al., 2009), which seems to be too low to be consistent with a mass wasting process. An incremental wedging model (*Turtle et al.,* 1998; *Melosh and Turtle,* 2004) explains ridge development as being due to a gradual forcing apart of the walls of a crack intruded by material from below that freezes within the crack, causing upward plastic deformation at the surface to construct the ridge. In this model, it is unclear what the source of the intruded material would be, or why it is so readily accessible by surface cracks.

The ridge model of *Greenberg et al.* (1998) attributes their formation to the cyclical extrusion of a slurry of lead ice created by exposure and instantaneous near-surface freezing of an underlying ocean during the opening of a crack by diurnal tidal stresses. During subsequent closure of the crack, the ice is squeezed onto the surface, gradually building piles of ice debris to either side of the central crack. A caveat to this model is the need for a very thin icy shell in order to reconcile the requirement of complete separation of the ice layer to expose the underlying ocean (e.g., *Rudolph and Manga,* 2009) with the fact that tidal stresses are typically very small (likely a few tens of kilopascals) and thus would quickly be overcome by overburden pressure with increasing depth. Furthermore, because of the density contrast, ocean water can only rise to a level about 10% of the total icy shell thickness down from the surface. It would therefore have become increasingly difficult for material to be squeezed up to the surface if the icy shell thickened through time, as is suggested by thermodynamic models and the evolution of surface geological features (see section 5.2), unless the underlying ocean is sufficiently pressurized to allow cryovolcanic eruption, which is unlikely to be the case on Europa (*Manga and Wang,* 2007).

Gaidos and Nimmo (2000) and *Nimmo and Gaidos* (2002) infer that ridge development is ultimately driven by frictional shear heating along an existing crack (see section 2.3.1), even for friction coefficients as low as 0.1. Shearing is driven by the ever-rotating diurnal tidal stress field (see section 4.1.5) with inferred diurnal timescale shear velocities of 10^{-6}–10^{-7} m s^{-1}. Subsequent heating results in an almost sevenfold increase in the local surface heat flux causing buoyant rising of warm ice toward the surface and resultant upwarping of a near-surface brittle layer to form a ridge. For shear velocities >~10^{-6} m s^{-1}, local melting along the shear zone will cause downward draining of any melt products and the production of void space that may promote sagging or lateral contraction. This model places only mild depth constraints on the preexisting cracks that get sheared (i.e., the cracks do not need to penetrate the icy shell to an underlying ocean), it is based on a proven deformation mechanism on Europa (i.e., shearing; see section 2.3), and is a process that has likely been occurring on Europa as long as there has been a tidally responding ocean beneath the icy shell. Caveats to the model include the lack of observable lateral offsets along the majority of ridges and the lack of a clear mechanism for how the buoyant upwelling ultimately constructs the ridges. The mechanism appears to resemble the linear diapirism model described above and the two ideas are probably not mutually exclusive and thus share similar caveats regarding the ridge construction process. However, a source of heating may also perhaps explain the relatively low outer slopes of ridges if viscoplastic flow is the dominant form of ridge slope modification (*Coulter et al.,* 2009). *Han and Showman* (2008) explicitly model a linear zone of thermal upwelling beneath a frictionally shear heated zone, producing narrow, laterally continuous, ridge-like features with heights of up to 120 m. Ridges are known to attain heights of more than twice this amount; however, this small disparity may perhaps be circumvented if there is a component of fault-perpendicular contraction during the shear process that contributes to the construction of ridges (*Nimmo and Gaidos,* 2002; *Vetter,* 2005; *Aydin,* 2006; *Patterson et al.,* 2006; *Kattenhorn et al.,* 2007; *Bader and Kattenhorn,* 2007) or additional buoyancy mechanisms such as depletion of salts during heating (cf. *Nimmo et al.,* 2003). Possible evidence for contraction across ridges is described in more detail in section 2.2.3, but essentially allows ridge development to accommodate convergence across weak zones caused by shear heating along cracks. The associated contraction of the brittle icy shell at the surface may develop a permanent positive relief structure, perhaps negating the problem of expected relaxation of buoyant-upwelling-induced ridges over the thermal diffusion timescale of ~10^7 yr (*Han and Showman,* 2008).

Regardless of the precise formation mechanism for ridges, the fact remains that ridge building has been an effective geological process on Europa. Considering the relatively young surface age based on crater densities (40–90 m.y.) (*Zahnle et al.,* 2003; see chapter by Bierhaus et al.) and the great number of ridges of different ages and orientations, each individual ridge must form in a relatively short period of time. *Greenberg et al.* (1998) suggest that ridges may form within 30,000 yr based on their tidal pumping model; however, that estimate is necessarily based on a number of uncertain assumptions regarding crack dilation and spacing, as well as the effectiveness of the ice extrusion process. *Melosh and Turtle* (2004) estimate 10,000 yr to form a ridge through an incremental ice-wedging process. *Gaidos and Nimmo* (2000) estimate that shear heating may result in buoyant uprising of warm ice at a rate that could conceivably construct a ridge in only ~10 yr. Presumably, the amount of time during which a crack may remain active (whether in dilation, shearing, or contraction) with the capability of developing a ridge is ultimately controlled by the amount of time over which the global tidal stresses drive crack activity. This timing may be controlled by the rate of nonsynchronous rotation, if present, relative to a tidally locked interior (see sections 4.1.6 and 5.1), which would eventually rotate an active crack away from a stress field conducive to crack activity. One cycle of nonsynchronous rotation takes in excess of 12,000 yr (*Hoppa et al.,* 1999b) and perhaps as much as 1.3 m.y. [cf. *Hoppa et al.* (2001), accounting for the revised surface age of Europa in the chapter by Bierhaus et al., and a factor of 3 uncertainty], suggesting that an estimate of a few tens of thou-

sands of years during which a crack can remain active and thus form a ridge may be reasonable.

2.1.2. Cycloids. Europa also exhibits unique features morphologically similar to ridges called cycloids, also referred to as *cycloidal ridges* or *flexūs*. Cycloids, first described from Voyager data (*Pieri,* 1981; *Lucchitta and Soderblom,* 1982; *Helfenstein and Parmentier,* 1983), are curved, cuspate cracks that form chains of multiple, concatenated segments extending hundreds to thousands of kilometers across the surface (Fig. 4). Each curved segment of a cycloid chain is linked to the adjacent one at an abrupt kink called a cusp. Individual segments are typically tens of kilometers long, measured in a direct line from cusp to cusp, but are locally up to several hundred kilometers long. The central crack is commonly, but not necessarily, flanked by ridges, implying that progressive ridge development occurs to either side of an initial crack, analogous to linear ridges described in section 2.1.1. In some cases, ultimate dilation of the cracks occurs to form cycloidal bands (see chapter by Prockter and Patterson). Cycloids are distinctly different from other tectonic cracks on Europa and, other than one possibly analogous feature in the south polar region of Enceladus, are unique in the solar system. Therefore, their mode of formation must also differ from other tectonic lineaments on Europa, implying significant variability in crack-driving processes during the long-term tectonic history.

Hoppa and Tufts (1999) and *Hoppa et al.* (1999a) proposed that cycloidal cracks form as a result of tensile cracking in response to diurnally varying tidal stresses produced by Europa's orbital eccentricity (these stresses are described in detail in section 4.1.5; also see chapter by Sotin et al.). As Europa orbits Jupiter, it is constantly being reshaped as the size and location of the tidal bulges change, producing a time-dependent diurnal tidal stress field. At any location on the surface during the orbital period, the orientations of the principal stresses rotate and the magnitudes oscillate. The stresses rotate counterclockwise in the northern hemisphere and clockwise in the southern hemisphere, 180° each orbit (while only magnitudes change along the equator). The individual cycloid segments are hypothesized to grow as tension fractures that propagate perpendicular to the rotating direction of maximum tensile stress, resulting in curved segments. Cracking begins when the tensile strength of europan ice is overcome and ceases when the tensile stress drops below the crack propagation strength, assumed to be less than the tensile strength. These parameters are unknowns on Europa; therefore, *Hoppa et al.* (1999a, 2001) estimated them in such a way so as to provide the best match between observed cycloid shapes and theoretical stress fields. This growth model for cycloids predicts that all northern hemisphere cycloids that are concave toward the equator grew from east to west, whereas all cycloids concave toward the poles grew from west to east. Similarly, northern hemisphere cycloids that are concave to the east are predicted to have grown from north to south, whereas cycloids that are concave to the west grew from south to north. The opposite sense of growth is true in all cases in the southern hemisphere. Also, because the diurnal stress characteristics are dependent on latitude and longitude, expected cycloid shapes are correspondingly variable across the surface of Europa, ranging from broadly curved to squarish (*Bart et*

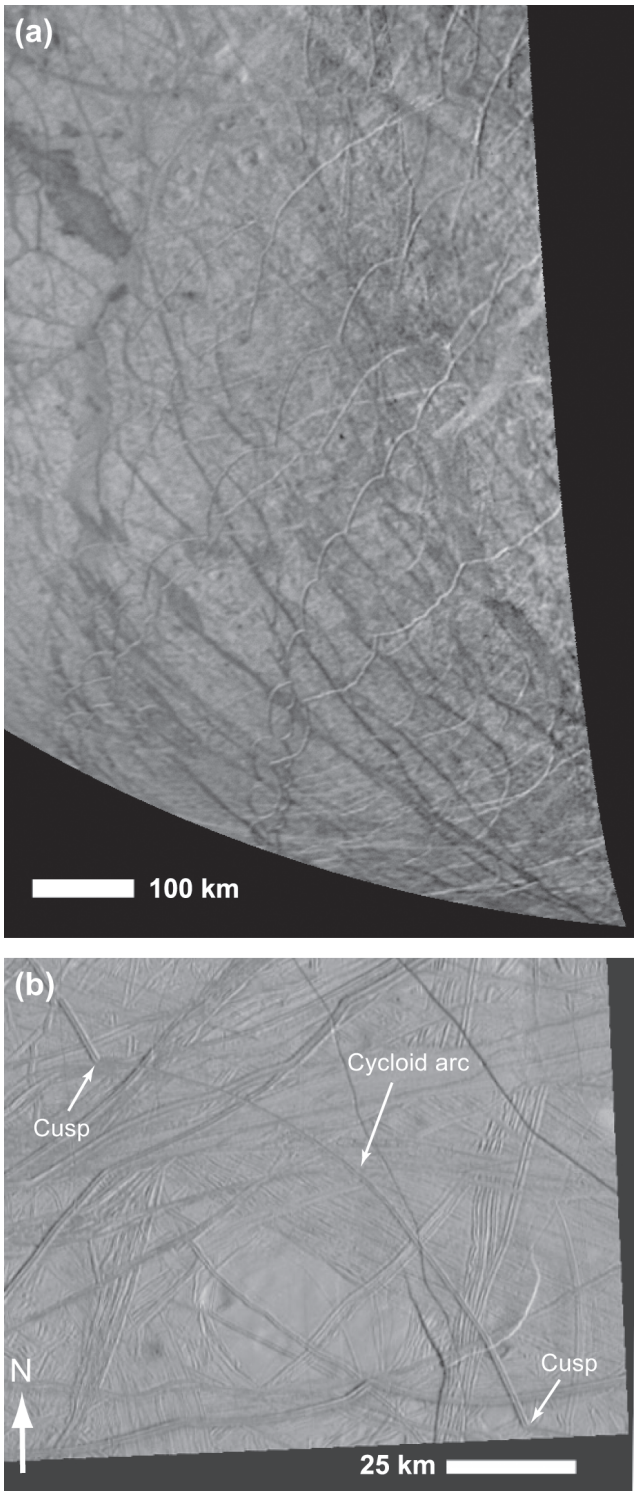

Fig. 4. **(a)** Voyager 2 image (c2065219) showing several chains of cycloidal ridges. **(b)** Example of a cycloidal fracture in the northern trailing hemisphere with ridge development along a small part of the arc (Galileo image 449961879, E15 orbit).

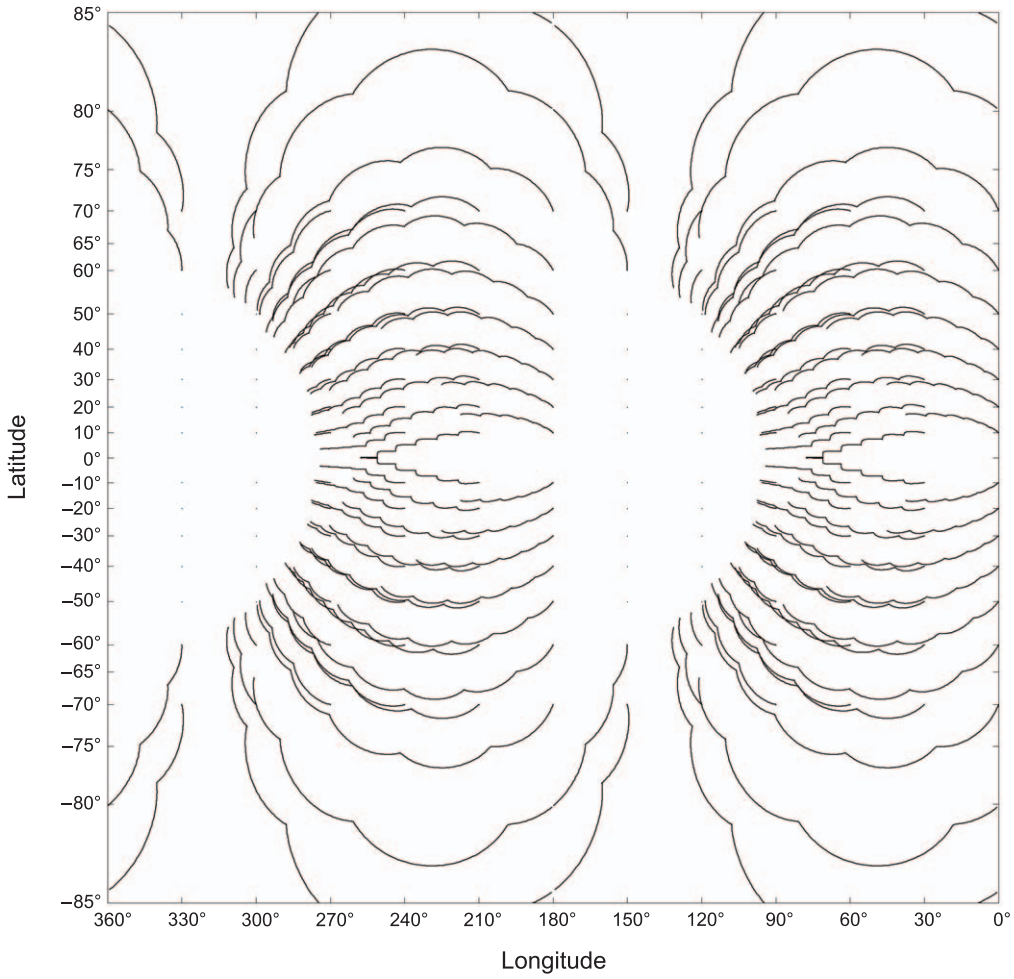

Fig. 5. Theoretical distribution of cycloids that grow from east to west (*Hurford et al.,* 2007a) in a stress field composed of a diurnal component plus stress due to 1° of nonsynchronous rotation. East-growing cycloids will have an opposite curvature in each hemisphere but a similar overall distribution.

al., 2003; *Hurford et al.,* 2007a). Cycloid chains commonly exhibit a large-scale curvature due to regional variability in global tidal stress fields. The growth of these broadly curved cycloid chains ultimately ceases when they propagate into an area where critical stress values are not attained, resulting in some regions where cycloids theoretically never form (Fig. 5).

The growth of a single cycloid arc is assumed to be a continuous process during the course of a europan day and must occur at a low crack propagation speed (~3–5 km/h) in order for curved segments to produce a match to the predicted stresses. Actual growth speeds may be much faster, albeit occurring in short, discrete spurts to produce a much lower effective propagation speed (*Lee et al.,* 2005). After cessation of growth of a cycloid arc, the next arc starts growing when the tensile strength of the ice is again overcome in the subsequent orbit; however, because the stresses rotate during the period of no crack growth, the new cycloid arc propagates at an angle away from the tip of the previous one, forming a sharp cusp. These rotated stresses resolve a component of shearing along the arrested cycloid segment immediately prior to the development of the cusp, inducing a concentration of stress at its tip that drives the development of the new cycloid arc (*Marshall and Kattenhorn,* 2005; *Groenleer and Kattenhorn,* 2008). In this way, cycloid cusps form identically to features called tailcracks that develop at the tips of strike-slip faults on Earth and elsewhere throughout the solar system, including Europa (see section 2.3.3). The tailcrack then continues to grow in tension to form a new cycloid arc, driven by the diurnal stresses. Ongoing shearing near cycloid cusps has also been suggested to be the cause of multiple tailcrack-like splays of fractures emanating from cusp regions, producing complex cusps (*Marshall and Kattenhorn,* 2005) that resemble horsetail fracture splays along terrestrial strike-slip faults.

2.1.3. Dilational bands. Also referred to as *pull-apart bands* (see chapter by Prockter and Patterson), dilational bands represent clear evidence of prolonged dilation in the icy shell and hence a resurfacing process on the icy moon. A dilational band is a tabular zone of new crustal material that intruded between the progressively dilating walls of a tension fracture (Fig. 6a). The surface of this material ap-

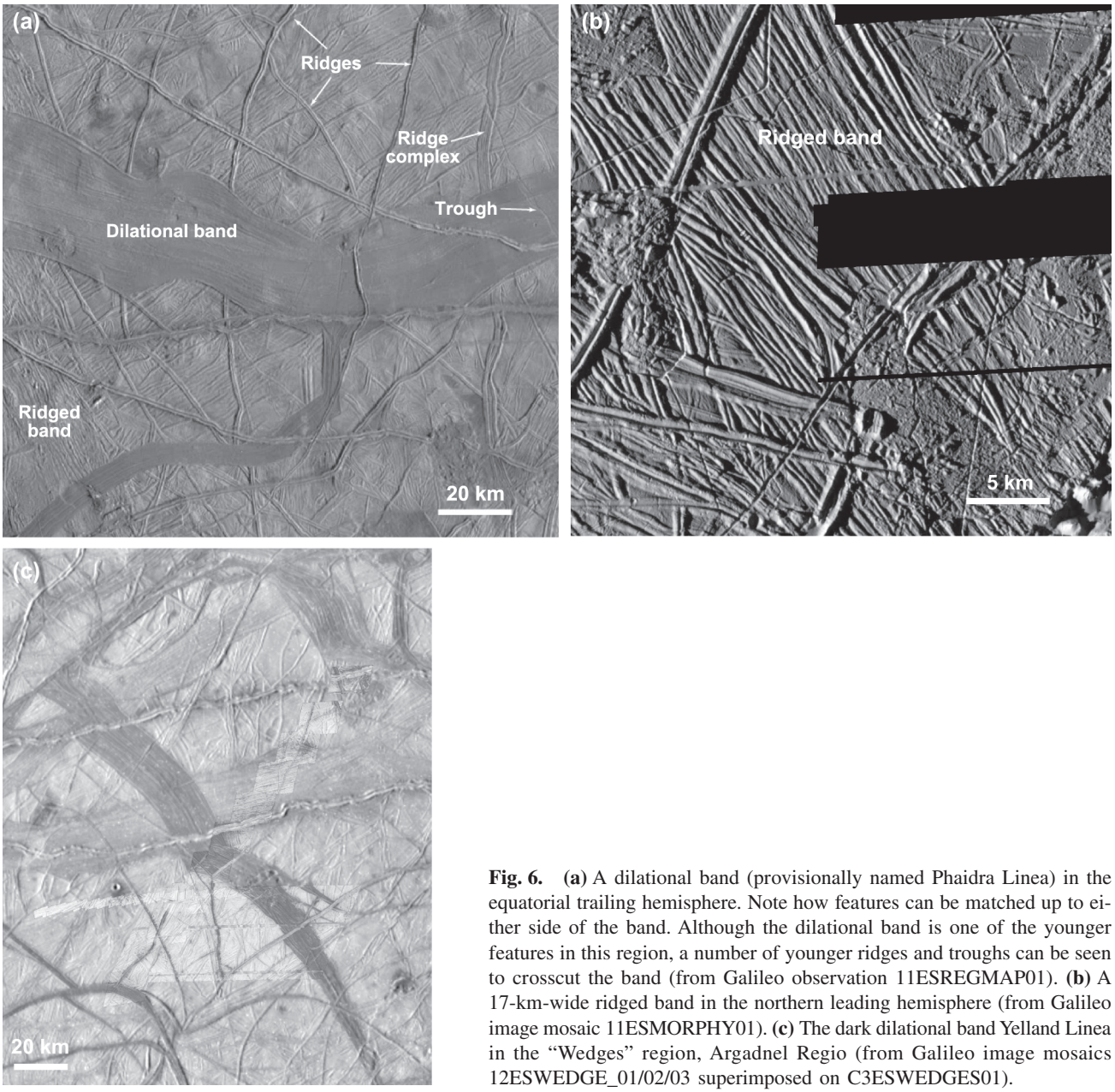

Fig. 6. **(a)** A dilational band (provisionally named Phaidra Linea) in the equatorial trailing hemisphere. Note how features can be matched up to either side of the band. Although the dilational band is one of the younger features in this region, a number of younger ridges and troughs can be seen to crosscut the band (from Galileo observation 11ESREGMAP01). **(b)** A 17-km-wide ridged band in the northern leading hemisphere (from Galileo image mosaic 11ESMORPHY01). **(c)** The dark dilational band Yelland Linea in the "Wedges" region, Argadnel Regio (from Galileo image mosaics 12ESWEDGE_01/02/03 superimposed on C3ESWEDGES01).

pears featureless in lower-resolution images, in which case the term *smooth band* can be used as a descriptor; however, if an internal geometry of fine lineations is observable (usually at medium to high resolution, as in Fig. 6a), the term *lineated band* may be used. Complete separation and infill of the surface is evidenced by the fact that the ridged plains to either side of a dilational band typically match up, implying that the dilational band material represents new surface area (*Schenk and McKinnon,* 1989*; Sullivan et al.,* 1998). The exact source of the dilational band material is unclear. Some have suggested that the dilation occurred across cracks that fully penetrated the icy shell, with the smooth material representing frozen portions of an exposed, underlying ocean (*Tufts et al.,* 2000). Alternatively, dilational bands may represent regions where the brittle portion of the icy shell dilated slowly enough that ductile ice underwent buoyant upwelling from deeper portions of the icy shell to fill in the dilational gap (*Pappalardo and Sullivan,* 1996; *Sullivan et al.,* 1998; *Prockter et al.,* 1999, 2002). The low albedo of most young dilational band material has been suggested to represent the effects of magnetospheric particle bombardment of endogenic sulfur-bearing compounds (*Kargel,* 1991; *Noll et al.,* 1995); however, continued exposure at the surface ultimately results in a brightening of the dilational band such that the oldest dilational bands have a similar albedo to the surrounding ridged plains (*Pappalardo and Sullivan,* 1996; *Geissler et al.,* 1998a; *Prockter et al.,* 1999, 2002), which historically resulted in use of the descriptor *bright bands*. Although tectonic plates (in the terrestrial sense) do not exist in the icy shell (see section 3), dilational bands represent a spreading phenomenon analogous to mid-ocean ridge spreading centers, mak-

ing europan dilational bands the only other known feature in the solar system where complete lithospheric separation has occurred. Similar to mid-ocean ridges, dilational bands stand higher than the surrounding plains by up to 200 m (*Prockter et al.,* 1999, 2002; *Nimmo et al.,* 2003) and may have a relatively reduced elastic thickness (in the range of a few hundred meters to a few kilometers) (*Prockter et al.,* 2002; *Billings and Kattenhorn,* 2005; *Stempel et al.,* 2005). Opening vectors across dilational bands indicate that both orthogonal and oblique dilations are common.

Similar to ridges, dilational bands can be hundreds of kilometers in length, implying a regional process responsible for the recorded period of spreading. Dilational band widths generally do not exceed ~30 km and are commonly only a few kilometers, suggesting that the process responsible for driving the dilation is unable to sustain spreading beyond a certain time and/or width limit. Nonetheless, a dilational band formation event likely represents a prolonged period of uninterrupted tectonic extension. Discrete episodes of dilation are evidenced by an internal fabric of fine lineaments within lineated bands (Fig. 6a) that commonly form a bilateral symmetry about a central axis and exhibit a consistent spacing on the order of ~500 m (*Sullivan et al.,* 1998; *Prockter et al.,* 1999, 2002; *Stempel et al.,* 2005). If these lineaments are normal faults, creating a type of lineated band called a *faulted band*, they may perhaps form a graben-like system centered about the middle of the dilational band (see section 2.1.5), with older faults being translated successively further away from the actively spreading central axis over time. At slow spreading rates, the faulted surface of the dilational band may become rugged, with tilted fault blocks creating repeating valleys and ramparts (*Prockter et al.,* 2002; *Stempel et al.,* 2005).

Some dilational bands have been noted to exhibit a maximum dilation near the center of the length of the band, with dilation decreasing toward either tip, such as Thynia Linea (*Pappalardo and Sullivan,* 1996) and Yelland Linea (Fig. 6c) (*Stempel et al.,* 2005). Such dilational bands resemble typical cracks in an elastic layer that are dilated by a regional tensile stress acting perpendicular to the feature. Nonetheless, some dilational bands are more rhomboidal where they occur in extensional stepover zones (i.e., pull-aparts) along strike-slip faults (see section 2.3.3) such as Astypalaea Linea in the southern antijovian region (*Tufts et al.,* 1999, 2000; *Kattenhorn,* 2004a) and wedge-shaped bands in Argadnel Regio (*Schulson,* 2002; *Kattenhorn and Marshall,* 2006), implying a localized tectonic phenomenon.

Although it is possible that the driving stress responsible for a dilational band also created the original crack across which dilation ensued, some dilational bands show evidence of raised flanks that appear to be the two halves of an erstwhile ridge. Hence, some dilational bands dilated preexisting cracks that had already developed ridges along their rims. Considering that ridge formation is not instantaneous but may take tens of thousands of years and involve a range of mechanisms (dilational, contractional, and shearing), the process responsible for dilational band formation is unlikely to be a natural endmember of the ridge formation process. Ridges simply provide weakness zones within the icy shell that may be utilized when the conditions conducive to dilational band formation occur. The actual spreading across dilational bands may be driven by underlying convection in a region of locally high heat flow (*Prockter et al.,* 2002), perhaps originally initiated by the cracking of the icy shell (cf. *Han and Showman,* 2008). This upwelling may explain why portions of ridged plains immediately adjacent to some dilational bands are also slightly elevated relative to the surroundings (*Nimmo et al.,* 2003). Comparisons to terrestrial midocean-ridge spreading models suggest strain rates in the range 10^{-15}–10^{-12} s^{-1} at europan dilational bands (*Nimmo,* 2004a,b; *Stempel et al.,* 2005), implying spreading rates of 0.2–40 mm yr^{-1}, similar to terrestrial mid-ocean ridge spreading rates. *Nimmo* (2004b) estimates a maximum duration of 10 m.y. for dilational band formation, with the observed narrow rift geometry of dilational bands implying a high strain rate or a relatively thick shell (but probably <15 km) at the time of dilational band formation. *Stempel et al.* (2005) estimate the duration of spreading to be in the range 0.1–30 m.y. (with lower estimates representing lower coefficients of friction of the ice), which is well within the limits of surface ages deduced from the cratering record (*Zahnle et al.,* 2003; see chapter by Bierhaus et al.). Nonetheless, the great number and different ages of dilational bands and other tectonic features on Europa suggest that dilational band activity is likely to be at the lower end of this duration estimate. This deduction is also supported by the requirement for self-similar stress conditions during the development of dilational bands that exhibit a uniform lineated texture, although some dilational bands may record a more complicated dilational/stress history. The needed stresses to drive spreading are on the order of a few megapascals (*Stempel et al.,* 2005), which are likely provided by nonsynchronous rotation (see section 4.1.6). Considering that nonsynchronous rotation would result in a gradually changing stress field in any area of dilational band formation, the duration of band formation must be less than the time it would take for nonsynchronous rotation to move the developing dilational band into a new stress state.

Some cycloidal cracks also show evidence of having dilated to form cycloidal dilational bands (*Marshall and Kattenhorn,* 2005), including Thynia Linea (*Pappalardo and Sullivan,* 1996; *Tufts et al.,* 2000), wedge-shaped bands in Argadnel Regio (*Prockter et al.,* 2002), and the prominent example of the "Sickle" (provisionally named Phaidra Linea) in the equatorial trailing hemisphere (*Tufts et al.,* 2000; *Prockter et al.,* 2002) (Fig. 6a). In these examples, the opening vector across each dilational band is constant, resulting in portions of the band having undergone oblique dilation relative to the margins.

An apparent type of lineated dilational band morphologically similar to a faulted band, but composed of ridges, is a tabular spreading zone referred to here as a *ridged band* (cf. *Figueredo and Greeley,* 2000, 2004) (Fig. 6b). *Stempel et al.* (2005) used this same terminology to refer to faulted

bands; however, we abandon that use of the nomenclature because ridges (which have an explicit meaning on Europa) are not the dominant feature in faulted bands. In low-resolution imagery, ridged bands may be mistaken for smooth bands if the internal lineated texture is not observable; however, ridged bands are essentially up to 60-km-wide complexes of multiple adjacent ridges and furrows (i.e., essentially dilational bands composed of ridges). Ridged bands appear to be analogous to the "Class 2 ridges" of *Greenberg et al.* (1998) and *Tufts et al.* (2000) and have also been classified as "complex ridges" (*Kattenhorn,* 2002; *Spaun et al.,* 2003). This latter terminology causes confusion and should be avoided in light of previous usages and to avoid confusion with the definition of a ridge complex as a zone of multiple superposed and interweaving ridges (see section 2.1.1). Ridged bands also represent zones of spreading in the icy shell but the infill process differs from smooth bands and faulted bands, although hybrid features may exist that take on the appearance of both smooth bands and ridged bands (*Tufts et al.,* 2000). Instead of upwelling of ductile material from below, ridged bands may represent a different form of spreading. One model invokes injection of material from below into discrete fractures, analogous to a terrestrial dike swarm. At the surface, each of these cracks may then take on the form of a ridge through some ridge-forming mechanism (see section 2.1.1). Like a dike swarm, there is no necessity for symmetry about a central crack, as the sequence of intrusion through vertical dike-like features may be somewhat random across the spreading zone (*Tufts et al.,* 2000). Nonetheless, bilateral symmetry is possible (e.g., *Kattenhorn,* 2002).

2.1.4. Troughs. Considering the lack of raised edifices along the crack margins, as typifies ridges, troughs are easily overlooked in images of the surface. They likely represent tension fractures in the ice shell that never developed into a more evolved landform, such as a ridge, and have been referred to simply as *cracks*. They have been acknowledged (*Figueredo and Greeley,* 2000, 2004; *Kadel et al.,* 2000; *Prockter et al.,* 2000; *Kattenhorn,* 2002) but have received little attention, despite being relatively common in high-resolution images of the surface. The majority of the tectonic features on Europa likely owe their beginnings to tension fracturing at the surface of the icy shell, starting as troughs.

Confining stress considerations dictate that most fractures are likely tension fractures that are initiated at the surface and then propagate downward. Whether or not the fractures completely penetrate the icy shell is dependent on the availability of stresses to overcome the overburden, which becomes increasingly difficult for thicker icy shells. Diurnal tidal stresses (see section 4.1.5) are rapidly overwhelmed by the overburden in the icy shell, which, for an ice density of 0.91 g/cm^3, increases at a rate of about 1.2 MPa/km. *Hoppa et al.* (1999a) suggest that fracture depths should thus not exceed ~65 m; however, consideration of crack-tip stresses increase this depth to a few hundred meters (*Lee et al.,* 2005; *Qin et al.,* 2007) and perhaps up to several kilometers when ice porosity effects are considered, allowing complete penetration of the icy shells if its thickness does not exceed 3 km. The addition of stress due to nonsynchronous rotation (see section 4.1.6) allows penetration depths of several kilometers (*Panning et al.,* 2006) to approaching 10 km (*Golombek and Banerdt,* 1990; *Leith and McKinnon,* 1996), perhaps allowing complete penetration of an icy shell in the thickness range 6–13 km for a plausible range of ice porosity (*Lee et al.,* 2005). If there has been more than 10 km of thickening of the icy shell through time (see section 4.1.8), sufficient stress may have been produced at the base of the icy shell to initiate cracking and permit complete penetration through the shell (*Manga and Wang,* 2007), with upward propagation aided by fluid pressure (cf. *Crawford and Stevenson,* 1988), in which case it would not be unreasonable to assume that tension fractures provide potential connection pathways between the surface and an underlying ocean. Nonetheless, viscoelastic relaxation in the lower part of the icy shell over the shell thickening timescale likely limits complete penetration by tension fractures to icy shells ≤2.5 km thick (*Rudolph and Manga,* 2009).

Troughs constitute the youngest tectonic features on Europa based on crosscutting relationships. Hence, they provide the most promising indicator of recent to current tectonic activity (see section 5.3). *Kattenhorn* (2002) showed that troughs make up a significant portion (the youngest 20%) of the tectonic history of the Bright Plains region. Although the surface geological history appears to record a transition from principally tectonic to predominantly cryomagmatic activity, with associated formation of regions of chaos and lenticulae (see section 5.2 and chapter by Doggett et al.), troughs have been noted to cross regions of chaos and thus may be very recent features.

Troughs vary greatly in geometry, scale, orientation, and location, reflecting differences in causal mechanisms driving fracturing (e.g., *Figueredo and Greeley,* 2004). A classification scheme for troughs is suggested here to address these differences (Fig. 7): (1) *Tectonic fractures* range in length from <10 km to hundreds of kilometers (Fig. 7a). They are presumably the result of global tidal stresses plus any other global, regional, or local contributing stress components that may drive global tectonics (see section 4). They exhibit a range of orientations and are characterized by linear or broadly curving geometries. They are sometimes segmented along their lengths or may show evidence of having formed by the coalescence of numerous segments, analogous to terrestrial joints. (2) *Cycloidal fractures* (Figs. 4b and 7b) are also tectonic fractures but are specifically the ridgeless progenitors to cycloidal ridges. They are distinct in their curved and cuspate nature, probably reflecting the dominant control of the diurnal stress field in their formation. Although cycloidal ridges are more common, relatively younger cycloidal fractures have also been identified (e.g., *Marshall and Kattenhorn,* 2005), indicating that cycloid development has persisted until at least geologically recent times. (3) *Tailcracks* emanate from the tips of strike-slip faults (Fig. 7b) and represent brittle accommodation of fault motion in the

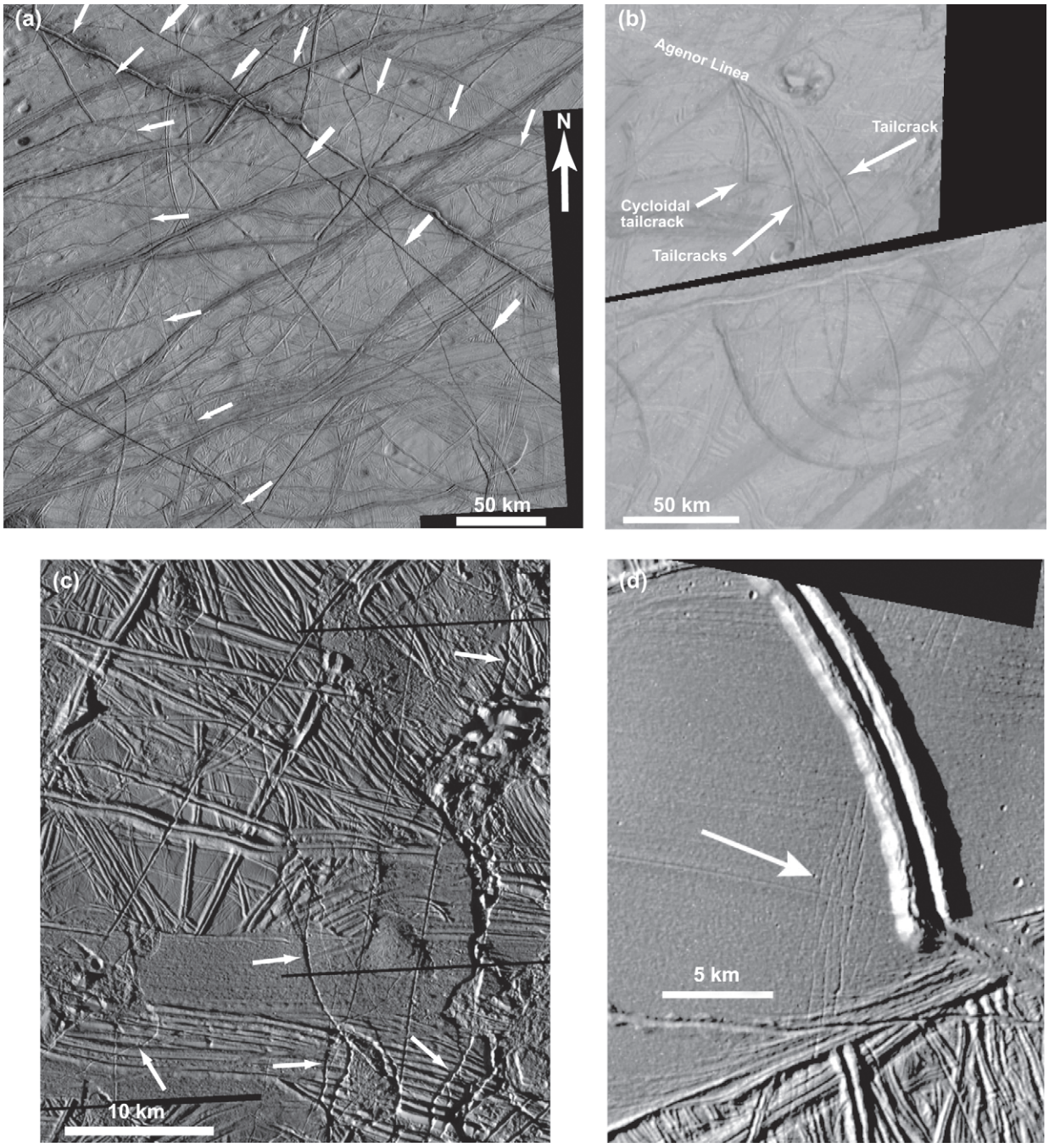

Fig. 7. Troughs (indicated by white arrows). **(a)** *Tectonic fractures* refer to any generic troughs induced by global deformation of the icy shell, such as due to tidal forcing (from Galileo mosaic 15ESREGMAP01). **(b)** *Tailcracks* form at the tip of a strike-slip fault (in this case, Agenor Linea) where localized tension is induced by fault motion. One tailcrack here is also a *cycloidal fracture* (see Fig. 4). From Galileo images 466664413 and 466665378, E17 orbit. **(c)** *Endogenic fractures* may be irregular and typically form adjacent to chaos, as occurs here in Galileo image mosaic 11ESMORPHY01. **(d)** *Fold hinge fractures* are caused by tension along anticlinal fold hinges. This example is within Astypalaea Linea, from Galileo image 466670113, E17 orbit. A fifth fracture type is a *flexure fracture* as occurs to either side of Androgeos Linea (see Fig. 2b) in response to elastic bending of the icy shell.

tensile quadrant of a fault tip (*Schulson,* 2002; *Kattenhorn,* 2004a; *Kattenhorn and Marshall,* 2006). Also referred to as horsetail splays or wing cracks in terrestrial analogs, they have been recognized in many locations on Europa such as the impressive example at the southeast end of Agenor Linea (*Prockter et al.,* 2000; *Kattenhorn,* 2004a). Tailcracks form in response to the locally perturbed stress field at the tip of a fault and thus do not provide a direct indicator of the global stress field at the time of their formation, except where the tailcracks extend far enough from the fault tip that their orientations are controlled by regional stresses. (4) *Endogenic fractures* are most commonly associated with

regions of chaos (Fig. 7c) and thus reflect a local process likely driven by thermal upwelling or diapirism in a convecting icy shell, which in turn disrupts the brittle carapace (*Collins et al.,* 2000; *Figueredo and Greeley,* 2004; *Schenk and Pappalardo,* 2004; *Mitri and Showman,* 2008). These fractures may also be associated with broad scale warping at the surface of the icy shell (e.g., Fig. 3b in *Prockter and Pappalardo,* 2000), which is also likely driven by an endogenic process. Thus, the orientations of endogenic fractures are not controlled by a global stress field. (5) *Flexure fractures* occur along the flanks of many large ridges (e.g., Fig. 2b) that have caused elastic flexing of the adjacent icy shell, probably due to the loading caused by their weight (*Tufts et al.,* 2000; *Hurford et al.,* 2005) and/or by withdrawal of material from beneath the ridge flanks (*Head et al.,* 1999). Flexing of the elastic portion of the icy shell alongside a ridge induces bending stresses that can exceed the tensile strength of the ice, at which point one or more fractures develops (*Billings and Kattenhorn,* 2005). (6) *Fold hinge fractures* (Fig. 7d) form in response to tensile bending stresses along the hinge lines of surface anticlines (see section 2.2.1), although such features appear to be relatively rare (*Prockter and Pappalardo,* 2000).

2.1.5. Normal faults. Although tensile fracturing is dominant, some of the extension of the icy shell occurred by normal faulting, evidenced by fault scarps that show a component of vertical motion. Tensile stresses are common in the shell (see section 4.1); however, normal faulting does not occur under conditions of absolute tension, only deviatoric tension. Normal faulting is possible when the minimum horizontal compressive stress is less than the overburden compressive stress by a sufficient amount to overcome the internal friction (*Beeman et al.,* 1988; *Pappalardo and Davis,* 2007). Compressive stresses are common in the icy shell during the tidal cycle, therefore adequate conditions for extensional shear failure are likely to be common.

The great majority of normal faults are inferred to constitute the fine striations within lineated bands (see section 2.1.3) that parallel the band boundaries, contributing to the similarity between dilational bands and terrestrial mid-ocean ridge spreading centers. Rare normal faults with significant vertical displacements (~300 m) have also been noted to crosscut ridged plains (*Nimmo and Schenk,* 2006), and it is possible that up to 1.5-km-deep troughs in the icy shell that define antipodal small-circle depressions in the leading and trailing hemispheres are also normal fault related (*Schenk et al.,* 2008). In lineated bands, bilateral symmetry about a central trough is reminiscent of repeating pairs of inward-dipping, graben-bounding faults that move progressively outward from the spreading axis with time. In high-resolution images (less than a few tens of meters per pixel), the striations in the lineated bands are clearly normal faults, showing smooth and highly reflective fault planes bounding rotated blocks of band material with low-albedo tilted upper surfaces. Mechanical interactions are evident in fault trace patterns, as well as relay ramps in overlap zones, analogous to terrestrial normal fault systems (*Kattenhorn,* 2002). Normal faults in lineated bands do not necessarily dip inward towards an axial trough but may dip consistently in one direction across the entire width of a band or be restricted to certain parts of the band only (*Kattenhorn,* 2002; *Prockter et al.,* 2002). This pattern of faulting is distinctly different to mid-ocean ridge rift zones and may imply that some dilational bands were extended by normal faulting at some time after initial band formation, perhaps due to the reduced brittle thickness of the dilational band relative to the surrounding ridged plains, causing the bands to act as necking instabilities that focused extension. It is unclear, however, why some dilational bands localize normal faulting (forming faulted bands) rather than localizing tension fractures (in which case, ridged bands may ultimately develop).

2.2. Compressive Tectonics

An apparent consequence of the great amount of extension on Europa is the need for corresponding contraction to provide a balanced surface area budget. Although Europa has likely undergone some amount of expansion due to cooling and thickening of the icy shell, the maximum likely extensional strain after even 100 m.y. of cooling would be ~0.35% (*Nimmo,* 2004a), which is insufficient to account for the amount of new surface area created at spreading bands, which occupy ~5% of the surface area in the pole-to-pole regional maps of the leading and trailing hemispheres (*Figueredo and Greeley,* 2004). Hence, some amount of contraction must have occurred during the visible tectonic history in order to create a balanced surface area budget. Given this need, contractional features might be expected to be as common on the surface as extensional features. In actuality, contractional deformation on Europa is visibly sparse and by no means obvious. *Greenberg et al.* (1999) contemplated whether much of the contraction may have been accommodated within areas of chaos terrain, which covers ~10% of the surface; however, no ultimate geological evidence arose to imply that chaos represents sites of contraction.

Part of the reason for an apparent lack of contractional features may be a historical emphasis on the many forms of extensional structures such as ridges and dilational bands, which are morphologically dominant; however, a potentially greater hindrance to the identification of contraction has been a failure to clearly recognize the manifestation of such deformation. In terrestrial settings, contraction may be accommodated variably over a range of scales. At the outcrop scale, small amounts of contraction may occur along deformation bands (tabular zones of cataclasis and porosity reduction in granular rocks) or along pressure-solution surfaces (sometimes called anticracks, where part of the rock is removed in solution resulting in a volume loss). At the regional scale, contraction is accommodated in brittle materials through the development of thrust faults (with associated mountain building) or elastic warping, and in ductile materials through folding. At the planetary scale, broad-

scale convergence occurs at subduction zones to accommodate the creation of new oceanic lithosphere at spreading ridges. Hence, any contraction on Europa is likely manifested through one or more of these mechanisms. There is no evidence for global plate tectonics on Europa (see section 3) and thus no removal of surface area along subduction zones; however, all other forms of contraction described above may be viable on Europa.

2.2.1. Folding. The first documented evidence for contraction on Europa was the identification of several parallel folds within a dilational band associated with the right-lateral strike-slip fault Astypalaea Linea (*Prockter and Pappalardo,* 2000). The folds are visible due to subtle differences in surface brightness and have a wavelength of ~25 km and crest-to-trough amplitudes of 250 ± 50 m (*Dombard and McKinnon,* 2006). In adjacent ridged terrain, the folds gradually disappear or are not resolvable, suggesting that dilational band material is more easily folded, perhaps due to a localized high heat flow (*Prockter,* 2001). Other telltale clues for the presence of the folds include clusters of bending-induced tensile cracks along the hinge lines of anticlines and compressive crenulations along the hinge lines of synclines (Fig. 7d). The high heat flow in a dilating band (see section 2.1.3) relative to adjacent ridged terrain, combined with a reduced ice thickness (*Billings and Kattenhorn,* 2005), causes dilational bands to become localized zones of crustal weakness that may be able accommodate contraction by folding. *Prockter and Pappalardo* (2000) suggest that sufficient compressive stress may accumulate to drive folding over <40° of nonsynchronous rotation of the icy shell, and also suggest that fold axis orientations are consistent with predicted stress fields. In contrast, *Mével and Mercier* (2002) suggest that late transpressive motion along Astypalaea Linea may have caused the localized folding. Over time, folds may relax away due to ductile flow of deeper, warm ice; however, *Dombard and McKinnon* (2006) suggest that such relaxation would occur so slowly relative to the age of Europa's surface (e.g., as little as 4% relaxation over 100 m.y.) that all folds that formed during the geologically visible past should still be apparent. Hence, the distinct scarcity of visible folding on Europa suggests that it is not a significant accommodator of crustal contraction and/or is difficult to recognize in existing images, and is certainly insufficient to balance out the amount of extension.

2.2.2. Convergence bands. A second candidate feature for localized contraction, first identified by *Sarid et al.* (2002), is a convergence band, across which a tectonic reconstruction reveals a zone of "missing" crust. These bands superficially resemble dilational bands caused by plate spreading in that they form broad zones that may be many kilometers wide and perhaps tens of kilometers long, and appear to disrupt the surrounding ridged terrain (*Greenberg,* 2004) (Fig. 8). They differ from dilational bands, however, in that their edges may be nonlinear or even inosculating, and one edge of the band is not necessarily a mirror image of the other side, unlike dilational bands that form by icy shell separation and spreading. Convergence bands are among the least-studied features on Europa; therefore, much work is still needed to fully characterize their broad-scale geometries, internal morphologies, and mechanical evolution. Nonetheless, existing studies imply two varieties of convergence bands: (1) those driven by motion along strike-slip faults, with resultant convergence adjacent to the fault in the tip-region compressional quadrants; and (2) those that develop along zones of preexisting weakness in the icy shell, such as dilational bands and dilational strike-slip faults.

Sarid et al. (2002) describe two sites in the trailing hemisphere where convergence is driven by motions along adjacent strike-slip faults (type 1 above). One example in the southern trailing hemisphere (in the Galileo regional image mosaic 17ESREGMAP01), between Argadnel Regio and Castalia Macula (Fig. 8a), is suggested to be a zone of convergence related to right-lateral motion along an approximately north-south-oriented strike-slip fault north of the zone of convergence. *Patterson et al.* (2006) describe evidence of dilational band development in the same vicinity. We infer that both processes may have occurred here at different times (early convergence with later dilation). Strike-slip fault driven convergence is suggested to have occurred in the marginal blocks alongside Astypalaea Linea (*Mével and Mercier,* 2002), resulting in up to 55% contraction along numerous distributed ridge-like crenulations (perhaps a related contractional mechanism to convergence bands). Evidence for strike-slip fault-related convergence bands is also presented by *Kattenhorn and Marshall* (2006), who characterize compressive stress concentrations in the tip regions of strike-slip faults in Argadnel Regio (see section 2.3.3).

Convergence bands that localize along sites of crustal weakness such as preexisting dilational bands (type 2 above) may also be driven by nearby strike-slip fault motions. This phenomenon appears to have occurred in the northern trailing hemisphere (Fig. 8b) example described by *Sarid et al.* (2002), although they did not recognize it as such. Several major strike-slip faults on Europa dilated during their development to become band-like (see section 2.3.3) and may have subsequently acted as loci for a component of convergence if conditions changed from transtensional to transpressional. Candidate site examples include the bright bands Corick Linea, Katreus Linea, and Agenor Linea (see chapter by Prockter and Patterson). Agenor Linea was interpreted by *Prockter et al.* (2000) to contain contractional features related to shear-related duplexing, suggesting transpression. *Greenberg* (2004) inferred 20 km of convergence across Corick Linea in order to match up offset features, resulting in the formation of a 5-km-wide convergence band, implying 75% shortening.

It is unclear how inferred contraction is physically accommodated within a convergence band. *Sarid et al.* (2002) describe an internal fabric of numerous subtle parallel striations. Conceivably, these could be the traces of thrust faults. In the 15ESREGMAP01 example (Fig. 8b), 8 km of convergence is accommodated within a band that is only 2.7 km wide, indicating 66% shortening. Even with a perhaps un-

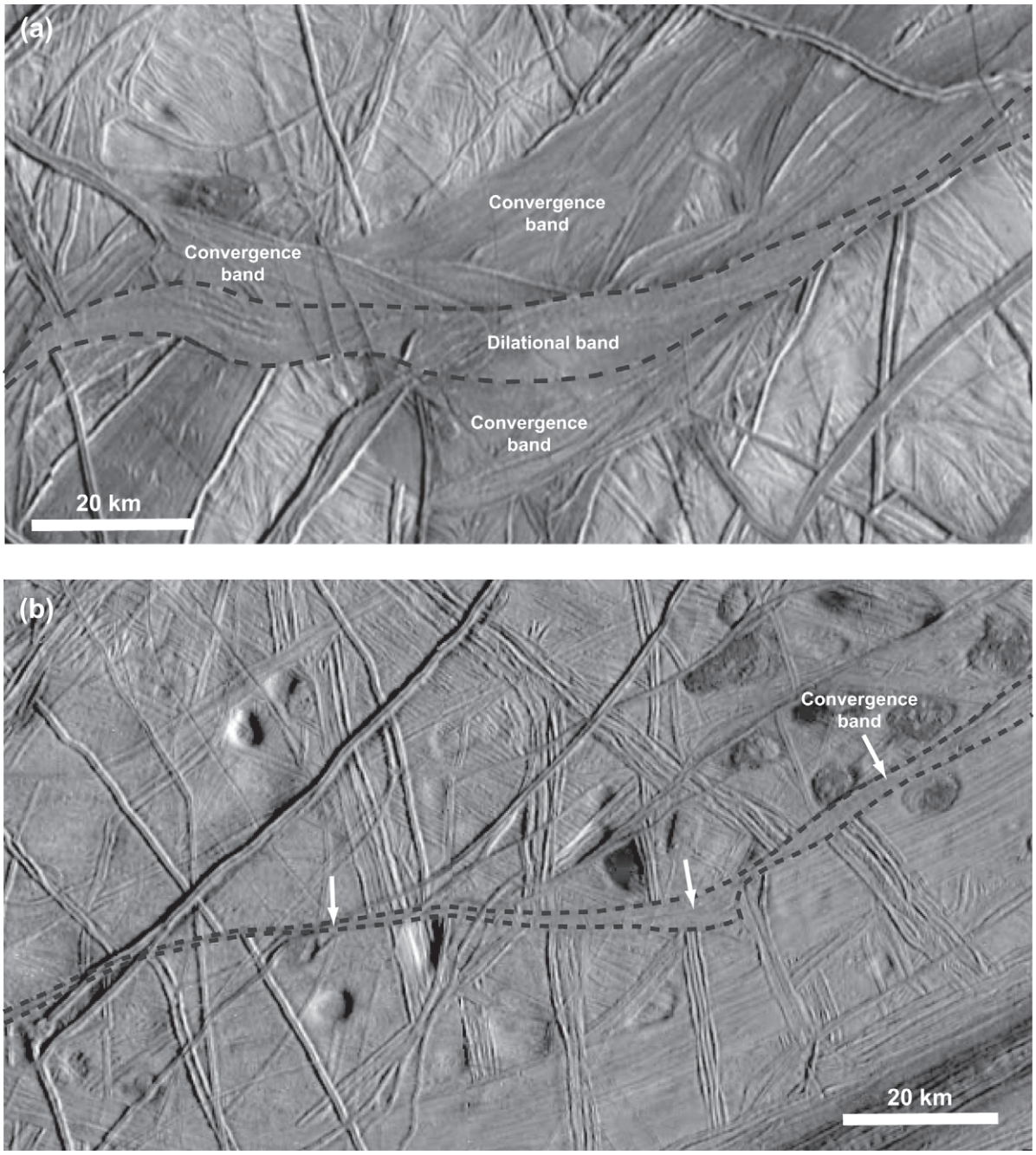

Fig. 8. Two sites of potential contraction in the icy shell, manifested as convergence bands. **(a)** Possible convergence bands where ~15 km of convergence may have occurred in the equatorial trailing hemisphere, near Castalia Macula. The inferred convergence bands resemble dilational bands but have irregular margins and do not have matching geology to either side of the band. This particular example is superimposed with a later dilational band that passes across the center of the convergence band (*Patterson et al.,* 2006). From Galileo mosaic 17ESREGMAP01. **(b)** An irregular convergence band (white arrowed zone between dashed lines) where ~8 km of crust appears to be missing, resulting in mismatches of older, crosscut features (from Galileo mosaic 15ESREGMAP01).

realistically small fault spacing of 100 m, each fault would need to accommodate 300 m of horizontal shortening, resulting in 170–300 m of vertical relief across each fault (depending on the fault dip, assumed to be in the range 30°–45°). These numbers would increase as the fault spacing increases. The convergence bands do not appear to display such rugged relief, perhaps casting doubt on thrust faulting as a mechanism for contraction. A related complicating factor is the relatively large amount of differential stress (up to 10 MPa by a depth of 3 km) required for thrust faults to develop on Europa (*Pappalardo and Davis,* 2007), which would hinder thrust fault development in the icy shell except at very shallow depths (perhaps less than a few hundred meters) due to the typical magnitudes of tidal stresses

(unless some other source of compressive stress exists). Other possible contractional mechanisms include actual volume loss within convergence bands due to remobilization of warm ice toward deeper portions of the icy shell, or compaction through porosity reduction (e.g., *Aydin,* 2006).

The documented large values of contraction at convergence bands should make them easy to identify through disruption of the continuity of the ridged plains, except perhaps where convergence occurs within preexisting dilational bands and the convergence is less than the original dilation. Convergence band-like features might be common in Europa images but may have been previously misidentified as dilational bands; therefore, they are potentially important tectonic features for balancing Europa's surface area budget. Additional work will be needed to test this hypothesis.

2.2.3. Contraction across ridges. A third possibility for sites of convergence on Europa is the ubiquitous double ridges that dominate the tectonic fabric of the icy shell, first suggested by *Sullivan et al.* (1997). The origin of ridges is an equivocal source of great dispute (see section 2.1.1). Some ridges show evidence for lateral offsets along them but the majority of ridges do not. Nonetheless, recent models (*Nimmo and Gaidos,* 2002) hypothesize that ridge formation may be driven by lateral shearing and frictional heating along cracks. An analysis of ridges containing relatively offset features (i.e., where relatively older lineaments have undergone apparent lateral displacements along a ridge) reveals that the offsets cannot be related to lateral shearing alone (*Patterson and Pappalardo,* 2002; *McBee et al.,* 2003; *Vetter,* 2005; *Patterson et al.,* 2006; *Bader and Kattenhorn,* 2007; *Kattenhorn et al.,* 2007). Although pure dilation across any lineament (e.g., a dilational band) cannot produce lateral offsets of features split apart by the dilation, convergence across a lineament will result in the production of apparent lateral offsets of all nonorthogonal crosscut features along the lineament that have nothing to do with lateral shearing.

Aydin (2006) identified ridge-like contraction lineaments, which he referred to as compaction bands or compactive shear bands in the case where lateral shearing also occurred. As used by *Aydin* (2006), the word "band" has no association or morphological resemblance to either dilational bands or convergence bands described earlier, but rather originates from terrestrial analogs called deformation bands, across which compaction can occur through the comminution of granular materials. We therefore avoid use of "compaction band" to describe these features, which morphologically resemble ridges. The amount of apparent lateral offset along a ridge is controlled by the amount of convergence as well as the relative angle α measured clockwise from the ridge toward any offset feature (Fig. 9). It is possible to differentiate between apparent offsets caused by convergence and those caused by true lateral shearing by examining the distribution of normalized *separation* as a function of α, where separation is the orthogonal distance between a linear feature on one side of a ridge and the projection of that same feature on the other side of the ridge (i.e., the conventional structural geologic definition of separation). Separation is uniquely related to α and the amount of convergence relative to the amount of true lateral shear motion (*Vetter,* 2005; *Bader and Kattenhorn,* 2008).

Apparent lateral offsets along ridges related to convergent motions raise the possibility that ridge development may, in some cases, be partially driven by contraction across sheared lineaments. Such a notion is congruent with the *Nimmo and Gaidos* (2002) frictional shear heating model for ridge development. Such heating may result in a more mobile wedge of ice alongside a shearing lineament, causing a localized zone of weakness in the icy shell where contraction may be accommodated. In this model, part of the loss of volume along the sheared lineament occurs by remobilization of warm ductile ice into the deeper parts of the shell or by localized melting and downward draining within the frictionally heated zone. Part of the near-surface convergence, however, is manifested through the construction of ridge edifices along the crack. The ridges could result from buoyant upwelling above the frictionally heated zone, buckling, or porosity reduction in near-surface ices, assuming an initially high enough porosity to allow volumetric compaction. Thus, the possibility exists that this is a plausible mechanism for ridge development, particularly because it is likely that all active lineaments on Europa are subject to shearing and thus heating during the europan day in response to the constantly rotating diurnal tidal stresses (see section 2.3.4). Those ridges that have been shown to exhibit a component of contraction across them invariably show a larger amount of strike-slip motion accompanying the contraction (*Vetter,* 2005), providing a strong argument that the contraction is related to the process of shearing. The implication of this mechanism for ridge development is that the majority of the elusive contraction in Europa's icy shell may, in fact, be accommodated across its most common type of feature (i.e., ridges), with only a minimal amount of convergence needed across any one ridge to allow for a balanced surface area budget. Unfortunately, other than a few prominent ridge examples, this hypothesis has not been convincingly demonstrated, plausibly because apparent offsets along ridges are below existing resolution limits, perhaps due to minimal amounts of convergence and/or lateral offsets. Therefore, any inferences about ridges as important accommodators of convergence remain mostly conceptual for the time being. An added complication is that many sheared ridges have been shown to exhibit evidence of dilation using the same technique (α vs. separation graphs) described above (*Bader and Kattenhorn,* 2008), indicating that ridges may be subject to a combination of dilational, convergent, and shearing motions during their history.

2.3. Lateral Shearing

2.3.1. Shear failure of ice. Lateral shearing refers to strike-slip motions along lineaments. Voyager images indi-

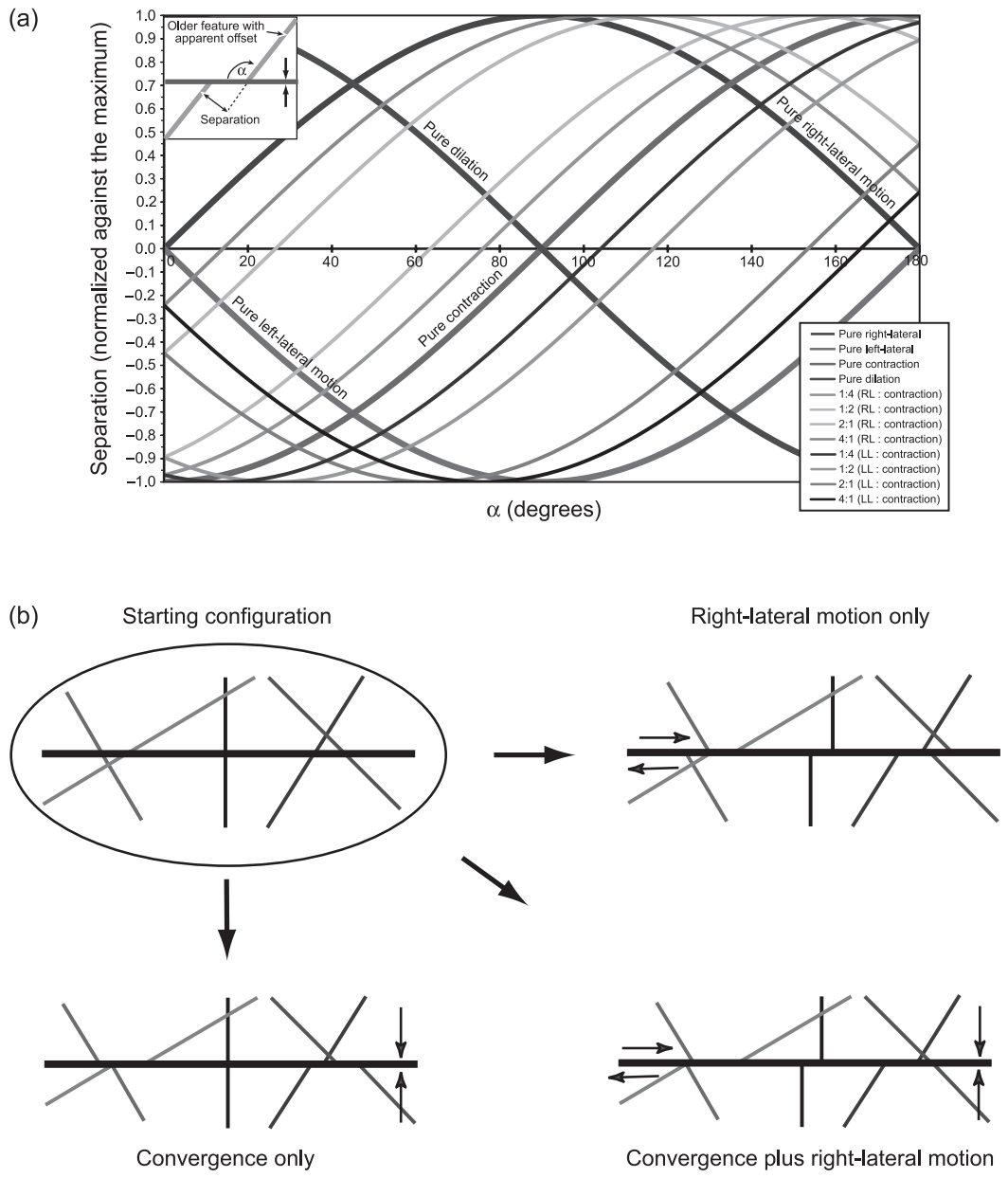

Fig. 9. See Plate 12. **(a)** Analytical curves can be used to differentiate the relative amounts of strike-slip motion (whether right-lateral or left-lateral) and contraction across a ridge/strike-slip fault based on the amount of separation between two halves of an apparently offset feature (inset, upper left). α is the angle measured from the ridge/strike-slip fault to the offset feature in a clockwise sense. A separate set of curves exists for the case of dilation plus strike-slip motion (*Vetter,* 2005). **(b)** Illustration of various configurations of mismatches of crosscut features in response to pure right-lateral motion, convergence only, or a combination (motion is along the thicker black line, representing a ridge or strike-slip fault). If α is 90°, offsets only occur if there is lateral motion. Pure convergence can produce a mixture of left- and right-lateral offsets, depending on α.

cated the presence of lateral offsets in the europan icy shell at scales of tens of kilometers (*Schenk and McKinnon,* 1989). On Earth, such motions may occur for two reasons: (1) through primary shear failure of rock in a stress field where the intermediate compressive principal stress (σ_2) is vertical and the horizontal differential stress ($\sigma_1 - \sigma_3$) exceeds the rock frictional strength; and (2) through reactivation of existing structures (faults and fractures) in response to a temporal change in the stress field relative to when the existing structures first formed. In the first case, approximately vertical strike-slip faults are produced on Earth and include transform plate boundary faults (such as the San Andreas fault) as well as intraplate faults. In the second case, any of the principal stresses could be vertical, resulting in oblique-slip motion in cases where the faults are not vertical.

On Europa, the second of these situations most certainly exists. The stress field changes constantly due to variations

in the tidal figure during each orbit (see section 4.1); therefore, any active lineament on Europa necessarily experiences shear stresses that could induce lateral shearing. If a crack is dilated during shearing (i.e., the normal stress is tensile), there is no frictional constraint on shear motion. For the case of sliding of a closed crack, the limiting factor is the coefficient of friction, μ, based on the Coulomb failure criterion: $\tau = S_0 + \mu\sigma_n$ at failure, where τ is shear stress, σ_n is normal stress, and S_0 is the inherent shear strength (cohesion) in the absence of normal stress.

The value of μ for europan ice is unknown but is almost certainly less than occurs in rocky materials and is commonly approximated on the basis of comparisons to terrestrial observations and laboratory experiments (*Beeman et al.,* 1988; *Rist and Murrell,* 1994; *Rist,* 1997; *Schulson,* 2009). Complications exist in that μ is likely affected by ice chemistry, sliding speed, and temperature, with the friction increasing as temperature decreases. Based on low-temperature (77–115 K) experiments on sawcut pure water ice, *Beeman et al.* (1988) provide perhaps the most appropriate estimate of μ applicable to europan conditions in the upper part of the icy shell, but even so, μ is variable depending on loading conditions. At low confining pressures ($P \leq 5$ MPa; or down to a depth of ~4 km on Europa), $\mu = 0.55$ and the inherent shear strength, $S_0 = 1$ MPa. Where $P \geq 10$ MPa (deeper than ~8 km), $\mu = 0.2$ and the inherent shear strength, $S_0 = 8.3$ MPa. Potential caveats to the laboratory technique include the 2–5 orders-of-magnitude-faster sliding velocities used than may occur on europan faults, which underestimates the friction coefficient (e.g., *Kennedy et al.,* 2000; *Fortt and Schulson,* 2004); a time-dependency to crack strength, increasing with the number of slip events or due to development of fault gouge; the usage of pure water ice; the possibility that frictionally heated ice along a shearing crack may experience a decreased friction coefficient (as has been suggested to occur on Enceladus) (*Smith-Konter and Pappalardo,* 2008); and the assumption of a preexisting fault.

The assumption of a preexisting fault is only problematic in attempting to make predictions about the orientations of primary shear fractures relative to the principal stresses. In laboratory experiments on water ice, this angle is commonly reported to be ~45° (*Durham et al.,* 1983; *Sammonds et al.,* 1989*; Rist and Murrell,* 1994; *Rist et al.,* 1994; *Rist,* 1997). Considering that the angle, θ, between a developing shear fracture and the maximum compressive principal stress, σ_1, is given by $\theta = 0.5 \tan^{-1}(1/\mu)$, an angle of 45° implies $\mu = 0$, which disagrees with deduced values of μ described above. *Schulson et al.* (1999) suggest that the 45° shear fracture angles were an artifact of the loading apparatus. They produced shear fractures in ice where $\theta = 30°$ (i.e., $\mu \approx 0.6$), more congruous with the low confining stress results of *Beeman et al.* (1988). If low sliding velocities (10^{-6}–10^{-7} m s^{-1}) (*Nimmo and Gaidos,* 2002) occur on Europa, μ may actually be in the range 0.6–0.8 (*Kennedy et al.,* 2000), creating shear fractures at $\theta = 25°$–30° to the orientation of σ_1, unless the ice is sufficiently warm (e.g., due to shear heating) that μ is reduced.

2.3.2. Lateral shear failure on Europa. Normal faults have already been shown to be a common form of extensional deformation (see section 2.1.5), therefore lateral shearing would tend to produce oblique-slip motions along them. *Kattenhorn* (2002) describes evidence of *en echelon* breakdown zones at the tips of normal faults within dilational bands, implying oblique motions during fault tip propagation. Nonetheless, vertical fractures predominate on Europa due to tensile failure perpendicular to the horizontal maximum extension direction. As a result, troughs, ridges, and dilational band margins are all likely to be vertical and prone to reactivation through lateral shearing as long as the fractures have not yet healed. Strike-slip motions along these features thus also fall into category 2 faults described in section 2.3.1. Whether or not category 1 strike-slip faults exist on Europa (i.e., due to primary shear failure) is still unclear, especially seeing as they may be impossible to decipher from the myriad other vertical cracks that underwent lateral shearing due to reactivation. Nonetheless, primary shear failure is ultimately dependent on whether or not the stress conditions favor strike-slip fault formation, exactly as it would on Earth. It should also be noted that lateral shearing has been noted in terrestrial ice shelfs (*Wilson,* 1960) and glaciers (e.g., during the rupture of the Denali fault in Alaska in 2002), but typically takes on the form of *en echelon* fracture arrays, with individual fractures oriented obliquely to the trend of the fault zone (*Haeussler et al.,* 2004). Very few analogous *en echelon* crack geometries have been described in europan strike-slip fault zones (e.g., *Prockter et al.,* 2000; *Michalski and Greeley,* 2002), and appear to be more commonplace within shear-reactivated dilational bands, perhaps implying that strike-slip motions typically reactivate existing cracks that initially formed in tension (cf. *Greenberg et al.,* 1998; *Tufts et al.,* 1999). In some instances, shearing across regions of closely spaced tension cracks may result in fragmentation along the developing shear zone (*Aydin,* 2006).

Any evaluation of the formation mechanisms for strike-slip faults on Europa must be placed within the context of the mechanics of shear failure of ice and must incorporate a candid analysis of the pros and cons of shear failure vs. tensile failure interpretations for europan lineaments showing apparent offsets (e.g., *Kattenhorn,* 2004b). For example, *Spaun et al.* (2003) suggest that northeast- and northwest-oriented ridges with strike-slip offsets in the equatorial trailing hemisphere formed as primary shear fractures because they form X-shaped patterns that superficially resemble conjugate shear sets, and because of their locations relative to expected nonsynchronous rotation stresses. Although the X-shapes are reminiscent of conjugate shear fractures, shear offsets are either absent or inconsistent along ridges of a particular orientation and no explicit crosscutting relationships exist, probably implying that the ridges are distinctly different in age. Also, potentially conjugate ridge sets

(i.e., X-shapes for ridges of similar stratigraphic age) show no consistent conjugate angle, 2θ, between them. This would not be expected for true conjugate sets as 2θ is explicitly controlled by the coefficient of friction of the ice, μ (see section 2.3.1), which should be somewhat consistent. Hence, there is currently no convincing geological evidence that primary shear failure of the icy shell, analogous to strike-slip faulting, produced global lineaments. Nonetheless, given that extensional shear failure is likely responsible for normal faults in the icy shell, the possibility that some lineaments formed through strike-slip shear fracturing cannot be dismissed.

2.3.3. Strike-slip fault morphologies. Lateral offsets can potentially occur along all lineament types (i.e., troughs, ridges, cycloids, and dilational and convergent bands), regardless of how they initially formed. Nonetheless, cumulative offsets that are large enough to be resolvable in Galileo images (generally hundreds of meters or more) typically occur along ridges and dilational bands. Accordingly, *Kattenhorn* (2004a) distinguishes two predominant types of strike-slip faults on Europa: ridge-like and band-like, based on their morphologic similarity to ridges and dilational bands (Fig. 10). The mechanical evolution of the two types of strike-slip faults is distinctly different. Ridges likely initiated as troughs (see section 2.1.1); therefore, any lateral shear motions along them probably happened later, potentially contributing to the process of ridge development. In the case of dilational bands (see section 2.1.3), the question arises as to whether strike-slip offsets along them happen prior, during, or after dilation. Strike-slip offsets across dilational bands are evidenced by the need for oblique closing to reconstruct older features affected by the dilation. Sigmoidal lineations within dilational band material may imply oblique dilation (i.e., concurrent dilation and strike-slip motion), as occurs along Astypalaea Linea; however, the timing of strike-slip motions along dilational bands cannot necessarily be determined based on band morphology alone (*Prockter et al.,* 2002).

Kattenhorn (2004a) and *Kattenhorn and Marshall* (2006) suggest that secondary cracks at fault tips, called tailcracks, provide insights into the mechanics of ridge-like vs. band-like strike-slip fault development. Tailcracks are secondary tension fractures commonly observed at the tips of strike-slip faults on Earth, and which have also been documented on Europa (see sections 2.1.4 and 4.2). The intersection of the fault and its associated tailcrack is manifested by a sharp kink, with an angle described by linear elastic fracture mechanics theory as being controlled by the ratio of shear stress to normal stress at the instant of tailcrack development. Hence, it is possible to determine whether or not a fault is dilating at the instant it is shearing laterally based on the geometry of its tailcracks. Using this line of reasoning, *Kat-*

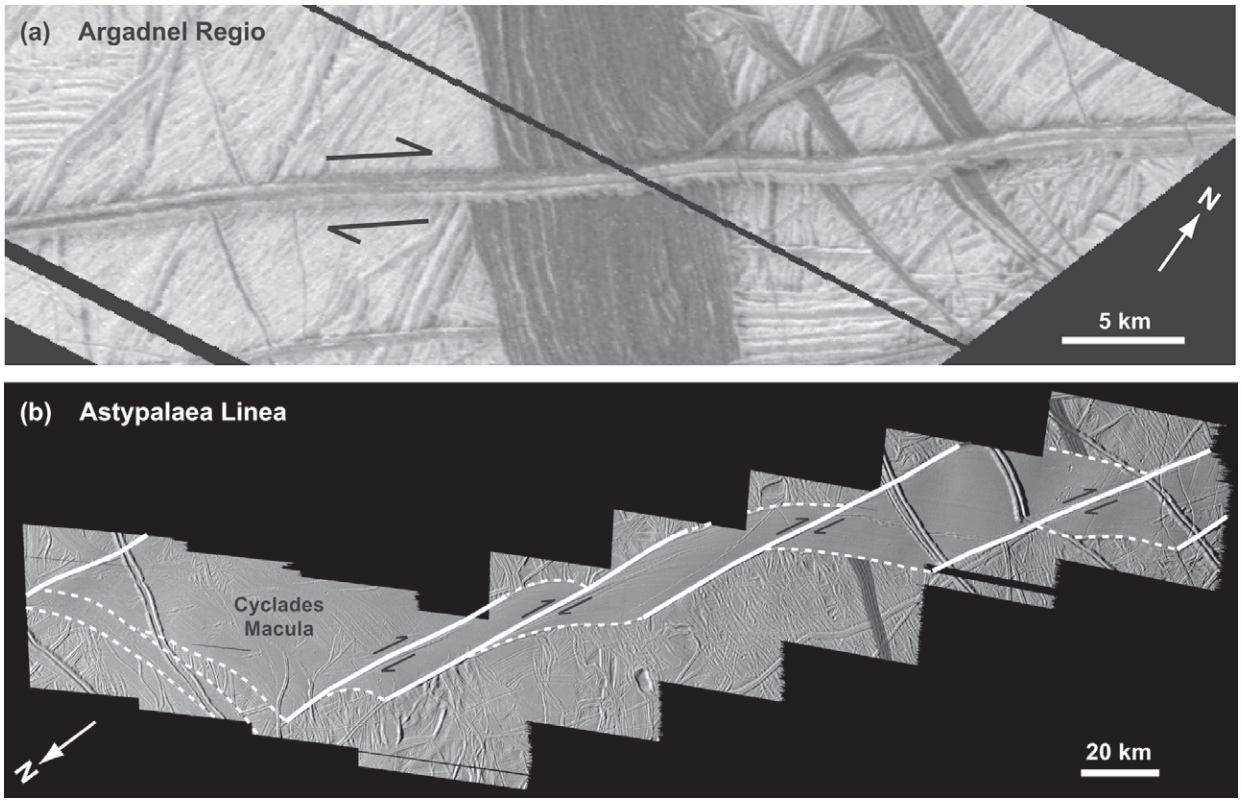

Fig. 10. Examples of strike-slip faults. **(a)** Unnamed right-lateral, ridge-like strike-slip fault cutting Yelland Linea in Argadnel Regio, from Galileo mosaic 12ESWEDGE_03. **(b)** A portion of the band-like strike-slip fault Astypalaea Linea in the southern antijovian region. White solid lines are fault segments that slipped right-laterally, producing dilational pull-aparts along linking cracks (white dashed lines). A ridge that was offset by 77 km (gray) illustrates the fault kinematics. From Galileo mosaic 17ESSTRSLP02.

tenhorn (2004a) showed that ridge-like faults (Fig. 10a) commonly undergo lateral shearing while slightly dilated or frictionally closed (see also *Aydin,* 2006), whereas the band-like faults they examined (Fig. 10b) accrue strike-slip offsets concomitant with significant dilation. Hence, many band-like strike-slip faults are essentially transtensional, oblique spreading zones. They exhibit typical lateral offsets of tens of kilometers (e.g., ~77 km along Astypalaea Linea) (*Kattenhorn,* 2004a) and lengths of up to ~1500 km (e.g., Agenor Linea) (*Prockter et al.,* 2000).

Despite these interpretations, band-like strike-slip faults should not be considered to be simply types of dilational bands, as some strike-slip motions almost certainly occur after dilation has ceased and may even be associated with some amount of later contraction. For example, the bright bands originally described from Voyager imagery, such as Agenor Linea (Fig. 7b) (*Schenk and McKinnon,* 1989), may reflect geologically recent reactivation of older dilational bands to create transpressional strike-slip faults. The interior structure of Agenor Linea is convoluted (unlike simple dilational bands) with some portions being reminiscent of transpressional duplexing along terrestrial fault zones (*Prockter et al.,* 2000). This duplexing probably occurred during shearing of the original band, with restraining bends developing because of the irregular geometry of the band margins. Tectonic annihilation of the margins of Agenor Linea during shearing may have resulted in ridged plains that cannot be matched from one side of the fault zone to the other, unlike dilational bands.

We infer that some band-like strike-slip faults are essentially ridge-like/band-like hybrids, in that the band portions of the fault formed as dilational pull-aparts along segmented ridge-like faults, where the sense of step between adjacent fault segments was the same as the sense of slip along them. A prominent example is the right-lateral fault Astypalaea Linea in the south-polar region (*Tufts et al.,* 1999; *Kattenhorn,* 2004a), where rhomboidal pull-apart bands formed between right-stepping ridge-like fault segments (e.g., Cyclades Macula). As a result of this formation mechanism, the interior striations of these bands (which trend perpendicular to the inferred spreading direction) are highly oblique to the overall trend of Astypalaea Linea.

As with distinctions between dilational bands and band-like faults, ridge-like strike-slip faults should not be considered to be simply types of ridges. Crosscut features that can be matched to either side of ridges (producing so-called piercing points that used to be together) typically show zero lateral offsets, indicating that measurable cumulative lateral offsets are not a requirement for ridge development. Nonetheless, some ridges do show appreciable lateral offsets, implying a long-term process of shearing and strike-slip accumulation, whereas troughs never show lateral offsets (*Hoppa et al.,* 1999c), suggesting that lateral motions may be an important aspect of the ridge building process. Ridge-like fault offsets are typically in the range of hundreds of meters to several kilometers (*Hoppa et al.,* 2000) but have been measured as high as 83 km (*Sarid et al.,* 2002). An important observation is that the lateral offset along a ridge-like fault does not scale with the length of the ridge, as would be true of terrestrial strike-slip faults and theoretical predictions for shear fractures based on linear elastic fracture mechanics (*Pollard and Segall,* 1987). For example, Agave Linea, which passes north of Conamara Chaos (Fig. 2a), is at least 2000 km long, yet shows lateral offsets of ~5 km, implying that it did not initiate or grow as a primary shear fracture but rather accrued a minor amount of lateral offset during subsequent movement. Therefore, models that favor ridge formation through primary shear failure of the icy shell do not seem justified in these cases. Nonetheless, frictional shearing may very well contribute to the ridge developmental process (*Nimmo and Gaidos,* 2002) (see section 2.1.1). Accordingly, tailcrack geometries along ridge-like faults confirm that frictional sliding of closed cracks commonly did occur to form these features (*Kattenhorn,* 2004a). The caveat to this model is that not all ridges show lateral offsets, implying two possible scenarios: (1) repeated forward and backward frictional shear motion along cracks during the diurnal cycle resulted in zero or unresolvable cumulative strike-slip offset but still produced enough total heat to drive ridge construction; or (2) frictional shearing is just one of perhaps several contributing factors to ridge development (see section 2.1.1), such that the absence of strike-slip motions does not preclude ridge formation. Neither scenario can be proven; however, the creation of apparent lateral offsets through a component of convergence, if present (see section 2.2.3), implies other processes may also contribute to ridge development. The upshot is that strike-slip motions are relatively common on Europa and that the lateral motions commonly utilize ridges and dilational bands, which must therefore act as planar weaknesses in the icy shell along which lateral shearing is accommodated.

2.3.4. Tidal walking. True strike-slip motions along faults are suggested to be driven by diurnal tidal stresses through a process informally referred to as tidal walking (*Hoppa et al.,* 1999c). In response to the constantly changing diurnal tidal stress field (see section 4.1.5), faults repeatedly experience tension then compression out of phase with left- and right-lateral shear stresses, because of the manner in which the tidal stress tensor resolves normal and shear stresses onto the fault surfaces. As with any fault or fracture, certain failure criteria rules apply. Where tension opens a crack, there would be no frictional resistance to shear motion; therefore, concomitant shearing should produce lateral offset. If a crack is closed, shear motion is limited by the frictional strength; therefore, lateral offsets can only be produced if the shear stress exceeds the normal stress multiplied by the coefficient of static friction, μ (i.e., the Coulomb failure criterion). Hence, the tidal walking theory implies that when the stress normal to a fault is tensile, the fault opens at the surface, allowing shear stress to produce a small amount of offset. The net sense of shear during this dilational phase, which depends on the extent to which the normal and shear stress curves are out of phase with each other (*Hoppa et al.,* 1999c; *Groenleer and Kattenhorn,* 2008), controls the sense of strike-slip offset. As

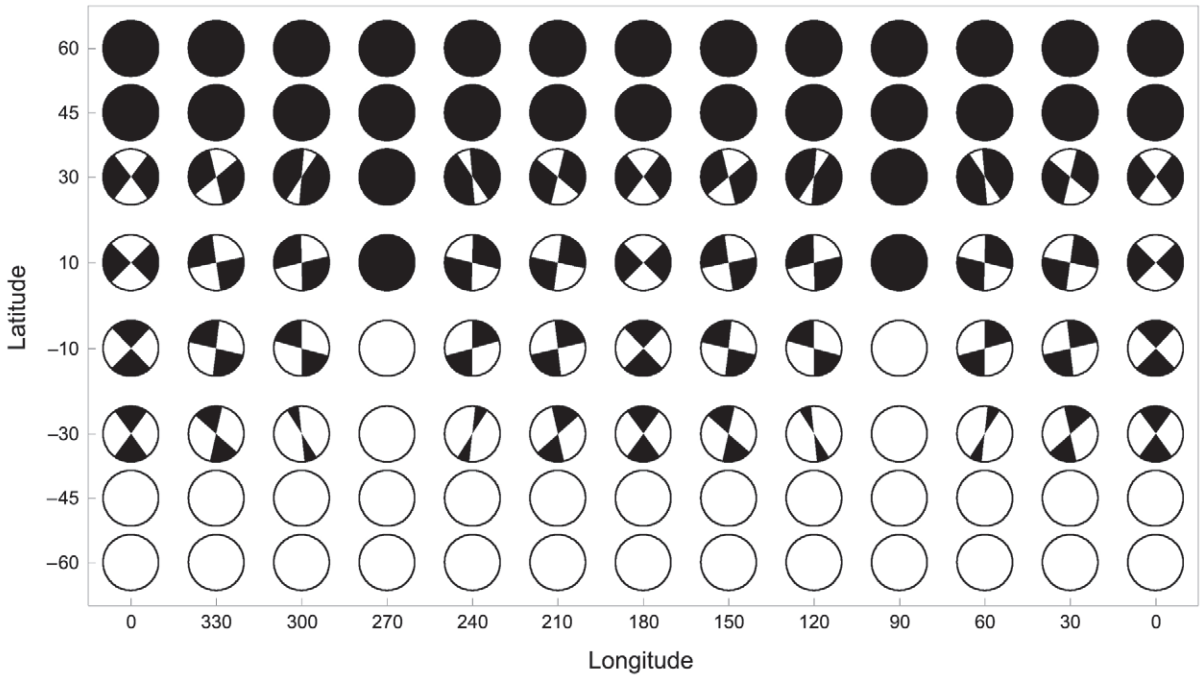

Fig. 11. Global pattern of strike-slip motion sense of faults of all orientations as a result of diurnal tidal stresses and the process of tidal walking. Fault orientations are indicated by the circular rose diagrams where the top of each circle is the 0° or north-south orientation. There is a prevalence of left-lateral motions (black) in the northern hemisphere and right-lateral motion (white) in the southern hemisphere.

the normal stress acting across the fault changes from tension to compression about half an orbit later, the fault surfaces must be in frictional contact. The friction along the fault then limits the ability of a changing sense of shear stress to completely remove the recently accrued offset. Consequently, after each diurnal cycle, the fault accumulates a small net sense of strike-slip offset along its length. Over many successive cycles of this process, the accumulation of a multitude of small strike-slip offsets produces a visible amount of strike-slip displacement.

The sense (left- or right-lateral) of strike-slip displacement along a fault depends on the orientation and location of the fault (Fig. 11). Poleward of 45° latitude, regardless of fault orientation, tidal walking must result in only left-lateral faults in the northern hemisphere and right-lateral faults in the southern hemisphere. A mixture of left- and right-lateral displacements is predicted in the midlatitudes, depending on fault orientation. Observations of many strike-slip fault offsets appear to support this theoretical expectation (*Hoppa et al.,* 2000). In the leading and trailing hemisphere Galileo regional mapping observations, *Sarid et al.* (2002) observed left-lateral faults in the high northern latitudes and right-lateral faults in the high southern latitudes; however, the transition to orientation-controlled offset sense was not observed to occur at the predicted 45° latitude. They posited that a small amount of polar wander may be responsible for the mismatch between tidal walking theory and their strike-slip fault observations.

Tidal walking provides a simple mechanism for driving strike-slip motions on Europa, with a similar phenomenon now suggested to be driving fault activity in the south polar region of Enceladus (*Hurford et al.,* 2007b; *Smith-Konter and Pappalardo,* 2008), possibly responsible for plume eruptions. Nonetheless, while band-like faults show consistent agreement with the predictions of tidal walking, there are exceptions for ridge-like faults (such as left-lateral ridge-like faults in the south-polar region) (*Kattenhorn,* 2004a). A potential caveat is that the theory does not incorporate the longer-term effects of nonsynchronous rotation stresses on strike-slip motions, which are expected to be important. For example, *Schulson* (2002) uses a frictional sliding calculation to infer that a significant amount of nonsynchronous rotation stress buildup would be needed to drive motion along a strike-slip fault with sufficient force to allow a developing tailcrack to penetrate down to a depth of 1 km into the icy shell. Considering that some tailcracks have developed into dilational bands, and thus must have penetrated sufficiently deep to reach viscoplastically deformable ice, nonsynchronous rotation stresses may indeed have been an important contributor to this process. A final caveat is that the tidal walking theory is currently conceptual, as it does not incorporate a quantitative test of shear motions using frictional failure criteria. In fact, the recent work involving tidal stresses acting on faults on Enceladus has produced a conceptual model for slip along faults that is based on the mechanics of strike-slip faults on Earth (*Smith-Konter and Pappalardo,* 2008). This newer model of tidally driven slip along faults might still be considered a form of tidal walking but its predictions of the sense of slip may be different in detail from the *Hoppa et al.* (1999c) model shown in Fig. 11.

2.3.5. Lateral shearing and cycloid growth. Although cycloids are probably tension fractures (see section 2.1.2),

lateral shearing is likely to play an important part in their developmental mechanics. *Marshall and Kattenhorn* (2005) highlighted geometrical similarities between cycloid cusps and tailcracks and developed a conceptual model that ascribed cusp formation to lateral shearing and tailcrack initiation in the tip region of a recently formed cycloid arc in response to the rotating diurnal stresses. The tailcrack then continues to grow in tension, forming the next cycloid arc in the chain. This model was bolstered by the demonstration of an excellent match between cusp angles and theoretical tailcrack angles predicted using linear elastic fracture mechanics equations and calculated tidal stress fields (*Groenleer and Kattenhorn,* 2008). The point in the orbit at which cusp development and new arc initiation occurs is therefore controlled by the interplay between resolved shear stress and normal stress in the tip region of the previously formed arc, not the timing of the maximum tensile principal stress during the orbit. This point in the orbit changes for each cycloid arc, depending on the orientation of the end region of the most recently formed arc.

3. LATERAL MOTIONS WITHOUT GLOBAL PLATE TECTONICS

Plate tectonics, in the terrestrial sense, implies that the entire brittle outer layer (lithosphere) is broken into numerous discrete fragments (plates) that move across the surface relative to each other in response to a combination of three types of motions along their boundaries: divergent, convergent, and transform. Europa contains a highly fractured outer layer (cryosphere), raising the issue of whether it too is broken into discrete plates with discernable boundaries. The existence of dilational bands on Europa (see section 2.1.3) indicates that new surface area was created through the process of complete separation of the icy shell and concurrent filling of the resultant lithospheric gap by material from below, analogous to mid-ocean ridge spreading centers. However, these tabular dilational gashes in the icy shell tend to vary in width along their lengths and may have discrete ends, or tips, indicating that they do not facilitate rigid motions of the two opposing sides away from the spreading site as typifies tectonic plates on Earth. Terrestrial plate tectonics has created a balance between surface area creation at mid-ocean ridges and surface area removal at subduction zones. In contrast, there are no known subduction zones on Europa (*Sullivan et al.,* 1998*; Prockter et al.,* 2002) and no obvious global pattern of tectonic plate boundaries that localize deformation. Rather, brittle deformation of the icy shell is globally pervasive, although the intensity of deformation may be localized (e.g., at dilational bands and major strike-slip faults). The locations of tensile fracturing or lateral shearing at any point in time is likely driven by the characteristics of the global tidal stress field, which is geographically variable (see section 4). However, any long-term reorientation of the icy shell, such as by nonsynchronous rotation (section 4.1.6) or polar wander (section 4.1.7), could move all locations on the moon's surface into optimal stress zones for brittle deformation at some point, allowing for the global pervasiveness of brittle fracturing. The upshot is that there is no indication of a terrestrial-like, global plate tectonic system on Europa. Accordingly, there is no known (or likely) driving mechanism for global plate tectonics either.

The problem remains that the repeated creation of tens-of-kilometers-wide dilational gashes in the icy shell must be somehow accommodated without global plate tectonics. Localized contractional features apparently do exist on Europa to accommodate some of the spreading occurring at dilational bands (see section 2.2), including convergence bands, ridges, and to a much lesser extent, folds. It is also possible that much of the opening across a band is accommodated elastically in the icy shell at timescales less than the Maxwell relaxation time. In a linear elastic half-space, a tension fracture causes significant elastic deformation within the material within which it is embedded out to a distance that scales with the smallest dimension of the crack (e.g., *Pollard and Segall,* 1987). On Europa, this dimension is likely to be the fracture depth for the case of fractures that do not fully penetrate the icy shell. For a very long tension fracture or dilational band, elastic deformation will mostly dissipate within about three crack depths perpendicularly away from the structure, which should be in the range of a few kilometers to a few tens of kilometers. If the crack fully penetrates the shell (a situation that has been proposed but never confirmed on Europa), elastic deformations will extend away from the crack out to a distance that scales with the crack length, as long as this length exceeds the shell thickness (also see *Sandwell et al.,* 2004). Hence, shell-penetrating cracks that extend hundreds of kilometers across the surface would cause elastic deformations in the adjacent icy shell out to distances of hundreds of kilometers. The point here is that dilations could conceivably be accommodated by elastic contractional strains alongside a dilating crack without the need for visible contractional deformation. Because dilational bands maintain a permanent dilation, the elastic deformation of the icy shell can only be dissipated by long-term viscous relaxation within the icy shell. Considering that the relaxation time for the cold outer brittle portion of the icy shell (~80 G.y.) (*Nimmo,* 2004a) exceeds the age of the solar system, ongoing opening of a dilational band should ultimately cause stored elastic energy within any elastically perturbed zone around the dilational band to be released through brittle deformation, such as shear failure (e.g., strike-slip faulting) or convergence along existing structures. Hence, some motions along structures may be driven by locally perturbed stresses alongside dilating bands rather than global tidal stresses.

Terrestrial strike-slip faults can be isolated or transcurrent intraplate faults or transform plate boundary faults. Isolated faults have distinct tips at the end of the fault trace, toward which the lateral offset decreases to zero from some maximum along the fault trace (commonly near the geometric center of the fault). In contrast, transcurrent and transform faults may be unconstrained by fault tips as a result of the presence of deformation belts, spreading centers, or subduction zones at either tip, allowing the fault to behave analogous to a rigid-body translation. In these cases, the

total offset along the fault may be approximately constant along the fault length. In the absence of global plate tectonics on Europa, one might expect only nontransform faults; however, palinspastic reconstruction of fault offsets can commonly be achieved via a rigid-body technique (e.g., Astypalaea Linea) (*Tufts et al.,* 1999; *Kattenhorn,* 2004a). This is possible because even in the absence of plate tectonics, fault-tip motions can potentially be accommodated by dilational bands where extension is needed and by convergence bands where contraction is needed (*Sarid et al.,* 2002*; Schulson,* 2002*; Kattenhorn and Marshall,* 2006). Nonetheless, it is not always possible to match up features across a palinspastically restored strike-slip fault using rigid translations because of variability in the amount of strike-slip displacement associated with elastic displacement gradients (e.g., *Vetter,* 2005). This behavior may suggest that isolated strike-slip faults exist on Europa with slip gradients along their lengths and should not be treated as rigid-body transforms in tectonic reconstructions.

Although the preceding discussion highlights the lack of global plate tectonics on Europa, rigid translations and rotations appear to have occurred locally along circumferentially detached portions of the icy shell (i.e., areas that are completely surrounded by prominent, active cracks with variable motion behaviors, analogous to plate boundary processes). These localized plate-like fragments of the icy shell have been referred to as microplates (*Schenk and McKinnon,* 1989; *Rothery,* 1992; *Sullivan et al.,* 1998; *Sarid et al.,* 2002) and sometimes form triple junctions where three microplates meet (*Patterson and Head,* 2007). The existence of these mostly intact portions of the icy shell that undergo lateral shifts or rotations justifies local usage of plate tectonic analysis techniques, similar to terrestrial analogs, despite the lack of a global plate tectonic system. Accordingly, *Patterson et al.* (2006) examined fault- and dilational band-bounded microplates, tens to hundreds of kilometers wide, in the equatorial region near Castalia Macula, northwest of Argadnel Regio, and were able to determine Euler poles of rotation. Nonetheless, the nonuniqueness of derived Euler poles using several adjacent microplates and a deduced deformation sequence implies nonrigid deformation within the microplates. In the absence of a known driving mechanism for any type of large-scale plate motion on Europa, small rotations of inferred microplates are ostensibly driven by differential motions induced by local tectonic activity along the microplate boundary (such as the opening of a dilational band), or in adjacent deforming regions. This process may be particularly common where the icy shell is heavily dissected by multiply oriented dilational bands (such as in Argadnel Regio) because dilational bands potentially form zones of weakness within the icy shell across which later deformation may be localized.

4. CAUSES OF TECTONIC DEFORMATION

Fractures on Europa are produced in response to stress in the icy shell. As described in previous sections of this chapter, a diverse range of tectonic features has been produced in response to these stresses, causing initial brittle failure of the ice and subsequent modification of these structures over time. Thus, the tectonic record preserves a record of the stresses experienced by the icy shell and holds the key to identifying the processes that imparted those stresses. We now highlight the processes that can create the stresses responsible for fractures in the europan shell at global, regional, and local scales (also see chapters by Nimmo and Manga, Sotin et al., and Bills et al.).

4.1. Global-Scale Stress

Some global-scale ridges span more than 50% of the circumference of Europa, so the stress conditions needed to form the fractures along which these ridges formed must have been global in scale. We therefore examine the range of plausible factors that may induce global-scale stress fields, which, at their essence, require a global change in shape of the satellite.

4.1.1. Thin shell approximation. Using Mercury as an example, *Melosh* (1977) showed that a global change in shape caused by a change in rotation rate produces stress that could drive the formation of tectonic features. In its simplest form, the model approximates the surface stress as occurring in a thin elastic shell that is decoupled from a fluid interior as it deforms. The horizontal strain in the shell induced by the tidally distorted interior results in stress on the surface, given by

$$\sigma_{\theta\theta} = -\frac{1}{3}\mu f\left(\frac{1+\nu}{5+\nu}\right)(5 + 3\cos 2\theta) \quad (1)$$

and

$$\sigma_{\phi\phi} = \frac{1}{3}\mu f\left(\frac{1+\nu}{5+\nu}\right)(1 - 9\cos 2\theta) \quad (2)$$

The quantity $\sigma_{\theta\theta}$ is the stress along the surface in the direction radial to the axis of symmetry, while $\sigma_{\varphi\varphi}$ is the stress along the surface in a direction orthogonal to the $\sigma_{\theta\theta}$ stress. Also, θ is the angular distance to any point on the surface measured with respect to the tidal distortion's axis of symmetry, f is the flattening, μ is the rigidity (shear modulus) of the shell, and ν is Poisson's ratio. Compressive stresses are defined here to be positive and tensional stresses negative. Flattening, f, is defined as $f = (r_{sym} - r_{orth})/r$ where r is the mean radius of the body, r_{sym} is the radius along the axis of deformation symmetry, and r_{orth} is the radius along an orthogonal axis. The flattening is positive when $r_{sym} > r_{orth}$, otherwise it is negative.

The thin shell approximation of surface stress is also applicable to Europa, where conservative estimates of tidal heating predict a H_2O layer that might be liquid underneath an icy shell (*Peale and Cassen,* 1978; *Moore,* 2006). Moreover, magnetometer measurements from Galileo strongly imply the existence of a liquid layer (*Kivelson et al.,* 2000).

A liquid ocean would decouple the icy shell from the interior of Europa. Although the thickness of the icy shell is not known, a range of techniques have constrained it to be probably less than 30 km (*Billings and Kattenhorn,* 2005, and references therein; see chapter by McKinnon et al.). In the absence of a good physical constraint on the thickness of the icy shell, the assumption that it behaves as a thin elastic layer is assumed to be valid. If this icy shell is on the order of 10 km thick, the stresses on its surface may still approximate a thin elastic shell (*Hurford,* 2005). A thicker icy shell is expected to have its upper portion acting elastically (*Williams and Greeley,* 1998; *Billings and Kattenhorn,* 2005; *Hurford et al.,* 2005) with deeper, warmer ice behaving viscously at low strain rates (*Rudolph and Manga,* 2009). Even so, the entire icy shell may still behave in a manner analogous to a thin elastic layer if deformed rapidly, such as at the timescale of diurnal stressing (*Wahr et al.,* 2009).

Although we describe the results of a thin shell approximation for the tidal stress, an alternative model that can account for thicker icy shells has been recently developed (*Wahr et al.,* 2009). Models of tidal stress for arbitrary icy shell thicknesses are based on standard techniques used to calculate tides on Earth (*Dahlen,* 1976). These models define the stress in terms of the material properties of the satellite at it surface and a description of the satellite's tidal deformation, which is given by tidal Love numbers h_2 and l_2. The models also assume that the satellite is composed of distinct layers, each defined by its own material properties: density ρ, viscosity η, rigidity μ, and compressibility λ. Measurements of the moment of inertia allow some constraints on the distribution of mass within the body (*Anderson et al.,* 1997). However, the structure of Europa's interior is poorly constrained.

4.1.2. Despinning. After the Voyager flybys, the pattern of global ridges on Europa (Fig. 1) was described as consisting of radial and concentric fractures resembling tension cracks near the sub- and antijovian points, while elsewhere on the surface, 60° intersections of fractures were interpreted as conjugate shear fractures (*Helfenstein and Parmentier,* 1980). This pattern suggested that cracks were produced by a change in shape of Europa by a tidal process and not by a change in shape controlled by the rotation of Europa. Early analysis favored a change in shape induced by a tidal response driven by Europa's changing distance from Jupiter because of its finite eccentricity (*Helfenstein and Parmentier,* 1980). In Europa's early history, it is expected that the entire satellite spun nonsynchronously; however, tidal torques would have changed its spin rate, despinning it on a timescale much shorter than the age of the solar system such that the satellite's solid interior now rotates synchronously (*Peale,* 1977; *Squyres and Croft,* 1986), although the decoupled icy shell may rotate nonsynchronously (see section 4.1.6). Nonetheless, even after reaching a synchronously rotating state, the spin rate will continue to change as Europa's orbit evolves. Outward orbital migration (*Yoder,* 1979) increases the semimajor axis length, forcing Europa's spin rate to decrease as tidal torques further slow its rotation rate in order to maintain a synchronous rotation state.

A spinning satellite in hydrostatic equilibrium deforms into a shape in which the force of gravity balances the centripetal force produced by its rotation. This deformation produces an oblate spheroid whose radius is depressed along an axis defined by the pole of rotation and enhanced along any orthogonal axis, extending through the equator. If the spin rate changes, then the oblateness of the spheroid will change in response and produce stress on the surface. Despinning reduces its oblateness ($\Delta f > 0$), producing a rebound of the radius along the axis of symmetry (through the rotational poles) and all-around tensile stress (i.e. $\sigma_{\theta\theta} < 0$ and $\sigma_{\varphi\varphi} < 0$) at latitudes poleward of ±48.2° (Fig. 12a). In the midlatitudes, meridional stresses (i.e., radial to the poles) are tensile while stresses in the orthogonal direction are compressive (i.e. $\sigma_{\theta\theta} < 0$ and $\sigma_{\varphi\varphi} > 0$). Tectonic features produced by this type of global stress pattern would most likely consist of radial and concentric tensile fractures centered on the polar regions of Europa. These have not been observed, suggesting that despinning is not responsible for the fracture patterns on Europa.

4.1.3. Orbital recession. The pattern of stress due to tidal deformation (as opposed to despinning) predicts a symmetry more consistent with the pattern of global fractures observed. Tidal deformation of Europa produces a prolate spheroid elongated along an axis connecting the center of Europa and Jupiter. Along any orthogonal axis the radius of the deformed body is depressed. The tide-raising potential, W, and the response of the body to that potential, denoted by the Love number h_2, determines the height of the tidal deformation given by $H = -h_2 W/g$, where g is the acceleration of gravity. The value of h_2 depends on the material properties and configuration of mass within Europa's interior. The tide-raising potential W depends strongly on the distance between Europa and Jupiter: $W = -GMa^{-3} R^2 (1.5 \cos^2 \theta - 0.5)$, where M is the mass of Jupiter, a is the semimajor axis of the orbit, R is the radius of Europa, and θ is the angular distance between any point on Europa's surface and the axis between the centers of Jupiter and Europa.

Since Jupiter rotates faster than Europa orbits, the tidal bulge raised on Jupiter by Europa is oriented slightly ahead of its position, providing orbital energy to Europa, which causes the orbit to migrate outward. As Europa's orbit migrates outward, the tide-raising potential deforming its surface decreases and the height of the tide raised on its surface is gradually reduced (*Squyres and Croft,* 1986). This change in shape ($\Delta f < 0$) should produce an all-around compressive stress on its surface ($\sigma_{\theta\theta} > 0$ and $\sigma_{\varphi\varphi} > 0$) in the region within 41.8° of the axis of symmetry, defined by the line between the centers of Europa and Jupiter (Fig. 12b). In the region between the compressive zones, the stresses are compressive radial to the axis of symmetry and tensile in the orthogonal direction ($\sigma_{\theta\theta} > 0$ and $\sigma_{\varphi\varphi} < 0$). If frac-

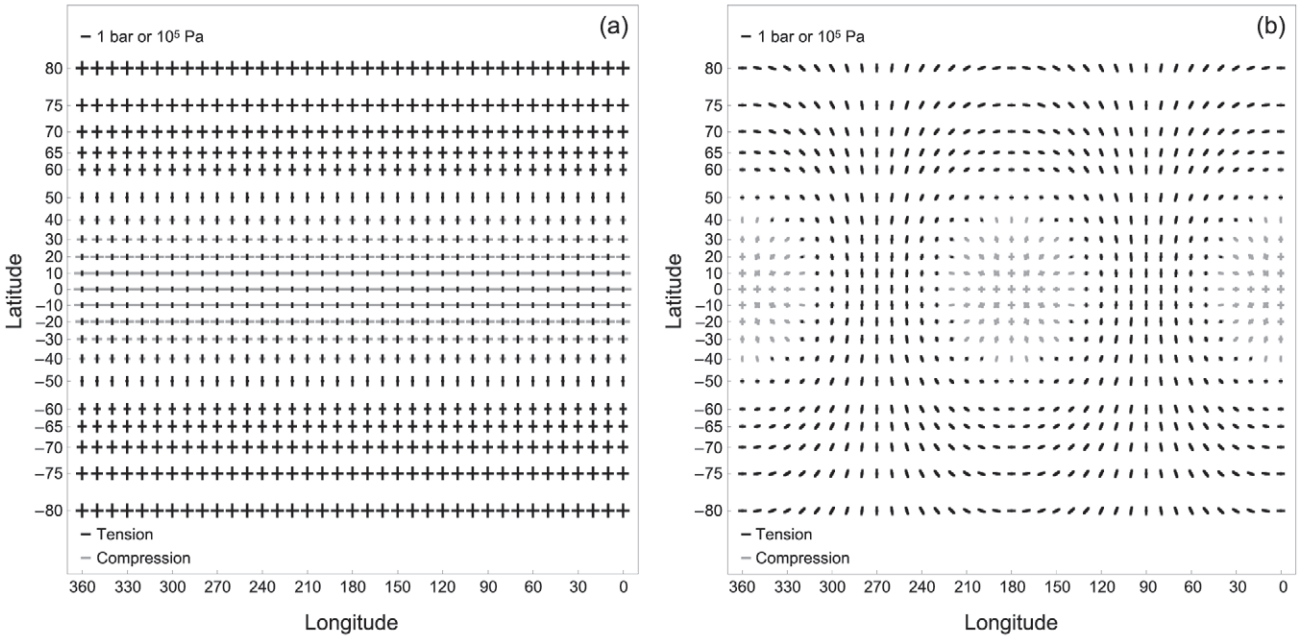

Fig. 12. **(a)** The stress field produced by a 5% decrease in Europa's rotation rate due to orbital recession and subsequent despinning. **(b)** The stress field produced by outward orbital migration, resulting in a 1% semimajor axis lengthening.

tures on Europa form mainly in tension, the stress from orbital recession would not produce fractures in the sub- and antijovian regions. Moreover, the cracks that would form between the sub- and antijovian regions would be radial to those regions. Hence, the stress field due to orbital recession also fails to produce tensile fractures in a pattern that matches Europa observations (Fig. 1).

4.1.4. Internal differentiation. During differentiation, mass within a body such as Europa is redistributed, with heavier materials moving toward the center. The redistribution of mass, along with any changes in material properties that occur, will change Europa's response to a tide-raising potential (cf. *Squyres and Croft,* 1986). This change manifests itself as a change in Europa's Love number h_2. As Europa's response to Jupiter's tide-raising potential changes, the prolateness of Europa is affected and the resulting change in shape produces stress on its surface.

Differentiation reduces Europa's response to a tide-raising potential, reducing the prolateness of the shape ($\Delta f < 0$). The resultant stress on the surface is similar to the stress produced by outward orbital migration: compressive in the region within 41.8° of the axis of symmetry, defined by the line between the centers of Europa and Jupiter. In the region between the compressive zones centered about the axis of symmetry, the stresses are compressive radial to the axis of symmetry and tensile in the orthogonal direction (i.e., analogous to Fig. 12b). Again, this stress field would not produce tension fractures in the sub- and antijovian regions but would produce cracks radial to those regions, which does not agree with the pattern of lineaments observed (Fig. 1). Moreover, the initial differentiation of Europa occurred early in its history, not long after its initial formation. Because Europa's surface is young (~40–90 m.y.), any tectonic features that formed as a result of the stress produced by differentiation have been erased by the formation of subsequent terrains.

4.1.5. Eccentricity and diurnal tidal stresses. If the semimajor axis were to migrate inward, the stress field would be the exact opposite of that described above for orbital recession, with a region of tension within 41.8° of the axis of symmetry. This stress field could produce tensile fractures in the sub- and antijovian regions as observed (Fig. 1). For this reason, *Helfenstein and Parmentier* (1983) proposed that global-scale lineaments formed in response to orbital eccentricity, e, which causes Europa's distance from Jupiter to change throughout the orbit, resulting in an oscillating diurnal tidal height response. At perijove, Europa is closer than average and the stresses near the sub- and antijovian points are tensile, allowing fractures to form. At apojove, Europa is farther than average and the stresses in this region are compressive. We now understand that this characterization of the stress field is incomplete. It neglects other important effects that orbital eccentricity has on tidal deformation, such as an oscillation in the longitudinal location of the tidal bulge, resulting in a poor match to tectonic patterns.

Because of Europa's finite eccentricity, as Europa moves from perijove to apojove, there is a small variation in the radial tide with an amplitude of $\Delta H = (9eh_2MR)/(4\pi\rho_{av}a^3)$ that affects f. In addition, Jupiter's angular position with respect to a fixed location above Europa's surface oscillates with an amplitude of 2e radians in longitude (and ε radi-

ans in latitude if there is a finite obliquity), changing slightly the angular distance θ of any point on the surface relative to the center of the tidal bulge. These two effects combine, yielding a diurnally varying component of the tide (*Greenberg et al.,* 1998; *Hurford et al.,* 2009).

The diurnal stress produced by Europa's orbital eccentricity thus changes throughout the orbit (Fig. 13). Zones of tension and compression along the equator migrate eastward throughout the day. The orientations of the principal stress axes rotate clockwise in the southern hemisphere and counterclockwise in the northern hemisphere, with 180° of rotation in principal stress orientations each orbit. This changing stress field provided the context for the development of the tidal walking hypothesis for strike-slip fault motions (see section 2.3.4) as well as for unraveling the patterns of cycloidal cracks on Europa (see section 2.1.2). Nonetheless, there are caveats to the use of the diurnal stress field pattern for unraveling all tectonic features. The constantly changing nature of the stress field makes it difficult to account for the extremely linear nature of most cracks, and the stress magnitudes are extremely small (on the order of a few tens of kilopascals) (*Hoppa et al.,* 1999a) such

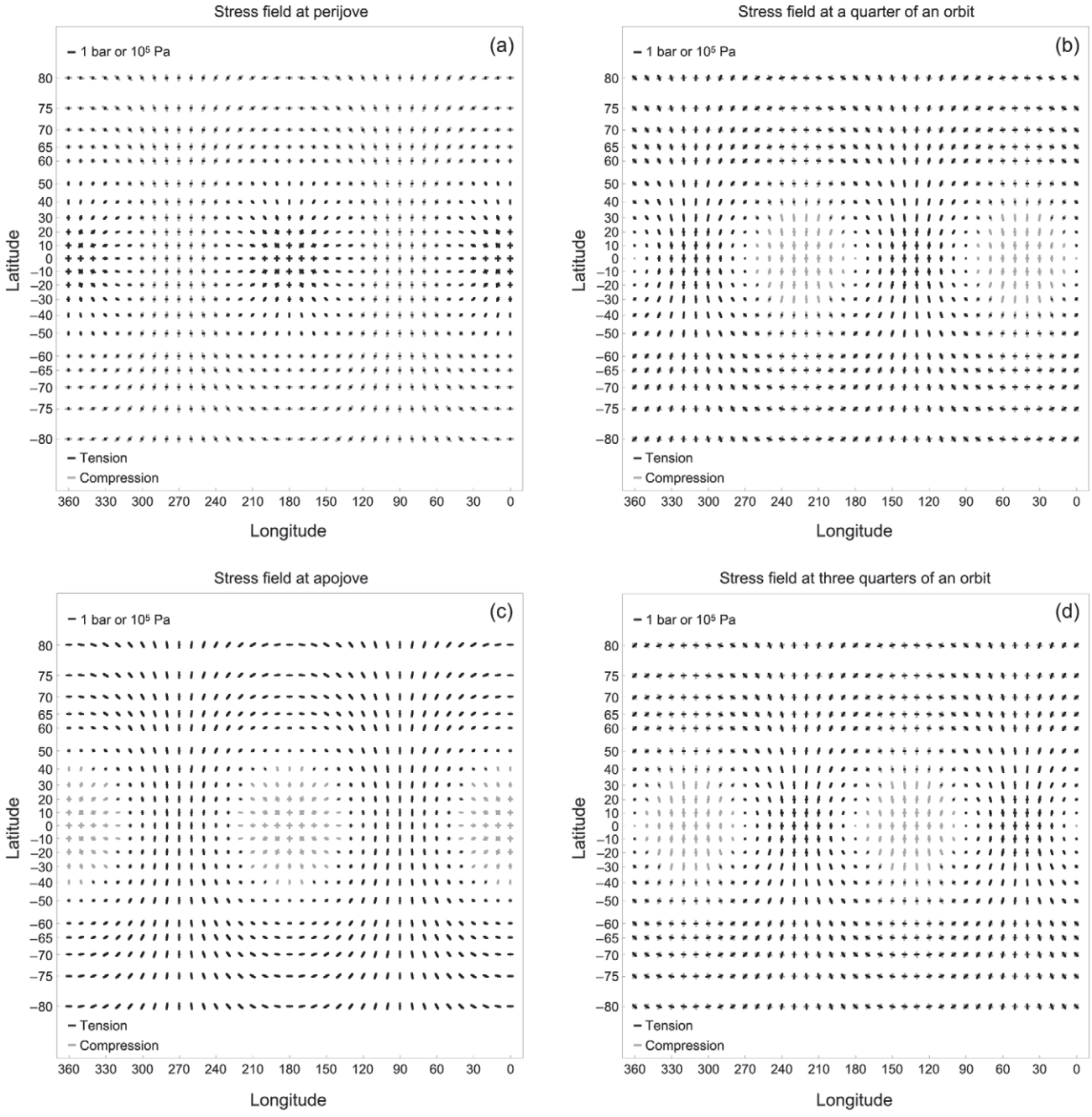

Fig. 13. Stresses produced by the diurnal oscillations of Europa's tidal bulge are shown in one-quarter orbital increments beginning at perijove. Zones of tension and compression along the equator migrate eastward throughout the day. The orientation of the principal stress axes rotate clockwise in the southern hemisphere and counterclockwise in the northern hemisphere, changing by 180° each orbit.

that it is has been questioned whether they are sufficient to overcome the likely tensile strength of ice at the low surface temperatures of Europa (*Harada and Kurita,* 2006). Also, diurnally varying tidal stresses cannot account for cycloids that cross the equator because of the mutually opposite rotation sense of stresses in each hemisphere. Such cycloids may provide evidence that there also exists a component of stress due to a small amount (perhaps ~0.1°) of obliquity that affected their formation patterns (*Hurford et al.,* 2006, 2009; *Sarid-Rhoden et al.,* 2009; see chapter by Bills et al.). The presence of a small forced libration (perhaps 150 m or so) of the decoupled icy shell over the diurnal period may also contribute a component of global stress (e.g., *Rambaux et al.,* 2007; *Hurford et al.,* 2008; *Van Hoolst et al.,* 2008; see chapter by Bills et al.). It is also possible that Europa's eccentricity has changed through time (see chapter by Sotin et al.), resulting in different diurnal stress field characteristics during the geological history. Nonetheless, pervasive fracturing of the icy shell and the existence of global-scale lineaments that are linear or broadly curved over great distances implies the existence of a higher-magnitude, static state of stress that dominates in controlling fracture geometries. Such a stress field may have been created in the icy shell through the process of nonsynchronous rotation.

4.1.6. Nonsynchronous rotation. Even though tidal torques work to force Europa to rotate synchronously, that rotation state can only be maintained if the orbit is circular or there exists a permanent and significant mass asymmetry within Europa (*Greenberg and Weidenschilling,* 1984). However, the Laplace resonance between Io, Europa, and Ganymede prevents tidal torques from circularizing Europa's orbit, forcing a small but finite orbital eccentricity. In a noncircular orbit, torques on Europa will tend to force it to rotate slightly faster than synchronous. This process would be accentuated by the potential development of thickness changes in an icy shell floating on a liquid ocean as tidal dissipation moves it toward thermal equilibrium (*Ojakangas and Stevenson,* 1989a). Gravitational torques from Jupiter acting on a variable thickness icy shell could induce nonsynchronous rotation on the thermal diffusion timescale (<10 m.y. per rotation), resulting in the shell attaining a state of dynamic equilibrium. Hence, as long as tidal heating within Europa prevented any permanent mass asymmetries from forming within the icy shell, the tidal torques may have forced Europa to rotate nonsynchronously (*Greenberg and Weidenschilling,* 1984), producing a significant contribution to the global stress state (*Helfenstein and Parmentier,* 1985).

Stresses from nonsynchronous rotation are caused by the reshaping of Europa as the location of the tidal bulge moves with respect to a fixed location on the surface. The actual amount of tidal deformation does not change, only the geographic location relative to the tidal bulges. The stress produced by 1° of nonsynchronous rotation produces an equatorial zone of tension to the west of the sub- and antijovian points and a zone of compression to the east of the sub- and antijovian points (Fig. 14). At high latitudes, the principal stresses ($\sigma_{\theta\theta}$ and $\sigma_{\phi\phi}$) have a range of magnitudes and signs. This stress field is broadly consistent with the pattern of ridges observed on the surface (Figs. 1 and 15). Therefore, although other sources of stress may contribute to global-scale crack formation, the stress from nonsynchronous rotation may be an important contributor to the global tectonics. Moreover, the amount of nonsynchronous rotation needed to produce stress of sufficient magnitude to allow tensile failure can be obtained within a few degrees of reorientation of the icy shell, assuming the rate at which the shell reorients is sufficiently rapid that stresses can accumulate elastically (*Harada and Kurita,* 2007; *Wahr et al.,* 2009). However, a far greater amount of cumulative nonsynchronous rotation is needed to account for the current longitudes of many fractures relative to their probable formation locations, if they indeed formed in response to nonsynchronous rotation (*McEwen,* 1986) (Fig. 15; see section 5.1).

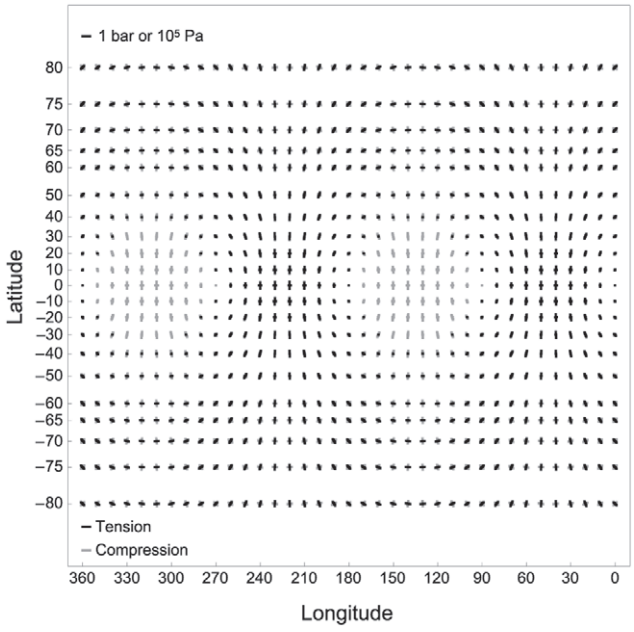

Fig. 14. The stress field produced by 1° of nonsynchronous rotation produces zones of tension just west of 0° and 180° longitude.

Geissler et al. (1998a,b) identified what appeared to be a systematic change in the azimuth of cracks over time, suggesting that Europa's surface has migrated eastward relative to the direction of Jupiter. Hence, at different times in the past, regions where cracks formed in a range of orientations may have been located within a zone of tension within the nonsynchronous rotation stress field, allowing these features to have formed as unrelated, superposed episodes of tension cracks that were subsequently translated eastward with respect to the zone of tension. As the icy shell migrated eastward, the changing orientation of the stress field at these locations resulted in new episodes of tension fracturing being superposed on older episodes, sometimes resulting in a seemingly conjugate pattern. Similar studies, utiliz-

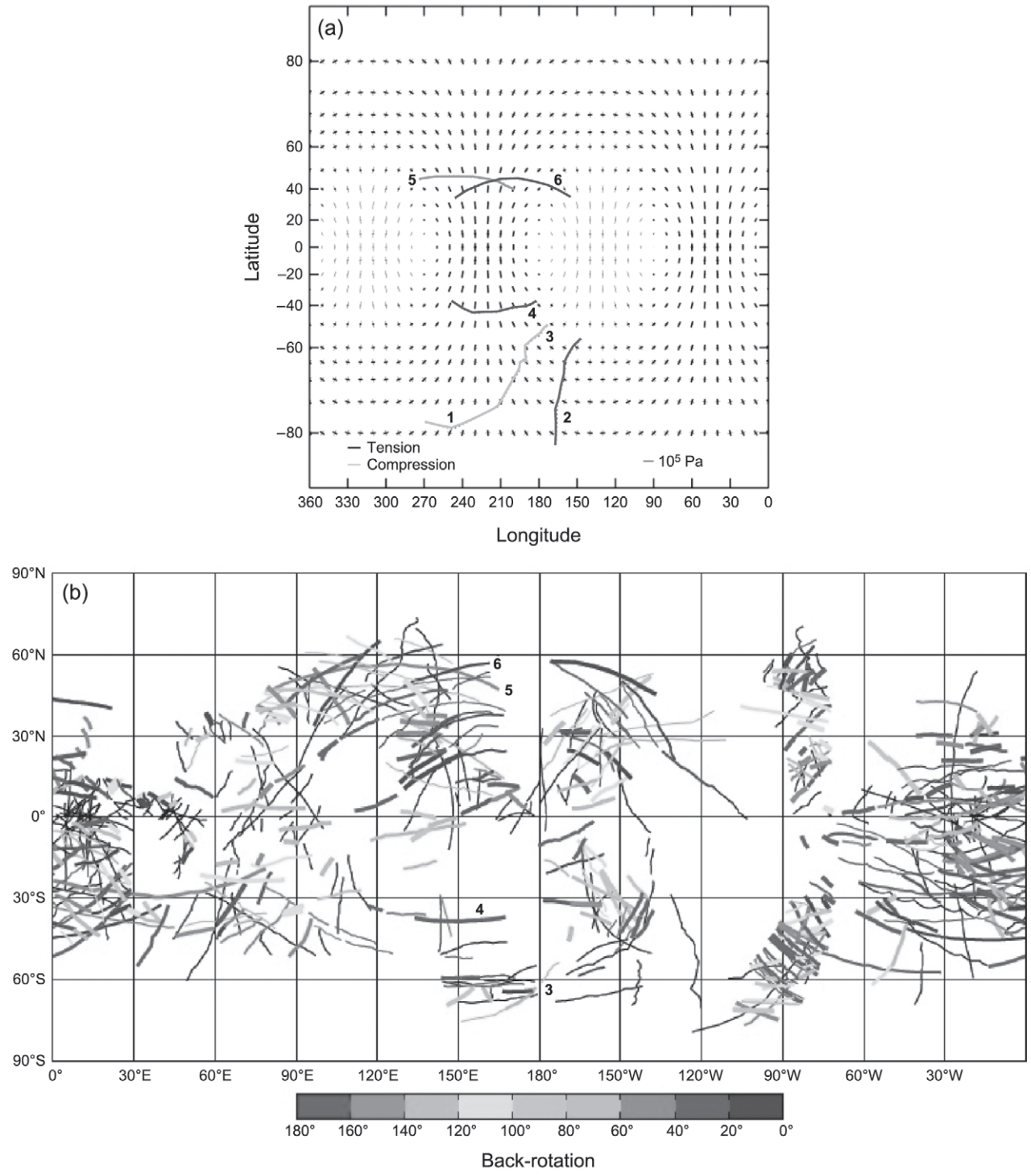

Fig. 15. See Plate 13. **(a)** The tidal stress-field produced by 1º of nonsynchronous rotation (*Greenberg et al.,* 1998) shows a good fit to the locations and orientations of several lineaments. The lineaments are numbered (1) Astypalaea, (2) Thynia, (3) Libya, (4) Agenor, (5) Udaeus, and (6) Minos Lineae. A better fit is produced if fractures are back-rotated westward in longitude relative to the stress field [by an amount given by their color coding, as defined in **(b)**] such that their orientations are perpendicular to the direction of maximum tension, providing a possible original longitude for the creation of the crack. **(b)** The global pattern of lineaments based on Galileo observations illustrates a range of orientations that cannot all be fitted to the same stress template, such as that shown in **(a)**, because they formed at different times. The lineaments are color coded to indicate how far westward they must be back-rotated in order to form perpendicular to the maximum tension produced by the stress of nonsynchronous rotation [map courtesy of Z. Selvans (Selvans et al., in preparation)]. Some of the numbered lineae in **(a)** are numbered accordingly in **(b)**.

ing higher-resolution data, have confirmed that a correlation between age and orientation exists (see section 5.1), and have been related to various interpretations of the effects of nonsynchronous rotation of the icy shell (*Figueredo and Greeley,* 2000; *Kattenhorn,* 2002; *Sarid et al.,* 2004, 2005, 2006; *Groenleer and Kattenhorn,* 2008).

4.1.7. Polar wander. Another potential contributor to the global stress state is provided by long-term latitudinal reorientation of the icy shell, or polar wander, in response to latitudinal changes in ice thickness as the icy shell thermally evolves (*Ojakangas and Stevenson,* 1989a,b). *Leith and McKinnon* (1996) explored the theoretical stress produced by this phenomenon and found only limited evidence for polar wander within observable crack patterns. *Sarid et al.* (2002) noted that the slip sense along some near-equatorial strike-slip faults did not agree with the predictions of tidal walking (see section 2.3.4) and that a small amount of polar wander since fault motions accrued may explain the distribution of the observed slip sense. However, finite obliquity is another potential mechanism for such aberrations (*Hurford et al.,* 2009) as well as the effects of convergence across ridges, which may create an apparent sense of offset in the absence of any actual strike-slip motions (see section 2.2.3). *Schenk et al.* (2008) interpret the locations and geometries of inferred extensional zones called small-circle depressions (SCDs) as being due to true polar wander. These curved depressions are up to 1.5 km deep and trace out segments of the arcs of almost perfect circles centered ~25° from the equator, forming an antipodal pattern in the leading and trailing hemispheres. The shapes and locations of the troughs are suggested to be consistent with the stress field that would result from 80° of polar wander. It is unclear what the timing of this hypothesized shell reorientation event may have been because other surface features are seemingly unaffected by the locations of the SCDs. The associated polar wander stress field (e.g., *Matsuyama and Nimmo,* 2008) has also not been compared to the orientations of the vast number of other tectonic features on Europa. Therefore, polar wander has yet to be shown to be a likely source of global stresses on Europa in terms of its potential contribution to the pattern of global tectonics.

4.1.8. Ice shell thickening. If Europa's icy shell increased in thickness relatively recently, the related stress may have contributed to tectonic activity (see chapter by Nimmo and Manga). For example, *Nimmo* (2004a) showed that for a nonconvecting icy shell that thickens in excess of 20 km, isotropic tensile stresses are produced within the icy shell, attaining magnitudes of perhaps 10 MPa at the surface, which are sufficient to induce tension fracturing and perhaps even shell-penetrating cracks (see also *Manga and Wang,* 2007). Because these stresses are isotropic, the principal stress orientations would still be controlled by the nonisotropic (e.g., tidal) components, which would thus control fracture orientations. This effect provides a potential solution to the mystery of tensile fracturing in equatorial compressive zones within the nonsynchronous rotation stress field, as described by *Spaun et al.* (2003) (see section 2.3.2). Another effect of an increasing icy shell thickness is a decreasing tidal response (e.g., a ~1% reduction if the shell thickens from 1 km to 10 km) (*Moore and Schubert,* 2000; *Hurford,* 2005), resulting in slightly reduced tidal stress magnitudes. Also, a change in ice thickness results in a change in the Love number, h_2, creating an additional component to the stress field similar to that induced by internal differentiation (see section 4.1.4).

4.2. Regional and Local Stress

Although global-scale stresses are responsible for the formation of the majority of the cracks on Europa's surface, regional and local scale stresses have also played an important role in the tectonic history. These stresses essentially represent regional and local perturbations to the global stress state and are significant for the tectonics if their magnitudes are on the order of the global stresses or higher. Although *regional* and *local* have somewhat arbitrary definitions, the important distinction is that they do not result from the global effects of tidal deformation or reorientation of the icy shell. Regional effects may encompass thousands of kilometers across the surface, depending on the causal factor. For example, endogenic processes such as thermal or compositional diapirism (see chapter by Barr and Showman) create upwelling that can impart regional stress conditions on an overlying stagnant lid. The formation of chaotic terrain, which represents the destruction of an earlier surface, is likely related to this process (*Collins et al.,* 2000; *Sotin et al.,* 2002; *Mitri and Showman,* 2008; see chapter by Collins and Nimmo). Chaos areas can only become disaggregated through the initial development of fractures that create loose blocks of brittle ice that are subsequently rafted around by the underlying motion of warmer ice and melt. Indeed, one of the types of tension fractures described in section 2.1.3, endogenic fractures, is specifically related to this phenomenon. The characteristics of the stress field caused by a diapir impinging on the brittle ice lid from below are not easily quantifiable, as they would likely depend on the shape and size of the diapir. Although the stress magnitudes are likely to be small (tens of kilopascals), they may be sufficient to drive deformation in the brittle lid (*Showman and Han,* 2005). A common observation is that endogenic fractures form concentric patterns about regions of chaos, suggesting that the causal stress field may be somewhat similar to that of an ascending bulge, analogous to upwarps above laccolith intrustions on Earth (*Jackson and Pollard,* 1988). Regional perturbations to the global stress state may also be imparted by large meteorite impacts, which can result in both radial and concentric fracture patterns for the case of complete shell penetration (*Melosh,* 1989), although radial fractures are not observed around the large impact site Tyre (*Kadel et al.,* 2000).

Local stress effects occur at scales on the order of hundreds of meters to perhaps hundreds of kilometers. The causal mechanism is typically apparent, usually related to an existing ridge, strike-slip fault, or fold, or to regions of

lenticulae (small disruptions related to underlying diapiric activity). For example, ridge constructs are up to several hundreds of meters high and their weight is expected to push down on the icy shell. As a result, the elastic portion of the shell flexes downward beneath the ridge, apparently producing secondary uplifts, or forebulges, to either side of the ridge, evident in subtle changes in shading and shadow patterns (*Tufts,* 1998; *Hurford et al.,* 2005). The resultant stresses induced by bending of the icy shell are sufficient to fracture the icy shell to either side of the ridge (Fig. 2b) and can be quantified using the equations describing the flexure of an elastic plate beneath a line-load (*Turcotte and Schubert,* 2002). *Billings and Kattenhorn* (2005) used these equations to formulate a relationship between elastic ice thickness and the distance from a ridge load to its flanking secondary cracks, allowing the thickness of the elastic portion of the icy shell to be constrained to between ~200 m and ~2400 m. Bending stresses are also responsible for the local development of surface cracks along the hinge lines of anticlinal folds, such as occurs within Astypalaea Linea (*Prockter and Pappalardo,* 2000).

Strike-slip faults produce local perturbations to the global stress field in response to lateral motions that create stress concentrations at the fault tips (*Kattenhorn,* 2004a). These stress fields are quantifiable (see section 2.3.3) and have been shown to be responsible for the development of secondary fractures at fault tips called tailcracks (see section 2.1.4) (*Prockter et al.,* 2000; *Schulson,* 2002; *Kattenhorn,* 2004a; *Kattenhorn and Marshall,* 2006). Tailcracks form in the locally perturbed stress field in the vicinity of a tip of a shearing fault or fracture. The remote (far-field) stresses govern the sense of slip on the fault itself while shear motion along the fault locally perturbs the stress field, creating near-tip quadrants of extension and compression, with an antisymmetric pattern at opposing tips. Tailcracks form in extensional quadrants and propagate away from the fault tip perpendicular to the direction of maximum local tension. A similar phenomenon is responsible for the development of cusps along cycloidal chains (*Groenleer and Kattenhorn,* 2008) in response to lateral shearing effects during the diurnal cycle. Compressive quadrants may also experience local deformation in the form of folds or anticracks, the latter having been suggested to exist in the "Wedges" region, Argadnel Regio (*Kattenhorn and Marshall,* 2006).

5. TECTONIC EVOLUTION OF EUROPA

5.1. Tectonic Evidence for Nonsynchronous Rotation

Theoretical considerations of nonsynchronous rotation stress fields (see section 4.1.6) and their match to the orientations of geologically recent large-scale lineaments prompts the search for direct evidence for extensive nonsynchronous rotation to determine its relative importance throughout Europa's visible tectonic history. Comparisons between lineament orientations on Europa and theoretical global stress fields suggest that many geologically recent lineaments did not form in their current longitudes (*McEwen,* 1986; *Greenberg et al.,* 1998; *Hoppa et al.,* 1999b). Instead, these lineaments are inferred to have translated longitudinally due to nonsynchronous rotation by a few tens of degrees (Fig. 15). Many locations on Europa show a complex sequence of multiply superposed lineaments with differing orientations, reflecting the dominant tensile stress orientation at that location at the time of lineament development. This is plausibly because the regional stress orientation changed as the icy shell migrated steadily eastward through time, rotating through a full 360° per nonsynchronous rotation cycle with a clockwise sense in the northern hemisphere and a counterclockwise sense in the southern hemisphere. Accordingly, lineament orientations have been suggested to display this rotation sense through time (*McEwen,* 1986; *Geissler et al.,* 1998a; *Figueredo and Greeley,* 2000; *Kadel et al.,* 2000; *Kattenhorn,* 2002). The amount of reorientation of the icy shell inferred from the tectonic history based on these studies is as little as 50° and up to 1000°, but may be much more depending on the amount of time between individual lineament formation events, which is unknown. A problem with these inferences is that changing fracture orientations do not directly indicate that nonsynchronous rotation actually occurred. Considering that nonsynchronous stress orientations sweep through all angles, it is not surprising that interpretations are equivocal. In fact, if one arbitrarily assumes that the sense of rotation of lineaments through time is the opposite of what would be expected in response to nonsynchronous rotation, the number of complete shell rotations needed to account for the full range of lineament orientations through time does not differ greatly to the nonsynchronous rotation result (*Sarid et al.,* 2004, 2005, 2006). Hence, although changing lineament rotations through time are certainly consistent with nonsynchronous rotation, this phenomenon does not provide direct proof that nonsynchronous rotation occurs.

Evidence for nonsynchronous rotation was suggested by *Hoppa et al.* (1999c) to be evident in the slip sense of strike-slip faults in equatorial areas, where the sense of cumulative slip in the context of the tidal walking model (see section 2.3.4) is completely dependent on the fault orientation. Some faults do not have the correct sense of slip for their orientation and location; however, back-rotation of a nonsynchronously rotated shell by up to 90° can place each fault at a longitude where the slip sense is compatible with expectations.

Additional evidence for icy shell reorientation, probably through nonsynchronous rotation, has emerged from studies of cycloids. *Hoppa et al.* (2001) show examples of southern hemisphere cycloids that could not have formed in their current locations but rather at locations up to 80° further to the west, after which nonsynchronous reorientation of the icy shell translated them eastward. *Hurford et al.* (2007a) reduced this estimate to 24° for these particular cycloids by accounting for the presence of a small amount of nonsynchronous rotation stress during cycloid growth,

indicating that reorientation of the icy shell is still necessary to fit the cycloid shapes. However, the inclusion of a small amount of obliquity may remove the need for a component of nonsynchronous rotation stress to account for the shapes of some cycloid examples (*Sarid-Rhoden et al.,* 2009). *Groenleer and Kattenhorn* (2008) document a history of numerous cycloidal episodes in the northern trailing hemisphere that necessitate at least 600° of nonsynchronous reorientation of the icy shell during the period of cycloid development alone (i.e., excluding all other lineament types). Crosscutting relationships among these cycloids imply a definitive age sequence that can best be reconciled with cycloid chains having formed during different nonsynchronous rotation cycles, lending credence to the idea that only a few cycloid chains form during each nonsynchronous rotation cycle.

The wide range of estimates of nonsynchronous rotation amounts may seem contradictory; however, disparate results likely reflect variances in both the types of features used to make the estimates and the differing resolutions of images studied in different regions. The combined studies suggest that the decoupled icy shell of Europa may have undergone almost three complete rotations relative to the rocky interior during the visible tectonic history, although this number may be much higher in reality. In support of this notion, given the 40–90-m.y. surface age of Europa (see chapter by Bierhaus et al.), nonsynchronous rotation must have occurred rapidly enough to accrue elastic stresses before they could be relieved viscously beyond the Maxwell relaxation time (*Harada and Kurita,* 2007; *Wahr et al.,* 2009). Given this rate of rotation, there have likely been numerous rotations of the icy shell relative to the interior during Europa's visible history. Nonetheless, if nonsynchronous rotation effects were relatively constant over the entire visible geological history, one might expect there to be a somewhat unchanging tectonic response throughout this time. On the contrary, Europa exhibits a diverse geological history with distinct temporal variability in the tectonic features that developed, implying that other factors need to be considered when examining the tectonic evolution of Europa, such as variations in the rate of nonsynchronous rotation (*Nimmo et al.,* 2005; *Hayne et al.,* 2006).

5.2. Temporal Changes in Tectonic Style

Previous sections of this chapter considered the range of tectonic features that pervasively deform the icy shell of Europa and the possible sources of stress responsible for those features. We now turn to the geological development of Europa inferred from the many episodes of tectonic events evident on the surface. Over the visible surface history of the icy shell, repeated fracturing events have left a remarkably coherent story regarding the tectonic evolution in the form of clearly identifiable crosscutting relationships. In so doing, tectonic features reveal that there has been a gradual change in the nature of deformation that points toward temporal variations in the thickness of the icy shell, processes occurring within the shell, and the response of the shell to tidal deformation.

Numerous studies aimed at unraveling the geological history of Europa have revealed significant changes through time (*Lucchitta and Soderblom,* 1982; *Prockter et al.,* 1999, 2002; *Figueredo and Greeley,* 2000; 2004; *Greeley et al.,* 2000; *Kadel et al.,* 2000; *Kattenhorn,* 2002; *Spaun et al.,* 2003; *Riley et al.,* 2006; *Doggett et al.,* 2007). A simple summary of these changes has early development of ridged plains (a multitude of closely spaced ridges) being followed by periods of ridge and band development, endogenic cryomagmatic disruption and cryovolcanism (chaos, lenticulae, and smooth plains) with some contemporaneous and subsequent ridge formation, and a late stage of tectonic fracturing (see chapter by Doggett et al.). Many lineaments were reactivated as strike-slip faults during the periods of tectonic activity. The following synthesis considers the individual evolution of the most prominent types of tectonic features that have been placed into a stratigraphic context.

5.2.1. Ridges. The oldest portions of the surface appear to consist of finely crenulated *ridged plains* or *subdued plains* that may represent the earliest visible ridges, with spacings on the order of hundreds of meters. Most of the ridged plains were subsequently destroyed by the repeated development of successively younger double ridges (i.e., a prominent central trough flanked by two raised rims) and dilational bands in a range of orientations. Older ridges appear to be more numerous, narrower, lower, and more closely spaced (tens to hundreds of kilometers) than relatively younger ridges (*Kadel et al.,* 2000*; Kattenhorn,* 2002*; Figueredo and Greeley,* 2004). Many of the prominent (and typically geologically young) global-scale ridges that cover broad portions of the europan surface have evolved into ridge complexes, forming the highest and widest ridge structures. Ridge development thus spans most of the geological history of the surface, although the youngest ridges could have formed many tens of degrees of nonsynchronous rotation in the past. Hence, it is unclear if ridges continue to form or if the processes responsible for their development (see section 2.1.1) still occur in the icy shell.

5.2.2. Cycloids. There has been some uncertainty as to whether cycloid development represents a geologically recent phenomenon on Europa. *Groenleer and Kattenhorn* (2008) show that there has been an extended period of cycloid development in the trailing hemisphere encompassing at least 600° of nonsynchronous rotation, with the most recent event occurring at least 30° of nonsynchronous rotation in the past. These cycloid-forming events were punctuated by periods of intervening linear ridge development, suggesting that there was an oscillation between the conditions conducive to cycloid and linear fracture formation, respectively. Although these oscillations are observed in specific areas, it is unknown whether or not a similar global temporal pattern of fracturing occurs or whether cycloid development in one region of Europa could have occurred contemporaneously with linear ridge development elsewhere. Regardless, whatever processes were responsible for

ridge construction continued regardless of whether cracks were linear or cycloidal, indicated by ridge development along the flanks of cycloids as well as linear fractures. Unlike linear ridges, however, cycloids have not been explicitly described from the earliest part of the geological history, raising the possibility that the initiation of the conditions needed to form cycloids occurred at some critical juncture during the tectonic history.

5.2.3. Dilational bands. There is also a wide range in the ages of dilational bands, some of which formed around the time of the earliest ridges (*Greeley et al.,* 2000; *Kattenhorn,* 2002); however, it is possible that the driving process behind dilational band development ceased on Europa even while ridge development continued. *Prockter et al.* (2002) indicate that there are always features younger than dilational bands, including troughs, ridges, and lenticulae. Nonetheless, dilational bands change in albedo from dark to light through time and the youngest dilational bands still have dark albedos. It is not known how quickly this lightening process occurs, so dilational bands could be many millions of years old. Dilational band widths are inferred to have decreased through time (*Figueredo and Greeley,* 2004), perhaps indicating a thinner icy shell and higher thermal gradients earlier in Europa's visible geological history. *Nimmo* (2004b) modeled the extension of icy shells and demonstrated a trade-off between strain rate and shell thickness in terms of whether wide or narrow rifts will develop. Narrow rifts are analogous to europan dilational bands and imply high strain rates or relatively thick icy shells. It is possible that changing shell thickness and strain rate conditions on Europa resulted in a transition in the mode of extension to no longer favor dilational band development. Hence, dilational bands rarely postdate chaos (see chapter by Prockter and Patterson). Those young dilational bands that appear to postdate chaos formation have dilated preexisting cycloids (*Figueredo and Greeley,* 2000); therefore, the initiation of the process responsible for cycloid development did not correspond to a termination of the process responsible for dilational band development, with both processes possibly overlapping with the period of chaos formation.

Figueredo and Greeley (2004) suggest that a long period of tectonic resurfacing by ridge and band development was followed by a rapid decrease in tectonic activity through time, concomitant with a steady increase in "cryovolcanic" activity that resulted in the formation of broad areas of chaos and lenticulae. These changes were attributed to the effects of a thickening icy shell that ultimately reached the threshold thickness required to induce solid-state convection, diapirism, and cryovolcanic resurfacing (*Pappalardo et al.,* 1999; *Barr et al.,* 2004; *Barr and Pappalardo,* 2005; see chapter by Nimmo and Manga). Nonetheless, an even younger period of trough development occurred (both linear and cycloidal), concomitant with recent cratering events. Considering that the visible geological history of Europa only spans around 2% of the total age of the satellite, it is not known if tectonic resurfacing and cryovolcanic processes occur in an oscillating cycle related to repeated thinning and thickening of the icy shell, perhaps associated with changes in Europa's orbital eccentricity (see chapters by Nimmo and Manga, Moore and Hussman, and Sotin et al.). A further complication is provided by the possibility of lateral variations in icy shell thickness due to latitudinal and longitudinal variations in tidal heating (*Ojakangas and Stevenson,* 1989a) and past tectonic modification of the icy shell (*Billings and Kattenhorn,* 2005). Regardless, the inferred thickening of the icy shell over the past 40–90 m.y. clearly influenced the tectonics.

5.3. Active Tectonics on Europa?

Although many bodies in the solar system show evidence of a remarkable geological history of tectonic activity (e.g., Mars, Venus, icy moons of Jupiter, Saturn, Uranus, and Neptune), evidence of current tectonic activity outside of Earth has been very elusive. With the recent discovery of eruptive water-ice plumes emanating from cracks (called "tiger stripes") in the south polar area of Saturn's icy moon Enceladus (*Porco et al.,* 2006; *Spencer et al.,* 2006), a relationship to active tectonics has been inferred, based on models of crack motions within a tidal stress field (*Hurford et al.,* 2007b; *Nimmo et al.,* 2007; *Smith-Konter and Pappalardo,* 2008). Any icy satellite with a liquid ocean beneath an icy shell that has apparently deformed due to the tidal response of the underlying ocean therefore provides a good candidate study for active tectonics. Hence, Europa is a promising candidate for active tectonics. It is generally accepted that a relatively thin icy shell (≤30 km) overlies a liquid ocean on Europa (see section 4.1.1) that experiences an oscillating tidal response due to its orbital eccentricity.

Despite the extensive body of work on the characterization and interpretation of europan tectonic features discussed in this chapter, this work could not directly answer the question of whether there is tectonic activity on Europa today. Past analyses demonstrated a good correlation between tidal stresses and tectonic lineaments, but focused on relatively old geological features such as ridges and dilational bands. Although some ridges can be placed into the youngest portions of the geological history (*Figueredo and Greeley,* 2000, 2004), especially cycloidal ridges, an analysis of ridge orientations or morphologies cannot be used to answer the question about active tectonics for three important reasons.

First, even geologically young cycloidal ridges currently occur in longitudinal locations (relative to the tidal bulges) that do not match the current tidal stress fields, suggesting that some amount of nonsynchronous rotation has occurred, implying at least several tens of thousands of years since those ridges formed (*Hoppa et al.,* 2001; *Hurford et al.,* 2007a; *Groenleer and Kattenhorn,* 2008). Although this is not a great period of time, geologically speaking, it must be remembered that the nonsynchronous rotation rate is still not well constrained and that these ridges are not the youngest tectonic features. Also, they could have formed 30° mod-

ulo 180° in the past (based on the global symmetry of the tidal stress field). The upshot is that cycloidal ridges do not provide proof of current tectonic activity.

Second, ridge-producing cracks may take a long time to construct their ramparts to either side of the crack (see section 2.1.1). The construction of a ridge is a late stage in an evolutionary process that begins with the development of a trough. It is not known how long this ridge-building process takes, mostly because many years of ridge analyses have still not conclusively determined their mode of development. Typical ridges may take tens of thousands of years to form and can only do so when optimally oriented with respect to the changing stress field during the nonsynchronous rotation process. Hence, ridges cannot be used to make inferences about current tectonic activity on Europa, even if they appear to be geologically young.

Third, the still-present topography of up to 200 m still observed along dilational bands and even higher elevations along ridges that date back through the ~40–90 m.y. of geological history indicates that topography can survive for long time periods and is thus unlikely to be an indicator of recent tectonics. *Dombard and McKinnon* (2006) suggest that appreciable topography may actually survive for >100 m.y. considering the low rate of viscous relaxation, although their results vary as a function of heat flow and surface temperature. *Nimmo et al.* (2003) show that compositional buoyancy due to lateral density differences in a cold, near-surface elastic layer (perhaps related to variability in either ice porosity or salt concentration) could explain prolonged topography that might otherwise be eradicated in less than 0.1 m.y. by ductile flow of ice from below an uncompensated surface load. *Luttrell and Sandwell* (2006) indicate that short-wavelength topography (~20 km), as would characterize ridges, can in fact be supported by the strength of the brittle portion of icy shell itself without the need for underlying support.

At least three factors have complicated attempts to make inferences about active tectonics on Europa:

1. There is a distinct lack of observational evidence for tectonic activity in the time interval between the imaging periods of the Voyager and Galileo spacecraft missions. A comparison of Voyager and Galileo images based on an iterative coregistration technique detected no evidence for deposition by plume activity (such as that which accompanies tectonic activity on Enceladus), nor any evidence for new fracturing during the 20-year interval between missions (*Phillips et al.,* 2000). The lack of inferred plume activity could simply be the result of negative buoyancy effects that hamper surface eruptions (*Crawford and Stevenson,* 1988), regardless of the fact that cracks might fully penetrate an icy shell that has substantially cooled and thickened (*Manga and Wang,* 2007). Hence, absent plumes do not necessarily imply no active tectonics. Additionally, no evidence for any geological (tectonic or otherwise) changes was discovered, so inferences regarding active tectonics are inconclusive. Part of the difficulty introduced into attempts at comparing these datasets is the low resolution of Voyager data and differences in photometric angles, which can dramatically alter the appearance and albedo of surface features. Future missions could be targeted to match Galileo coverage at high resolutions, which may increase the chances of measuring geological changes (*Phillips and Chyba,* 2003).

2. Inferences about tectonic activity based on the geological history in general have been inconclusive. Based on the low density of craters relative to the expected impact flux rate, Europa's surface appears to be geologically young (average age of 40–90 m.y.). This raises the likelihood that tectonic resurfacing has been a geologically recent process that may continue today. Although references have been made to "recent" tectonic lineaments on Europa (e.g., *Geissler et al.,* 1998a), inferences about what features are geologically recent are commonly thwarted by analyses of higher-resolution images that reveal comparatively younger geological features (tectonic fractures and endogenically driven chaos and lenticulae). Europa has experienced numerous changes in tectonic style over its visible history, with a prevalence of endogenically driven surface disruption in the recent geological history (see section 5.2). Nonetheless, a younger period of postchaos fracturing has been noted in several studies (*Kadel et al.,* 2000; *Figueredo and Greeley,* 2000, 2004; *Doggett et al.,* 2007), implying that the development of chaos did not equate to the cessation of tectonic activity on Europa. Although these geological studies point to a high likelihood that there was a geologically young period of tectonic activity, they have not unequivocally determined whether such activity is ongoing.

3. Theoretical stresses in a thickening icy shell allow ongoing fracturing but imply a reduction or cessation of tidally driven tectonic activity. Geological inferences of a thickening icy shell based on convincing evidence that the threshold thickness for solid-state convection was attained (*Barr et al.,* 2004; *Barr and Pappalardo,* 2005; see chapter by Barr and Showman) has led to the development of theoretical models to address the impact of a thickening icy shell on the tidal stress field. As a result of the decrease in tidal deformation as an icy shell thickens, and the fact that tidal stresses are relatively small even in a thin icy shell, there may be a decreasing likelihood of tidally driven tectonic activity through time on Europa (*Hurford,* 2005), reflected in the apparent transition from tectonic resurfacing to cryovolcanic resurfacing (see section 5.2). Hence, processes such as cycloid development and tidal walking along strike-slip faults, which are driven primarily by diurnal tidal stresses, may decline. Nonetheless, tensile stresses produced by expansion of a thickening icy shell (in the 10 MPa range) can far exceed those induced by diurnal or nonsynchronous rotation effects and could promote surface fracturing (see section 4.1.8). Because the stresses are isotropic, orientations of tectonic features will still be controlled by the nonisotropic components of the total stress field (e.g., tidal stresses), even if they are small. Thus, theoretical considerations show that the potential for sufficiently high stresses exists to promote active tectonics that can be reconciled with the current tidal stress state. Nonetheless, it cannot be

proven whether or not tectonic activity actually exists. Although thickening of the icy shell may have indeed induced changes in the tectonic style on Europa through time, as well as plausibly initiating convective overturn and cryovolcanism, it did not necessarily herald the death knell for tectonics.

The question of active tectonics on Europa is open ended. Its importance for understanding the interior dynamics of this icy world, as well as providing potential access pathways to the subsurface ocean, will undoubtedly motivate future studies in this direction, particularly in the context of future mission goals and design (e.g., *Sandwell et al.,* 2004; *Panning et al.,* 2006; see chapter by Greeley et al.).

6. CONCLUDING REMARKS

The icy shell of Europa has experienced pervasive deformation that has resulted in a wide range of tectonic features over the 40–90-m.y. visible history. This deformation was driven by a number of factors, whether global, regional, or local. The two most important global contributors to stresses were probably diurnal tidal deformation induced by a tidally responding subsurface ocean and a longer timescale longitudinal reorientation of the icy shell relative to its tidal bulges by nonsynchronous rotation.

Such stress fields commonly produced tensile components, resulting in ubiquitous extensional deformation. Tension fractures at the surface were reworked over many tens of thousands of years to form ridges. These ridges, composed of raised rims to either side of a central fracture, likely formed in response to a combination of extensional, compressive, and shear-related processes. Complete separation of the icy shell is evidenced by the development of dilational bands, which formed in response to tidally driven extension and endogenic processes such as local upwelling of ductile portions of the shell. Cycloidal fractures provide a strong indication that the diurnal stress field dominated in the creation of tectonic features at times, although this may have been more common later in the geological history, potentially as a result of a decrease in the rate of nonsynchronous rotation stress build-up as the icy shell gradually thickened. Long, linear, or curvilinear fractures likely formed in response to dominant nonsynchronous rotation stresses. Extension through normal faulting is seemingly rare within the ridged plains but commonplace within dilational bands, which resemble terrestrial mid-ocean ridges in many respects. Long-term changes in the orientations of multiply superposed extensional lineaments strongly suggest a temporally variable stress field, ostensibly in response to nonsynchronous rotation of the icy shell.

Contractional deformation is required to balance the surface area budget in light of the new surface area created at dilational bands, which exceeds the amount that would be expected purely as a result of icy shell thickening and expansion. Initially elusive in Galileo images, mounting evidence suggests that contraction may be common on Europa. Although folding is not likely to be globally significant, convergence bands and ubiquitous ridges are plausibly prominent accommodators of contraction. Unanswered questions remain regarding where convergence bands preferentially develop and whether contraction across ridges contributes to ridge construction in tandem with shearing and frictional heating.

Lateral shearing is common as a result of the constantly changing orientations of principal stresses predicted on the diurnal timescale as well as over longer time periods due to nonsynchronous rotation. As long as a fracture has not healed, it can potentially be reactivated by shear stresses that resolve onto the fracture plane from the tidal stress field. These shear stresses may induce strike-slip motions, which may or may not be frictionally resisted along the crack depending on whether the concomitant normal stresses are compressive or tensile (i.e., whether the crack is closed or dilated during the shearing). Active fractures should undergo cycles of tension and compression, as well as backward and forward motion, over the course of the europan day. These motions may result in a slow ratcheting with a preferred motion sense depending on location and crack orientation, ultimately accumulating visible strike-slip offsets; this process is referred to as tidal walking. Convergence across ridges may also produce apparent lateral offsets, resembling those created by strike-slip motions.

Europa is clearly one of the most tectonically diverse bodies in the solar system. Its crack-riddled surface has left a trail of clues for unraveling its deformation and stress history. The moon likely reached the pinnacle of its tectonic activity a long time ago (perhaps millions of years). Gradual thickening of the icy shell may have ultimately resulted in the attainment of a threshold thickness for convectional overturn. This thickening may have resulted in a reduced tidal response, a slower rate of nonsynchronous rotation, and thus smaller global stresses, causing a decrease in the amount of tectonic activity. Nonetheless, tectonic features have been noted to postdate endogenically driven disruptions of the surface that formed regions of chaos. It is probable that tectonic activity has continued to the current day on Europa, with driving stresses plausibly being composed partly of small magnitude tidal components in addition to a large isotropic tension created by the expansion of the icy shell. As with Cassini's encounter with an obviously active Enceladus, it is seems likely that future Europa missions may very well be met with a few surprises.

Acknowledgments. The authors thank G. W. Patterson and R. Pappalardo for their insightful and constructive comments on the original manuscript and acknowledge NASA for its financial support of the authors' research efforts. Useful discussions with L. Prockter, W. Patterson, P. Schenk, and C. Coulter helped improve this work.

REFERENCES

Anderson J. D., Lau E. L., Sjogren W. L., Schubert G., and Moore W. B. (1997) Europa's differentiated internal structure: Inference from two Galileo encounters. *Science, 276,* 1236–1239.

Aydin A. (2006) Failure modes of the lineaments on Jupiter's moon, Europa: Implications for the evolution of its icy crust.

J. Struct. Geol., 28, 2222–2236.

Bader C. E. and Kattenhorn S. A. (2007) Formation of ridge-type strike-slip faults on Europa. *Eos Trans. AGU, 88,* Fall Meet. Suppl., Abstract P53B–1243.

Bader C. E. and Kattenhorn S. A. (2008) Formation mechanisms of europan ridges with apparent lateral offsets. In *Lunar and Planetary Science XXIX,* Abstract #2036. Lunar and Planetary Institute, Houston (CD-ROM).

Barr A. C. and Pappalardo R. T. (2005) Onset of convection in the icy Galilean satellites: Influence of rheology. *J. Geophys. Res., 110,* E12005, DOI: 10.1029/2004JE002371.

Barr A. C., Pappalardo R. T., and Zhong S. (2004) Convective instability in ice I with non-Newtonian rheology: Application to the icy Galilean satellites. *J. Geophys. Res., 109,* E12008, DOI: 10.1029/2004JE002296.

Bart G. D., Greenberg R., and Hoppa G. V. (2003) Cycloids and wedges: Global patterns from tidal stress on Europa. In *Lunar and Planetary Science XXIV,* Abstract #1396. Lunar and Planetary Institute, Houston (CD-ROM).

Beeman M., Durham W. B., and Kirby S. H. (1988) Friction of ice. *J. Geophys. Res., 93,* 7625–7633.

Billings S. E. and Kattenhorn S. A. (2005) The great thickness debate: Ice shell thickness models for Europa and comparisons with estimates based on flexure at ridges. *Icarus, 177,* 397–412.

Collins G. C., Head J. W. III, Pappalardo R. T., and Spaun N. A. (2000) Evaluation of models for the formation of chaotic terrain on Europa. *J. Geophys. Res., 105(E1),* 1709–1716.

Cordero G. and Mendoza B. (2004) Evidence for the origin of ridges on Europa by means of photoclinometric data from the E4 Galileo orbit. *Geofís. Intl., 43,* 301–306.

Coulter C. E., Kattenhorn S. A., and Schenk P. M. (2009) Topographic profile analysis and morphologic characterization of Europa's double ridges. In *Lunar and Planetary Science XL,* Abstract #1960. Lunar and Planetary Institute, Houston (CD-ROM).

Crawford G. D. and Stevenson D. J. (1988) Gas-driven water volcanism and the resurfacing of Europa. *Icarus, 73,* 66–79.

Dahlen F. (1976) The passive influence of the oceans upon the rotation of the earth. *Geophys. J. R. Astron. Soc., 46,* 363–406.

Doggett T., Figueredo P., Greeley R., Hare T., Kolb E., Mullins K., Senske D., Tanaka K., and Weiser S. (2007) Global geologic map of Europa. In *Lunar and Planetary Science XXXVIII,* Abstract #2296. Lunar and Planetary Institute, Houston (CD-ROM).

Dombard A. J. and McKinnon W. B. (2006) Folding of Europa's icy lithosphere: An analysis of viscous-plastic buckling and subsequent topographic relaxation. *J. Struct. Geol., 28,* 2259–2269.

Durham W. B., Heard H. C., and Kirby S. H. (1983) Experimental deformation of polycrystalline H_2O ice at high pressure and low temperature: Preliminary results. *Proc. Lunar Planet. Sci. Conf. 14th,* in *J. Geophys. Res., 88,* B377–B392.

Figueredo P. H. and Greeley R. (2000) Geologic mapping of the northern leading hemisphere of Europa from Galileo solid-state imaging data. *J. Geophys. Res., 105,* 22629–22646.

Figueredo P. H. and Greeley R. (2004) Resurfacing history of Europa from pole-to-pole geological mapping. *Icarus, 167,* 287–312.

Finnerty A. A., Ransford G. A., Pieri D. C., and Collerson K. D. (1981) Is Europa surface cracking due to thermal evolution? *Nature, 289,* 24–27.

Fortt A. L. and Schulson E. M. (2004) Post-terminal compressive deformation of ice: Friction along Coulombic shear faults. *Eos Trans. AGU, 85,* T13A–05.

Gaidos E. J. and Nimmo F. (2000) Tectonics and water on Europa. *Nature, 405,* 637.

Geissler P. E. and 16 colleagues (1998a) Evolution of lineaments on Europa: Clues from Galileo multispectral imaging observations. *Icarus, 135,* 107–126.

Geissler P. E. and 15 colleagues (1998b) Evidence for non-synchronous rotation of Europa. *Nature, 391,* 368–370.

Giese B., Wagner R., Neukum G., Sullivan R., and the Galileo SSI Team (1999) Doublet ridge formation on Europa: Evidence from topographic data. 31st DPS Meeting Abstracts, *Bull. Am. Astron. Soc., 31(4),* 62.08.

Golombek M. P. and Banerdt W. B. (1990) Constraints on the subsurface structure of Europa. *Icarus, 83,* 441–452.

Greeley R. and 17 colleagues (2000) Geologic mapping of Europa. *J. Geophys. Res., 105,* 22559–22578.

Greenberg R. (2004) The evil twin of Agenor: Tectonic convergence on Europa. *Icarus, 167,* 313–319.

Greenberg R. and Weidenschilling S. J. (1984) How fast do Galilean satellites spin? *Icarus, 58,* 186–196.

Greenberg R., Geissler P., Hoppa G., Tufts B. R., Durda D. D., Pappalardo R., Head J. W., Greeley R., Sullivan R., and Carr M. H. (1998) Tectonic processes on Europa: Tidal stresses, mechanical response, and visible features. *Icarus, 135,* 64–78.

Greenberg R., Hoppa G. V., Tufts B. R., Geissler P., and Riley J. (1999) Chaos on Europa. *Icarus, 141,* 263–286.

Groenleer J. M. and Kattenhorn S. A. (2008) Cycloid crack sequences on Europa: Relationship to stress history and constraints on growth mechanics based on cusp angles. *Icarus, 193,* 158–181.

Han L. and Showman A. P. (2008) Implications of shear heating and fracture zones for ridge formation on Europa. *Geophys. Res. Lett., 35,* L03202, DOI: 10.1029/2007GL031957.

Haeussler P. J., Schwartz D. P., Dawson T. E., Stenner H. D., Lienkaemper J. J., Sherrod B., Cinti F. R., Montone P., Craw P. A., Crone A. J., and Personius S. F. (2004) Surface rupture and slip distribution of the Denali and Totschunda faults in the 3 November 2002 M 7.9 earthquake, Alaska. *Bull. Seismol. Soc. Am., 94(6B),* S23–S52.

Harada Y. and Kurita K. (2006) The dependence of surface tidal stress on the internal structure of Europa: The possibility of cracking of the icy shell. *Planet. Space Sci., 54,* 170–180.

Harada Y. and Kurita K. (2007) Effect of non-synchronous rotation on surface stress upon Europa: Constraints on surface rheology. *Geophys. Res. Lett., 34,* L11204, DOI: 10.1029/2007GL029554.

Hayne P. O., Sleep N. H., and Lissauer J. J. (2006) Thickness variations in Europa's icy shell: Stress and rotation effects. In *Europa Focus Group Workshop Abstracts, Vol. 5* (R. Greeley, ed.), pp. 53–54. Arizona State Univ., Tempe.

Head J. W., Pappalardo R. T., and Sullivan R. (1999) Europa: Morphological characteristics of ridges and triple bands from Galileo data (E4 and E6) and assessment of a linear diapirism model. *J. Geophys. Res., 104,* 24223–24236.

Helfenstein P. and Parmentier E. M. (1980) Fractures on Europa: Possible response of an ice crust to tidal deformation. *Proc. Lunar Planet. Sci. Conf. 11th,* pp. 1987–1998.

Helfenstein P. and Parmentier E. M. (1983) Patterns of fracture and tidal stresses on Europa. *Icarus, 53,* 415–430.

Helfenstein P. and Parmentier E. M. (1985) Patterns of fracture and tidal stresses due to nonsynchronous rotation: Implications for fracturing on Europa. *Icarus, 61,* 175–184.

Hoppa G. V. and Tufts B. R. (1999) Formation of cycloidal features

on Europa. In *Lunar and Planetary Science XXX,* Abstract #1599. Lunar and Planetary Institute, Houston (CD-ROM).

Hoppa G. V., Tufts B. R., Greenberg R., and Geissler P. E. (1999a) Formation of cycloidal features on Europa. *Science, 285,* 1899–1902.

Hoppa G., Greenberg R., Geissler P., Tufts B. R., Plassmann J., and Durda D. D. (1999b) Rotation of Europa: Constraints from terminator and limb positions. *Icarus, 137,* 341–347.

Hoppa G., Tufts B. R., Greenberg R., and Geissler P. (1999c) Strike-slip faults on Europa: Global shear patterns driven by tidal stress. *Icarus, 141,* 287–298.

Hoppa G., Greenberg R., Tufts B. R., Geissler P., Phillips C., and Milazzo M. (2000) Distribution of strike-slip faults on Europa. *J. Geophys. Res., 105,* 22617–22627.

Hoppa G. V., Tufts B. R., Greenberg R., Hurford T. A., O'Brien D. P., and Geissler P. E. (2001) Europa's rate of rotation derived from the tectonic sequence in the Astypalaea region. *Icarus, 153,* 208–213.

Hurford T. A. (2005) Tides and tidal stress: Applications to Europa. Ph.D. thesis, Univ. of Arizona, Tucson.

Hurford T. A., Beyer R. A., Schmidt B., Preblich B., Sarid A. R., and Greenberg R. (2005) Flexure of Europa's lithosphere due to ridge-loading. *Icarus, 177,* 380–396.

Hurford T. A., Bills B. G., Sarid A. R., and Greenberg R. (2006) Unraveling Europa's tectonic history: Evidence for a finite obliquity? In *Lunar and Planetary Science XXXVII,* Abstract #1303. Lunar and Planetary Institute, Houston (CD-ROM).

Hurford T. A., Sarid A. R., and Greenberg R. (2007a) Cycloidal cracks on Europa: Improved modeling and non-synchronous rotation implications. *Icarus, 186,* 218–233.

Hurford T. A., Helfenstein P., Hoppa G. V., Greenberg R., and Bills B. G. (2007b) Eruptions arising from tidally controlled periodic openings of rifts on Enceladus. *Nature, 447,* 292–294.

Hurford T. A., Bills B. G., Greenberg R., Hoppa G. V., and Helfenstein P. (2008) How libration affects strike-slip displacement on Enceladus. In *Lunar and Planetary Science XXXIX,* Abstract #1826. Lunar and Planetary Institute, Houston (CD-ROM).

Hurford T. A., Greenberg R., Bills B. G., and Sarid A. R. (2009) The influence of obliquity on europan cycloid formation. *Icarus,* DOI: 10.1016/j.icarus.2009.02.036.

Jackson M. D. and Pollard D. D. (1988) The laccolith-stock controversy: New results from the southern Henry Mountains, Utah. *Geol. Soc. Am. Bull., 100,* 117–139.

Kadel S. D., Fagents S. A., and Greeley R. (1998) Trough-bounding ridge pairs on Europa: Considerations for an endogenic model of formation. In *Lunar and Planetary Science XXIX,* Abstract #1078. Lunar and Planetary Institute, Houston (CD-ROM).

Kadel S. D., Chuang F. C., Greeley R., Moore J. M., and the Galileo SSI Team (2000) Geological history of the Tyre region of Europa: A regional perspective on europan surface features and ice thickness. *J. Geophys. Res., 105,* 22657–22669.

Kargel J. S. (1991) Brine volcanism and the interior structures of asteroids and icy satellites. *Icarus, 94,* 368–390.

Kattenhorn S. A. (2002) Nonsynchronous rotation evidence and fracture history in the Bright Plains region, Europa. *Icarus, 157,* 490–506.

Kattenhorn S. A. (2004a) Strike-slip fault evolution on Europa: Evidence from tail-crack geometries. *Icarus, 172,* 582–602.

Kattenhorn S. A. (2004b) What is (and isn't) wrong with both the tension and shear failure models for the formation of lineae on Europa. In *Workshop on Europa's Icy Shell: Past, Present, and Future,* pp. 38–39. LPI Contribution No. 1195, Lunar and Planetary Institute, Houston.

Kattenhorn S. A. and Marshall S. T. (2006) Fault-induced perturbed stress fields and associated tensile and compressive deformation at fault tips in the ice shell of Europa: Implications for fault mechanics. *J. Struct. Geol., 28,* 2204–2221.

Kattenhorn S. A., Groenleer J. M., Marshall S. T., and Vetter J. C. (2007) Shearing-induced tectonic deformation on icy satellites: Europa as a case study. In *Workshop on Ices, Oceans, and Fire: Satellites of the Outer Solar System,* pp. 74–75. LPI Contribution No. 1357, Lunar and Planetary Institute, Houston.

Kennedy F. E., Schulson E. M., and Jones D. E. (2000) The friction of ice on ice at low sliding velocities. *Philos. Mag. A., 80,* 1093–1110.

Kivelson M. G., Khurana K. K., Russell C. T., Volwerk M., Walker R. J., and Zimmer C. (2000) Galileo magnetometer measurements: A stronger case for a subsurface ocean at Europa. *Science, 289,* 1340–1343.

Lee S., Pappalardo R. T., and Makris N. C. (2005) Mechanics of tidally driven fractures in Europa's ice shell. *Icarus, 177,* 367–379.

Leith A. C. and McKinnon W. B. (1996) Is there evidence for polar wander on Europa? *Icarus, 120,* 387–398.

Lucchitta B. K. and Soderblom L. A. (1982) The geology of Europa. In *The Satellites of Jupiter* (D. Morrison, ed.), pp. 521–555. Univ. of Arizona, Tucson, Arizona.

Luttrell K. and Sandwell D. (2006) Strength of the lithosphere of the Galilean satellites. *Icarus, 183,* 159–167.

Malin M. C. and Pieri D. C. (1986) Europa. In *Satellites* (J. A. Burns and M. S. Matthews, eds.), pp. 689–717. Univ. of Arizona, Tucson, Arizona.

Manga M. and Wang C.-Y. (2007) Pressurized oceans and the eruption of liquid water on Europa and Enceladus. *Geophys. Res. Lett., 34(7),* L07202, DOI: 10.1029/2007GL029297.

Marshall S. T. and Kattenhorn S. A. (2005) A revised model for cycloid growth mechanics on Europa: Evidence from surface morphologies and geometries. *Icarus, 177,* 341–366.

Matsuyama I. and Nimmo F. (2008) Tectonic patterns on reoriented and despun planetary bodies. *Icarus, 195,* 459–473.

McBee J. H., Hartmann D., and Collins G. C. (2003) Strain across ridges on Europa. In *Lunar and Planetary Science XXXIV,* Abstract #1783. Lunar and Planetary Institute, Houston (CD-ROM).

McEwen A. S. (1986) Tidal reorientation and the fracturing of Jupiter's moon Europa. *Nature, 321,* 49–51.

Melosh H. J. (1977) Global tectonics of a despun planet. *Icarus, 31,* 221–243.

Melosh H. J. (1989) *Impact Cratering: A Geologic Process.* Oxford Univ., New York. 245 pp.

Melosh H. J. and Turtle E. P. (2004) Ridges on Europa: Origin by incremental ice wedging. In *Lunar and Planetary Science XXXV,* Abstract #2029. Lunar and Planetary Institute, Houston (CD-ROM).

Mével L. and Mercier E. (2002) Geodynamics on Europa: Evidence for a crustal resorption process. In *Lunar and Planetary Science XXXIII,* Abstract #1476. Lunar and Planetary Institute, Houston (CD-ROM).

Michalski J. R. and Greeley R. (2002) En echelon ridge and trough structures on Europa. *Geophys. Res. Lett., 29,* 1498, DOI: 10.1029/2002GL014956.

Mitri G. and Showman A. P. (2008) A model for the temperature-

dependence of tidal dissipation in convective plumes on icy satellites: Implications for Europa and Enceladus. *Icarus, 195,* 758–764.

Moore W. B. (2006) Thermal equilibrium in Europa's ice shell. *Icarus, 180,* 141–146.

Moore W. B. and Schubert G. (2000) The tidal response of Europa. *Icarus, 147,* 317–319.

Nimmo F. (2004a) Stresses generated in cooling viscoelastic ice shells: Application to Europa. *J. Geophys. Res., 109,* E12001, DOI: 10.1029/2004JE002347.

Nimmo F. (2004b) Dynamics of rifting and modes of extension on icy satellites. *J. Geophys. Res., 109,* E01003, DOI: 10.1029/2003JE002168.

Nimmo F. and Gaidos E. (2002) Strike-slip motion and double ridge formation on Europa. *J. Geophys. Res., 107,* 1–8.

Nimmo F. and Schenk P. (2006) Normal faulting on Europa: Implications for ice shell properties. *J. Struct. Geol., 28,* 2194–2203.

Nimmo F., Pappalardo R. T., and Giese B. (2003) On the origins of band topography, Europa. *Icarus, 166,* 21–32.

Nimmo F., Pappalardo R. T., and Moore W. M. (2005) Icy satellite shell thickening: Consequences for non-synchronous rotation rates and stresses. *Eos Trans. AGU, 86(52),* Fall Meet. Suppl., Abstract P22A-05.

Nimmo F., Spencer J. R., Pappalardo R. T., and Mullen M. E. (2007) Shear heating as the origin of the plumes and heat flux on Enceladus. *Nature, 447,* 289–291.

Noll K. S., Weaver H. A., and Gonnella A. M. (1995) The albedo spectrum of Europa from 2200 Å to 3300 Å. *J. Geophys. Res., 100,* 19057–19059.

Ojakangas G. W. and Stevenson D. J. (1989a) Thermal state of an ice shell on Europa. *Icarus*, *81,* 220–241.

Ojakangas G. W. and Stevenson D. J. (1989b) Polar wander of an ice shell on Europa. *Icarus, 81,* 242–270.

Panning M., Lekic V., Manga M., Cammarano F., and Romanowicz B. (2006) Long-period seismology on Europa: 2. Predicted seismic response. *J. Geophys. Res., 111,* E12008, DOI: 10.1029/2006JE002712.

Pappalardo R.T. and Davis D. M. (2007) Where's the compression? Explaining the lack of contractional structures on icy satellites. In *Workshop on Ices, Oceans, and Fire: Satellites of the Outer Solar System,* pp. 108–109. LPI Contribution No. 1357, Lunar and Planetary Institute, Houston.

Pappalardo R. T. and Sullivan R. J. (1996) Evidence for separation across a gray band on Europa. *Icarus, 123,* 557–567.

Pappalardo R.T. and 31 colleagues (1999) Does Europa have a subsurface ocean? Evaluation of the geological evidence. *J. Geophys. Res., 104,* E10, 24015–24055.

Patterson G. W. and Head J. W. (2007) Kinematic analysis of triple junctions on Europa. In *Workshop on Ices, Oceans, and Fire: Satellites of the Outer Solar System,* pp. 110–111. LPI Contribution No. 1357, Lunar and Planetary Institute, Houston.

Patterson G. W. and Pappalardo R. T. (2002) Compression across ridges on Europa. In *Lunar and Planetary Science XXXIII,* Abstract #1681. Lunar and Planetary Institute, Houston (CD-ROM).

Patterson G. W., Head J. W., and Pappalardo R. T. (2006) Plate motion on Europa and nonrigid behavior of the icy lithosphere: The Castalia Macula region. *J. Struct. Geol., 28,* 2237–2258.

Peale S. J. (1977) Rotation histories of the natural satellites. In *Planetary Satellites* (J. Burns, ed.), pp. 87–112. Univ. of Arizona, Tucson.

Peale S. J. and Cassen P. (1978) Contribution of tidal dissipation to lunar thermal history. *Icarus, 36,* 245–269.

Phillips C. B. and Chyba C. F. (2003) Methods for detecting current geological activity on Europa. *Forum on Concepts and Approaches for Jupiter Icy Moon Orbiter,* Abstract #9018. LPI Contribution No. 1163, Lunar and Planetary Institute, Houston.

Phillips C. B., McEwen A. S., Hoppa G. V., Fagents S. A., Greeley R., Klemaszewski J. E., Pappalardo R. T., Klaasen K. P., and Breneman H. H. (2000) The search for current geologic activity on Europa. *J. Geophys. Res., 105,* 22579–22597.

Pieri D. C. (1981) Lineament and polygon patterns on Europa. *Nature, 289,* 17–21.

Pollard D. D. and Segall P. (1987) Theoretical displacements and stresses near fractures in rock: With applications to faults, joints, veins, dikes, and solution surfaces. In *Fracture Mechanics of Rock* (B. K. Atkinson, ed.), pp. 277–349. Academic, London.

Porco C. C. and 24 colleagues (2006) Cassini observes the active south pole of Enceladus. *Science, 311,* 1393–1401.

Prockter L. M. (2001) Creation and destruction of lithosphere on Europa: From bands to folds. In *Lunar and Planetary Science XXXII,* Abstract #1452. Lunar and Planetary Institute, Houston (CD-ROM).

Prockter L. M. and Pappalardo R. T. (2000) Folds on Europa: Implications for crustal cycling and accommodation of extension. *Science, 289,* 941–943.

Prockter L. M., Pappalardo R. T., Sullivan R., Head J. W., Patel J. G., Giese B., Wagner R., Neukum G., and Greeley R. (1999) Morphology and evolution of europan bands: Investigation of a seafloor spreading analog. In *Lunar and Planetary Science XXX,* Abstract #1900. Lunar and Planetary Institute, Houston (CD-ROM).

Prockter L. M., Pappalardo R. T., and Head III J. W. (2000) Strike-slip duplexing on Jupiter's icy moon Europa. *J. Geophys. Res., 105,* 9483–9488.

Prockter L. M., Head J., Pappalardo R., Sullivan R., Clifton A. E., Giese B., Wagner R., and Neukum G. (2002) Morphology of europan bands at high resolution: A mid-ocean ridge-type rift mechanism. *J. Geophys. Res., 107,* 1–26.

Qin R., Buck W. R., and Germanovich L. (2007) Comment on "Mechanics of tidally driven fractures in Europa's ice shell" by S. Lee, R. T. Pappalardo, and N. C. Makris (2005, *Icarus 177,* 367–379). *Icarus, 189,* 595–597.

Rambaux N., Karatekin Ö., and Van Hoolst T. (2007) Europa's librations and ice shell thickness. *Soc. Franc. Astron. Astrophys., SF2A,* 1–6.

Riley J., Greenberg R., and Sarid A. (2006) Europa's South Pole region: A sequential reconstruction of surface modification processes. *Earth Planet. Sci. Lett., 248,* 808–821.

Rist M. A. (1997) High-stress ice fracture and friction. *J. Phys. Chem., 101,* 6263–6266.

Rist M. A. and Murrell S. A. F. (1994) Ice triaxial deformation and fracture. *J. Glaciol., 40,* 305–318.

Rist M. A., Jones S. J., and Slade T. D. (1994) Microcracking and shear fracture in ice. *Ann. Glaciol., 19,* 131–137.

Rothery D. A. (1992) *Satellites of the Outer Planets*. Clarendon, Oxford. 208 pp.

Rudolph M. L. and Manga M. (2009) Fracture penetration in planetary ice shells. *Icarus, 199,* 536–541.

Sammonds P. R., Murrell S. A. F., and Rist M. A. (1989) Fracture of multi-year sea ice under triaxial stresses: Apparatus description and preliminary results. *J. Offshore Mech. Arct.*

Eng., 111, 258–263.

Sandwell D., Rosen P., Moore W., and Gurrola E. (2004) Radar interferometry for measuring tidal strains across cracks on Europa. *J. Geophys. Res., 109,* E11003, DOI: 10.1029/2004JE002276.

Sarid A. R., Greenberg R., Hoppa G., Hurford T. A., Tufts R., and Geissler P. (2002) Polar wander and surface convergence of Europa's ice shell: Evidence from a survey of strike-slip displacement. *Icarus, 158,* 24–41.

Sarid A. R., Greenberg R., Hoppa G. V., Geissler P., and Preblich B. (2004) Crack azimuths on Europa: Time sequence in the southern leading face. *Icarus, 168,* 144–157.

Sarid A. R., Greenberg R., Hoppa G. V., Brown D. M., and Geissler P. (2005) Crack azimuths on Europa: The G1 lineament sequence revisited. *Icarus, 173,* 469–479.

Sarid A. R., Greenberg R., and Hurford T. A. (2006) Crack azimuths on Europa: Sequencing of the northern leading hemisphere. *J. Geophys. Res., 111,* E08004, DOI: 10.1029/2005JE002524.

Sarid-Rhoden A. R., Militzer B., Huff E. M., Hurford T. A., Manga M., and Richards M. (2009) Implications for Europa's obliquity from cycloid modeling. In *Lunar and Planetary Science XL,* Abstract #1891. Lunar and Planetary Institute, Houston (CD-ROM).

Schenk P. and McKinnon W. B. (1989) Fault offsets and lateral crustal movement on Europa: Evidence for a mobile ice shell. *Icarus, 79,* 75–100.

Schenk P. M. and Pappalardo R. T. (2004) Topographic variations in chaos on Europa: Implications for diapiric formation. *Geophys. Res. Lett., 31,* L16703, DOI: 10.1029/2004GL019978.

Schenk P., Matsuyama I., and Nimmo F. (2008) True polar wander on Europa from global-scale small-circle depressions. *Nature, 453,* 368–371.

Schulson E. M. (1987) The fracture of ice I_h. *J. Phys. (Paris), Colloque C1, 48,* 207–218.

Schulson E. M. (2001) Brittle failure of ice. *Engrg. Fract. Mech., 68,* 1839–1887.

Schulson E. M. (2002) On the origin of a wedge crack within the icy crust of Europa. *J. Geophys. Res., 107,* 5107, DOI: 10.1029/2001JE001586.

Schulson E. M. (2009) Frictional sliding of cold ice. In *Lunar and Planetary Science XL,* Abstract #1795. Lunar and Planetary Institute, Houston (CD-ROM).

Schulson E. M., Iliescu D., and Renshaw C. E. (1999) On the initiation of shear faults during brittle compressive failure: A new mechanism. *J. Geophys. Res., 104,* 695–705.

Showman A. P. and Han L. (2005) Effects of plasticity on convection in an ice shell: Implications for Europa. *Icarus, 177,* 425–437.

Smith B. A. and the Voyager Imaging Team (1979) The Galilean satellites of Jupiter: Voyager 2 imaging science results. *Science, 206,* 951–972.

Smith-Konter B. and Pappalardo R. T. (2008) Tidally driven stress accumulation and shear failure of Enceladus's tiger stripes. *Icarus, 198,* 435–451.

Sotin C., Head J. W. III, and Tobie G. (2002) Europa: Tidal heating of upwelling thermal plumes and the origin of lenticulae and chaos melting. *Geophys. Res. Lett., 29,* DOI: 10.1029/2001GL013844.

Spaun N. A., Pappalardo R. T., and Head J. W. III (2003) Evidence for shear failure in forming near-equatorial lineae on Europa. *J. Geophys. Res., 108(E6),* 5060, DOI: 10.1029/2001JE001499.

Spencer J. R., Pearl J. C., Segura M., Flasar F. M., Mamoutkine A., Romani P., Buratti B. J., Hendrix A. R., Spilker L. J., and Lopes R. M. C. (2006) Cassini encounters Enceladus: Background and the discovery of a south polar hot spot. *Science, 311,* 1401–1405.

Squyres S. W. and Croft S. K. (1986) The tectonics of icy satellites. In *Satellites* (J. A. Burns and M. S. Matthews, eds.), pp. 293–341. Univ. of Arizona, Tucson.

Stempel M. M., Barr A. C., and Pappalardo R. T. (2005) Model constraints on the opening rates of bands on Europa. *Icarus, 177,* 297–304.

Sullivan R. and 15 colleagues (1997) Ridge formation on Europa: Examples from Galileo high resolution images. *GSA Annual Convention, Abstr. with Progr., 29,* A-312.

Sullivan R. and 12 colleagues (1998) Episodic plate separation and fracture infill on the surface of Europa. *Nature, 391,* 371–373.

Tufts B. R. (1998) Lithospheric displacement features on Europa and their interpretation. Ph.D. thesis, Univ. of Arizona, Tucson. 288 pp.

Tufts B. R., Greenberg R., Hoppa G., and Geissler P. (1999) Astypalaea Linea: A large-scale strike-slip fault on Europa. *Icarus, 141,* 53–64.

Tufts B. R., Greenberg R., Hoppa G., and Geissler P. (2000) Lithospheric dilation on Europa. *Icarus, 146,* 75–97.

Turcotte D. L. and Schubert G. (2002) *Geodynamics,* 2nd edition. Cambridge Univ., New York. 456 pp.

Turtle E. P., Melosh H. J., and Phillips C. B. (1998) Tectonic modeling of the formation of europan ridges. *Eos Trans. AGU, 79,* F541.

Van Hoolst T., Rambaux N., Karatekin Ö., Dehant V., and Rivoldini A. (2008) The librations, shape, and icy shell of Europa. *Icarus, 195,* 386–399.

Vetter J. C. (2005) Evaluating displacements along europan ridges. M.S. thesis, Univ. of Idaho, Moscow.

Wahr J., Selvans Z. A., Mullen M. E., Barr A. C., Collins G. C., Selvans M. M., and Pappalardo R. T. (2009) Modeling stresses on satellites due to nonsynchronous rotation and orbital eccentricity using gravitational potential theory. *Icarus, 200,* 188–206.

Williams K. K. and Greeley R. (1998) Estimates of ice thickness in the Conamara Chaos region of Europa. *Geophys. Res. Lett., 25,* 4273–4276.

Wilson G. (1960) The tectonics of the 'Great Ice Chasm', Filchner Ice Shelf, Antarctica. *Proc. Geol. Assoc., 71,* 130–138.

Yoder C. F. (1979) How tidal heating on Io drives the Galilean resonance locks. *Nature, 279,* 767–770.

Zahnle K., Schenk P., Levison H., and Dones L. (2003) Cratering rates in the outer solar system. *Icarus, 163,* 263–289.